Bifuran-imide: A Stable Furan Building Unit for Organic Electronics

Sandip V. Mulay[a], Benny Bogoslavky[b], Idan Galanti[a], Ehud Galun[c] and Ori Gidron[a]*

[a] Institute of Chemistry, The Hebrew University of Jerusalem Edmond J. Safra Campus, Jerusalem, Israel. E-mail: ori.gidron@mail.huji.ac.il

[b] The Laboratory for Molecular Structure Analysis, The Institute of Chemistry, The Hebrew University of Jerusalem, The Edmond J. Safra Campus, Jerusalem, Israel.

[c] Head of Materials Division, R&T Base Unit, DDR&D IMOD, Hakirya, Tel Aviv, Israel

Contents

S1 General Information

The reagents and chemicals used here are commercially available and were used without further purification unless otherwise stated. Flash chromatography (FC) was performed using CombiFlash SiO_2 columns. The compounds 3,3'-dibromo-2,2'-bifuran,[1] 2-octyldodecylamine,[2] and *N*-(2-octyldodecyl)-2,2′-bithiophene-3,3′-dicarboximide[2] were synthesized according to the previously reported procedures. ^1H and ^{13}C NMR spectra were recorded in solution on a Bruker-AVIII 400 MHz and 500 MHz spectrometer using tetramethylsilane (TMS) as the external standard. The spectra were recorded using chloroform-*d* and methanol-*d4* as solvents. Chemical shifts are expressed in δ units. IR spectra were obtained as $CHCl_3$ solutions placed as a thin film on CaF pallet using Nicolet 6700 FT-IR spectrometer. High resolution mass spectra were measured on a HR Q-TOF LCMS. Molecular weights and size distribution were determined by gel permeation chromatography (GPC) in chloroform (with 0.025% toluene as internal standard) against polystyrene standards with a flow rate of 1 mL/min. GPC was performed on a Polymer Standards Service (PSS) system consisting of a linear M column composed of a styrene-divinylbenzene (CDV) copolymer network (*i.e.*, a PSS SDV linear M column), refractive index and UV detectors (Thermo). Data analysis and standard calibration (with PS standards) were performed using PSS WinGPC UniChrom software V8.20, Build 5350. Thermogravimetric analysis (TGA) and Differential Scanning Calorimetry (DSC) measurements were carried out simultaneously with a NETZSCH STA 449F3 Jupiter instrument at a heating rate of 5 °C min^{-1} under N_2. Melting points were determined using DSC by taking the peak maximum at a scan rate of 5 °C min^{-1} and Fisher-Johns melting point apparatus. Cyclic voltammetry (CV) measurements were performed using a Bio-Logic SP-150 Potentiostat in a standard three-electrode setup. Pt wire, Ag/AgCl wire, and Pt disk electrode were used as the counter electrode, pseudo-reference electrode, and working electrode, respectively. Dichloromethene (DCE) containing 0.1 M 0.1 M tetrabutylammonium perchlorate was used as the solvent. A ferrocene/ferrocenium redox couple was used as an internal reference for all measurements. UV-vis absorption and fluorescence spectra of synthesized compounds were recorded on an Agilent Technologies Cary series UV-Vis-NIR spectrophotometer. Fluorescence measurements were carried out with a Horiba Scientific Fluoromax-4 spectrofluorometer. Absolute fluorescence quantum yield measurements were performed using Quanta-Phi integrating sphere connected to Fluoromex-4. Fluorescence lifetime measurements were performed using Fluoro-Hub-B, equipped with NanoLed-390 as light source.

S2 Synthetic Procedure

3,3'-Dibromo-2,2'-bifuran (1)[1]

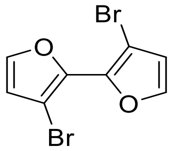

A solution of lithium diisopropylamide (LDA; 37.4 mL, 2.0 M in hexane) was added dropwise to a solution of 3-bromo-furan (10 g, 68.04 mmol) in 60 mL dry tetrahydrofuran (THF) at -78 °C under N_2. The reaction mixture was then stirred under the same conditions. After 1.5 h, $CuCl_2$ (10 g, 74.8 mmol) was added as a single portion and the resulting solution was allowed to reach room temperature slowly and was stirred overnight. The reaction mixture was then added into 100 mL water with 5 g glycine at 0 °C, filtered, and the filtrate was extracted with diethyl ether (3 × 80 mL), dried (Na_2SO_4), and concentrated. The residue obtained was purified by flash column chromatography on silica gel with hexane as eluent to give **1** as a white solid (6.7 g, 69%). **^{1}H NMR** (400 MHz, chloroform-*d*) δ 7.47 (d, *J* = 1.9 Hz, 2H), 6.55 (d, *J* = 1.9 Hz, 2H).

2,2'-Bifuran-3,3'-dicarboxylic acid (2)

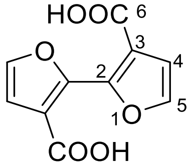

To a solution of *n*-BuLi (31.2 mL, 50.0 mmol, 1.6 M in hexane) in dry THF (50 mL), 3,3'-dibromobifuran (**1**) (5.84 g, 20.0 mmol) in dry THF (40 mL) was added dropwise over a period of 30 minutes at -70 °C. The resulting solution was stirred at -70 °C until it becomes white slurry (about 2 hours). To the slurry was added dry ice (7.0 g, 160.0 mmol) at -70 °C. Then, the mixture was gradually warmed to room temperature. After stirring for 5 hours at room temperature, the reaction mixture was quenched with methanol (5 mL), and the solvent was removed under reduced pressure. The crude product was purified by flash column chromatography on silica gel using AcOH/CH_2Cl_2/methanol (1:95:4) as eluent to give **2** as a light yellow solid (3.38 g, 76%). **^{1}H NMR** (400 MHz, methanol-*d*) δ 7.68 (d, *J* = 2.0 Hz, 2H; H–C(5)), 6.87 (d, *J* = 1.9 Hz, 2H, H–C(4)); **^{13}C**

NMR (101 MHz, methanol-*d*) δ 165.75 (2 C(6)), 147.34 (2 C(2)), 145.11 (2 C(5)), 121.08 (2 C(3)), 112.99 (2 C(4)); **HRMS** (ESI) calcd for $C_{10}H_7O_6$ 223.0243, found 223.0237 $(M + H)^+$.

2,2'-Bifuran-3,3'dicarboxylic anhydride (3)

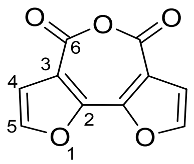

A solution of (2,2'-bifuran)-3,3'-dicarboxylic acid (**2**) (3.3 g, 14.9 mmol) in acetic anhydride (100 mL) was stirred under reflux conditions for 12 h. Acetic anhydride was removed by distillation under reduced pressure. The residue thus obtained was purified by flash column chromatography on silica gel using hexane/ethyl acetate (4:1) as eluent to give anhydride **3** as a light yellow solid (2.46 g, 81%), mp 205-206 °C. **^{1}H NMR** (400 MHz, chloroform-*d*) δ 7.61 (d, *J* = 1.6 Hz, 2H; H–C(5)), 7.11 (d, *J* = 1.6 Hz, 2H; H–C(4)); **^{13}C NMR** (101 MHz, chloroform-*d*) δ 154.35 (2 C(6)), 145.35 (2 C(2)), 144.74 (2 C(5)), 116.27 (2 C(3)), 113.93 (2 C(4)); **IR** (ν_{max}) 3149, 3123, 2924, 2859, 1730, 1704, 1627, 1497, 1446, 1295, 1266, 1161, 1131, 1093 cm^{-1}; **HRMS** (ESI) calcd for $C_{10}H_5O_5$ 205.0137, found 205.0130 $(M + H)^+$.

N-Hexyl-2,2'-bifuran-3,3'-dicarboximide (BFI-H)

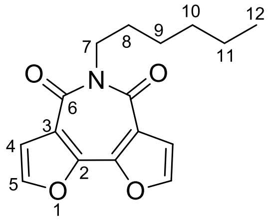

To a solution of anhydride **3** (2.04 g, 10.0 mmol) in dry CH_2Cl_2 (100 mL) was added a solution of 1-hexylamine (1.6 mL, 12.0 mmol) in CH_2Cl_2 (20 mL) dropwise under N_2. After addition, the reaction mixture was stirred under reflux for 12 h. The reaction mixture was cooled to room temperature and then $SOCl_2$ (1.1 mL, 15.0 mmol) was added dropwise. The reaction mixture was again refluxed for 15 h. The reaction was quenched with a saturated aqueous (sat. aq.) solution of $NaHCO_3$ (50 mL). The separated aqueous layer was extracted with CH_2Cl_2 (2 × 50 mL), dried (Na_2SO_4), filtered, and concentrated. The residue obtained was purified by flash column chromatography on silica gel using hexane and ethyl acetate (4:1) as eluent to give **BFI-H** as a white solid (2.53 g, 88%), mp 72 °C. **^{1}H NMR** (500 MHz, chloroform-*d*) δ 7.54 (d, *J* = 1.9 Hz, 2H; H–C(5)), 7.15 (d, *J* = 1.9 Hz, 2H; H–C(4)), 4.21 (t, *J* = 7.8, 2H; –C*H₂*(7)), 1.69-1.63 (m, 2H; –C*H₂*(8)), 1.42-1.30 (m, 6H; –C*H₂*(9-11), 0.88 (t, *J* = 7.1 Hz, 3H; –C*H₃*(12)); **^{13}C NMR** (101 MHz, chloroform-*d*) δ 160.42 (2 C(6)), 143.64 (2 C(5)), 143.49 (2 C(2)), 120.40 (2 C(3)), 114.17 (2 C(4)), 45.29 (C(7)), 31.65 (C(10)), 27.61 (C(8)), 26.98 (C(9)), 22.71 (C(11)), 14.17 (C(12)); **IR** (ν_{max}) 3131, 2956, 2930, 2858, 1666, 1630, 1579, 1569, 1508, 1467, 1383, 1339, 1316, 1288, 1225, 1193, 1168, 1140, 1112, 1093, 1051 cm^{-1}; **HRMS** (ESI) calcd for $C_{16}H_{18}NO_4$ 288.1230, found 288.1254 (M+H)$^+$.

N-Hexyl-5-bromo-2,2'-bifuran-3,3'-dicarboximide (4a)

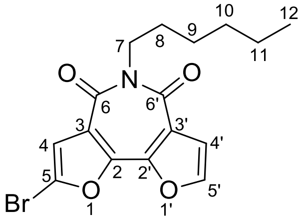

Bromine (0.18 mL, 3.6 mmol) and a catalytic amount of $FeCl_3$ (10 mg, 2 mol%) were added to a solution of imide **BFI-H** (0.862 g, 3.0 mmol) in CH_2Cl_2 (40 mL) and the reaction mixture was stirred in the dark for 4 h. After completion of the reaction, it was quenched using a sat. aq. solution of Na_2SO_3 and stirred for a further 30 min. The reaction mixture was poured into CH_2Cl_2 (150 mL) and washed with water (2 × 100 mL), brine, dried (Na_2SO_4), filtered, and concentrated. The residue obtained was purified by flash column chromatography on silica gel using hexane and CH_2Cl_2 (1:1) as eluent to give **4a** as a white solid (0.62 g, 56%), mp 94-96 °C. **^{1}H NMR** (500 MHz, chloroform-*d*) δ 7.55 (d, *J* = 1.9 Hz, 1H; H–C(5')), 7.15 (d, *J* = 1.9 Hz, 1H; H–C(4')),7.07 (s, 1H; H–C(4)), 4.18 (t, *J* = 7.8, 2H; –C*H₂*(7)), 1.67-1.61 (m, 2H; –C*H₂*(8)), 1.40-1.30 (m, 6H; –C*H₂*(9-11)), 0.88 (t, *J* = 7.1 Hz, 3H; –C*H₃*(12)); **^{13}C NMR** (125 MHz, chloroform-*d*) δ 160.09 (C(6)), 159.37 (C(6')), 144.59 (C(2')), 143.95 (C(5')), 142.45 (C(2)), 125.67 (C(3)), 121.92 (C(5)), 120.45 (C(3')), 115.58 (C(4)), 114.28 (C(4')), 45.40 (C(7)), 31.64 (C(10)), 27.57 (C(8)), 26.96 (C(9)), 22.71 (C(11)), 14.18 (C(12)); **IR** (ν_{max}) 3149, 3122, 2971, 2953, 2935, 2869, 2848, 1656, 1622, 1575, 1523, 1500, 1453, 1426, 1375, 1337, 1273, 1242, 1221, 1182, 1150, 1125, 1100, 1061, 1037 cm^{-1}; **HRMS** (ESI) calcd for $C_{16}H_{17}BrNO_4$ 366.0341, found 366.0357 (M+H)$^+$.

N-Hexyl-5,5'-dibromo-2,2'-bifuran-3,3'-dicarboximide (4b)

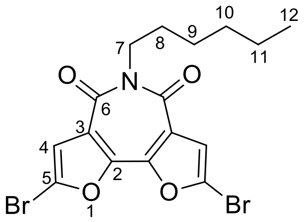

Bromine (0.62 mL, 12.0 mmol) and a catalytic amount of $FeCl_3$ (10 mg, 2 mol%) were added to a solution of imide **BFI-H** (0.862 g, 3.0 mmol) in CH_2Cl_2 (40 mL) and the reaction mixture was stirred in the dark for 4 h. After completion of the reaction, it was quenched using a sat. aq. solution of Na_2SO_3 and stirred for a further 30 min. The reaction mixture was poured into CH_2Cl_2 (150 mL) and washed with water (2 × 100 mL), brine, dried (Na_2SO_4), filtered, and concentrated. The residue obtained was purified by flash column chromatography on silica gel using hexane and ethyl acetate (9:1) as eluent to give **4b** as a white solid (1.29 g, 97%), mp 133-135 °C. **^{1}H NMR** (500 MHz, chloroform-*d*) δ 7.06 (s, 2H; H–C(4), 4.16 (t, *J* = 7.8, 2H; –C*H₂*(7)), 1.65-1.59 (m, 2H; –C*H₂*(8)), 1.38-1.29 (m, 6H; –C*H₂*(9-11)), 0.88 (t, *J* = 7.1 Hz, 3H; –C*H₃*(12)); **^{13}C NMR** (125 MHz, chloroform-*d*) δ 159.06 (2 C(6)), 143.52 (2 C(2)), 126.12 (2 C(3)), 121.92 (2 C(5)), 115.69 (2 C(4)), 45.51 (C(7)), 31.62 (C(10)), 27.52 (C(8)), 26.93 (C(9)), 22.71 (C(11)), 14.18 (C(12)); **IR** (ν_{max}) 3125, 3102, 2919, 2871, 2852, 1668, 1621, 1581, 1525, 1500, 1462, 1376, 1333, 1272, 1231, 1174, 1107, 1091, 1067 cm^{-1}; **HRMS** (ESI) calcd for $C_{16}H_{16}Br_2NO_4$ 445.9421, found 445.9435 $(M+H)^+$.

N-Hexyl-5-(tributylstannyl)-2,2'-bifuran-3,3'-dicarboximide (5)

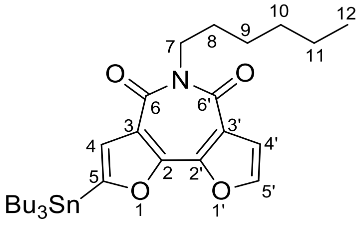

A solution of lithium diisopropylamide (LDA; 0.55 mL, 2.0 M in hexane, 1.1 mmol) was added dropwise to a solution of *N*-hexyl-2,2'-bifuran-3,3'-dicarboximide **(BFI-H)** (287 mg, 1.0 mmol) in dry THF (15 mL) at -85 °C under N_2 and stirred for 1 h. Bu_3SnCl (0.33 mL, 1.2 mmol) was added dropwise, and the reaction mixture was allowed to reach room temperature and stirred for 2 h. The mixture was quenched with water, extracted with CH_2Cl_2 (2 × 40 mL), dried (Na_2SO_4), filtered, and evaporated. The residue obtained was purified by flash column chromatography on silica gel basified with trimethylamine using hexane as eluent to give **5** as a colorless oil (300 mg, 52%). **^{1}H NMR** (400 MHz, chloroform-*d*) δ 7.53 (d, *J* = 1.9 Hz, 1H), 7.25 (s, 1H), 7.15 (d, *J* = 1.9 Hz, 1H), 4.22 (t, *J* = 7.7, 2H), 1.68-1.55 (m, 8H), 1.39-1.30 (m, 12H), 1.20-1.15 (m, 6H), 0.90 (t, *J* = 7.2 Hz, 12H); **^{13}C NMR** (101 MHz, chloroform-*d*) δ 165.72, 160.90, 160.65, 147.59, 144.09, 143.22, 125.17, 120.64, 119.33, 114.05, 45.19, 31.67, 28.97 (3C), 27.67, 27.25 (3C), 27.01 22.72, 14.18, 13.74 (3C), 10.59 (3C); **IR** (ν_{max}) 3130, 2956, 2925, 2871, 2854, 1664, 1632, 1579, 1520, 1489,1447, 1373, 1338, 1298, 1237, 1189, 1155, 1133, 1094, 1066 cm^{-1}; **HRMS** (ESI) calcd for $C_{28}H_{44}NO_4Sn$ 578.2292, found 578.2290 (M+H)$^+$.

Bis (*N*-hexyl-2,2'-bifuran-3,3'-dicarboximide) (2BFI-H)

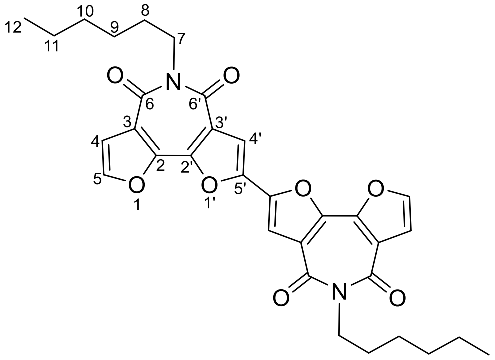

$Pd(PPh_3)_4$ (23 mg, 0.02 mmol) was added to a solution of *N*-hexyl-5-bromo-2,2'-bifuran-3,3'-dicarboximide **(4a)** (146 mg, 0.40 mmol) and *N*-hexyl-5-(tributylstannyl)-2,2'-bifuran-3,3'-dicarboximide **(5)** (300 mg, 0.52 mmol) in dry and degassed toluene (10 mL), and the reaction mixture was stirred at 90 °C for 24 h under nitrogen. Then reaction mixture was cooled to room temperature and the solvent was evaporated under reduced pressure. The residue obtained was purified by flash column chromatography on silica gel using hexane and dichloromethane (1:8) as eluent to give **2BFI-H** as a yellow solid (140 mg, 61%), mp 218 °C; **^{1}H NMR** (500 MHz, chloroform-*d*) δ 7.60 (d, *J* = 1.9 Hz, 2H; H–C(5)), 7.47 (s, 2H; H–C(4')), 7.18 (d, *J* = 1.9 Hz; H–C(4)), 4.21 (t, *J* = 7.8, 4H; –CH_2(7)), 1.71-1.63 (m, 4H; –CH_2(8)), 1.42-1.30 (m, 12H; –CH_2(9-11)), 0.89 (t, *J* = 7.1 Hz, 6H; –CH_3(12)); **^{13}C NMR** (125 MHz, chloroform-*d*) δ 160.06 (2 C(6)), 159.80 (2 C(6')), 144.78 (2 C(5')), 144.26 (2 C(5)), 143.30 (2 C(2')), 142.62 (2 C(2)), 121.78 (2 C(3)), 121.40 (2 C(3')), 114.54 (2 C(4)), 111.44 (2 C(4')), 45.42 (2 C(7)), 31.66 (2 C(10)), 27.60 (2 C(8)), 26.98 (2 C(9)), 22.73 (2 C(11)), 14.19 (2 C(12)); **IR** (ν_{max}) 3154, 3123, 2955, 2927, 2927, 2856, 1666, 1628, 1577, 1490, 1452, 1377, 1333, 1305, 1237, 1192, 1160, 1133, 1100, 1069 cm^{-1}; **HRMS** (ESI) calcd for $C_{32}H_{33}N_2O_8$ 573.2237, found 573.2229 $(M+H)^+$.

Tris (*N*-Hexyl-2,2'-bifuran-3,3'-dicarboximide) (3BFI-H)

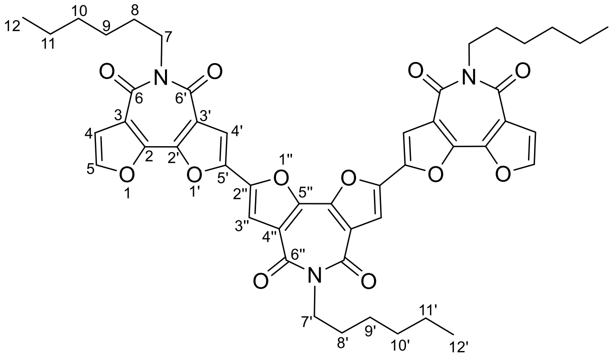

Tetrakis(triphenylphosphine)palladium ($Pd(PPh_3)_4$; 15 mg, 0.013 mmol) was added to a solution of *N*-hexyl-5,5'-dibromo-2,2'-bifuran-3,3'-dicarboximide **(4b)** (111 mg, 0.25 mmol) and *N*-hexyl-5-(tributylstannyl)-2,2'-bifuran-3,3'-dicarboximide **(5)** (432 mg, 0.75 mmol) in dry and degassed toluene (10 mL), and the reaction mixture was stirred at 90 °C for 24 h under nitrogen. Then reaction mixture was cooled to room temperature and the solvent was evaporated under reduced pressure. The residue obtained was purified by flash column chromatography on silica gel using dichloromethane and ethyl acetate (95:5) as eluent to give **3BFI-H** as a yellow solid (96 mg, 45%), mp 294 °C; **^{1}H NMR** (500 MHz, chloroform-*d*) δ 7.63 (d, *J* = 1.9 Hz, 2H; H–C(5)), 7.52 (s, 2H; H–C(3")), 7.45 (s, 2H; H–C(4')), 7.18 (d, *J* = 1.8 Hz, 2H; H–C(4)), 4.20 (t, *J* = 7.6, 6H; –CH_2(7)), 1.67 (quint, J = 7.6 Hz, 6H; –CH_2(8)), 1.43-1.33 (m, 18H; –CH_2(9-11)), 0.90 (t, *J* = 7.1 Hz, 9H; –CH_3(12)); **^{13}C NMR** (125 MHz, chloroform-*d*) δ 160.01 (2 C(6)), 159.68 (2 C(6')), 159.41 (2 C(6")), 145.28 (2 C(2')), 144.49 (2 C(2")), 144.39 (2 C(5)), 143.41 (2 C(5")), 142.52 (2 C(2)), 142.28 (2 C(5')), 122.72 (2 C(4")), 121.81 (2 C(3)), 121.56 (2 C(3')), 114.59 (2 C(4)), 112.00 (2 C(3")), 111.66 (2 C(4')), 45.56 (1 C(7')), 45.43 (2 C(7)), 31.66 (3 C(10)), 27.61 (2 C(8)), 27.59 (1 C(8')), 26.99 (3 C(9)), 22.75 (3 C(11)), 14.21 (3 C(12)); **IR** (ν_{max}) 3128, 2955, 2923, 2854, 1661, 1622, 1574, 1508, 1490, 1447, 1377, 1332, 1303, 1275, 1247, 1167, 1132, 1097, 1070, 1046 cm^{-1}; **HRMS** (ESI) calcd for $C_{48}H_{47}N_3O_{12}Na$ 880.3052, found 880.3041 $(M + Na)^+$.

N-(2-octyldodecyl)-2,2'-bifuran-3,3'-dicarboximide (BFI-OD)

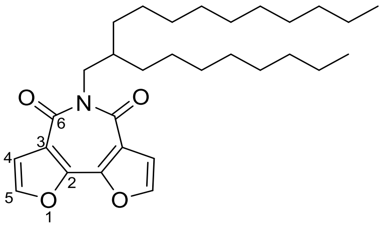

To a solution of anhydride **3** (1.5 g, 7.34 mmol) in dry CH_2Cl_2 (80 mL) was added a solution of 2-octyldodecylamine (2.4 g, 8.07 mmol) in CH_2Cl_2 (20 mL) dropwise under N_2. After addition, the reaction mixture was stirred under reflux for 12 hr. The reaction mixture was cooled to room temperature and then $SOCl_2$ (0.87 mL, 12.0 mmol) was added dropwise. The reaction mixture was again refluxed for 15 hr. The reaction was quenched using a sat. aq. solution of $NaHCO_3$ (20 mL). The aqueous layer was extracted with CH_2Cl_2 (2 × 80 mL), dried (Na_2SO_4) and concentrated. The residue obtained was purified by flash column chromatography on silica gel using hexane and ethyl acetate (9:1) as eluent to give **BFI-OD** as a colorless oil (2.81 g, 79%). **^{1}H NMR** (500 MHz, chloroform-*d*) δ 7.54 (d, *J* = 1.9, 2H; H–C(5)), 7.16 (d, *J* = 1.9, 2H; H–C(4)), 4.24 (d, *J* = 7.2, 2H; –CH_2-CH), 1.91-1.86 (m, 1H; –CH_2-C*H*), 1.38-1.18 (m, 32H; 16(CH_2)), 0.87 (t, *J* = 7.1 Hz, 3H; (CH_3)), 0.86 (t, *J* = 6.8 Hz, 3H; (CH_3)); **^{13}C NMR** (125 MHz, chloroform-*d*) δ 160.84 (2 C(6)), 143.60 (2 C(5)), 143.41 (2 C(2)), 120.41 (2 C(3)), 114.35 (2 C(4)), 48.56, 36.45, 32.07, 32.03, 31.85 (2C), 30.21 (2C), 29.79, 29.77, 29.74, 29.69, 29.48, 29.44, 26.65 (2C), 22.82, 22.80, 14.25 (2C); **IR** (ν_{max}) 3133, 2955, 2925, 2854, 1668, 1633, 1580, 1508, 1466, 1379, 1314, 1283, 1187, 1140, 1116, 1050, 1030 cm^{-1}; **HRMS** (ESI) calcd for $C_{30}H_{46}NO_4$ 484.3427, found 484.3421 (M + H)$^+$.

N-(2-octyldodecyl)- 5,5'-dibromo-2,2'-bifuran-3,3'-dicarboximide (4c)

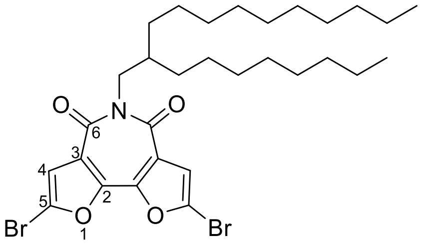

Bromine (0.32 mL, 6.0 mmol) and a catalytic amount of $FeCl_3$ (5 mg, 2 mol%) were added to the solution of *N*-(2-octyldodecyl)-2,2'-bifuran-3,3'-dicarboximide **(BFI-OD)** (0.73 g, 1.5 mmol) in CH_2Cl_2 (40 mL) and the reaction mixture was stirred in the dark for 4 hr. After completion of the reaction it was quenched using a sat. aq. solution of Na_2SO_3 and stirred for a further 30 min. The reaction mixture was poured into CH_2Cl_2 (100 mL) and washed with water (2 × 60 mL), brine, dried (Na_2SO_4), filtered, and concentrated. The residue obtained was purified by flash column chromatography on silica gel using hexane and ethyl acetate (9:1) as eluent to give **4c** as a colorless oil (0.93 g, 96%). **^{1}H NMR** (500 MHz, chloroform-*d*) δ 7.07 (s, 2H; H–C(4)), 4.19 (d, *J* = 7.3, 2H; –CH_2-CH), 1.86-1.81 (m, 1H; –CH_2-C*H*), 1.34-1.18 (m, 32H; 16(CH_2)), 0.87 (t, *J* = 7.0 Hz, 3H; (CH_3)), 0.86 (t, *J* = 7.0 Hz, 3H; (CH_3)); **^{13}C NMR** (125 MHz, chloroform-*d*) δ 159.46 (2 C(6)), 143.45 (2 C(2)), 126.08 (2 C(3)), 121.92 (2 C(5)), 115.86 (2 C(4)), 48.76, 36.37, 32.08, 32.06, 31.80 (2C), 30.18 (2C), 29.80 (2C), 29.74, 29.70, 29.50, 29.46, 26.60 (2C), 22.84, 22.83, 14.27 (2C); **IR** (ν_{max}) 3146, 2925, 2854, 1671, 1633, 1585, 1528, 1501, 1458, 1377, 1331, 1264, 1219, 1167, 1119, 1088, 1061 cm^{-1}; **HRMS** (ESI) calcd for $C_{30}H_{44}Br_2NO_4$ 642.1617, found 642.1598 (M + H)$^+$.

N-(2-octyldodecyl)-5,5'-bis(tributylstannyl)-2,2'-bifuran-3,3'-dicarboximide (6)

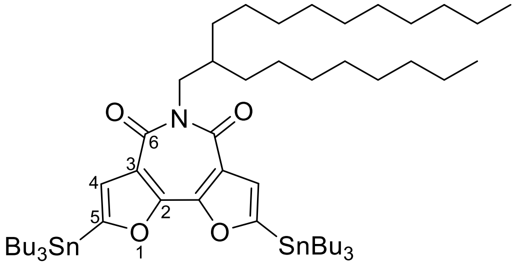

A solution of LDA (0.42 mL, 2.0 M in hexane, 0.84 mmol) was added dropwise to a solution of *N*-(2-octyldodecyl)-2,2'-bifuran-3,3'-dicarboximide **(BFI-OD)** (185 mg, 0.38 mmol) in dry THF (15 mL) at -85 °C under N_2 and stirred for 1 h. Bu_3SnCl (0.23 mL, 0.84 mmol) was added dropwise, and the reaction mixture was allowed to reach room temperature and stirred for 2 h. The mixture was quenched with water, extracted with CH_2Cl_2 (2 × 40 mL), dried (Na_2SO_4), filtered, and evaporated. The residue obtained was purified by flash column chromatography on silica gel basified with trimethylamine using hexane as eluent to give **6** as a colorless oil (331 mg, 81%). **^{1}H NMR** (400 MHz, chloroform-*d*) δ 7.25 (s, 2H; H–C(4)), 4.25 (d, *J* = 7.1, 2H; –CH_2-CH), 1.93-1.86 (m, 1H; –CH_2-C*H*), 1.64-1.56 (m, 12H; 6(CH_2) 1.42-1.13 (m, 56H; 28(CH_2)), 0.91 (t, *J* = 7.0 Hz, 18H; (CH_3)), 0.87 (t, *J* = 7.0 Hz, 3H; (CH_3)), 0.86 (t, *J* = 7.0 Hz, 3H; (CH_3)); **^{13}C NMR** (125 MHz, chloroform-*d*) δ 164.87 (2C), 161.55 (2C), 148.06 (2C), 125.30 (2C), 119.45 (2C), 48.45, 36.62, 32.08, 32.06, 31.93 (2C), 30.26 (2C), 29.81, 29.80 (2C), 29.73, 29.50, 29.46, 29.01 (6C),

27. 30 (6C), 26.77 (2C), 22.84, 22.82, 14.27 (2C), 13.79 (6C), 10.62 (6C); **IR** (ν_{max}) 3132, 2957, 2625, 2871, 2854, 1665, 1633, 1580, 1520, 1490, 1446, 1377, 1340, 1295, 1248, 1236, 1189, 1152, 1133, 1096, 1065, 1027 cm^{-1}; **HRMS** (ESI) calcd for $C_{54}H_{97}NO_4Sn_2$ 1062.5534, found 1062.5573 $(M)^+$.

Poly- *N*-(2-octyldodecyl)-2,2'-bifuran-3,3'-dicarboximide (poly(BFI-OD))

$Pd(PPh_3)_4$ (29 mg, 5 mol%) was added to a solution of *N*-(2-octyldodecyl)-5,5'-dibromo-2,2'-bifuran-3,3'-dicarboximide **(4c)** (321 mg, 0.50 mmol) and *N*-(2-octyldodecyl)-5,5'-bis(tributylstannyl)-2,2'-bifuran-3,3'-dicarboximide **(6)** (531 mg, 0.50 mmol) in dry and degassed dimethylformamide (DMF; 10 mL), and the reaction mixture was stirred at 90 °C for 24 h under nitrogen. The reaction mixture was then allowed to cool to room temperature and poured into 200 mL of methanol, and the precipitate was collected by filtration to give 530 mg of orange solid. The crude material was transferred to a Soxhlet extractor and extracted for 48 h with methanol and a further 24 h with acetone, and then recovered by extraction with hexane. The hexane solution was concentrated, and the polymer precipitated with 150 mL of methanol, filtered, and dried to give **poly(BFI-OD)** as an orange solid (350 mg 36%). **^{1}H NMR** (500 MHz, chloroform-*d*) δ 7.5 (bs, 2H), 4.20 (bs, 2H), 1.80 (bs, 1H), 1.64-1.00 (m, 32H), 0.75 (bs, 6H); **^{13}C NMR** (125 MHz, chloroform-*d*) δ 159.19, 144.98, 141.82, 122.94, 112.04, 48.82, 36.52, 32.10, 30.31, 30.16, 29.94, 29.86, 29.82, 29.76, 29.58, 29.55, 26.77, 22.87, 14.29, 14.26; **IR** (ν_{max}) 3149, 2925, 2854, 1667, 1634, 1510, 1463, 1445, 1377, 1311, 1259, 1219, 1171, 1115, 1092, 1043 cm^{-1}; **GPC** (30 °C) Molecular weight Mn = 12.5 kDa, Mw = 26.6 kDa, PDI = 2.1.

S3 Supporting Figures

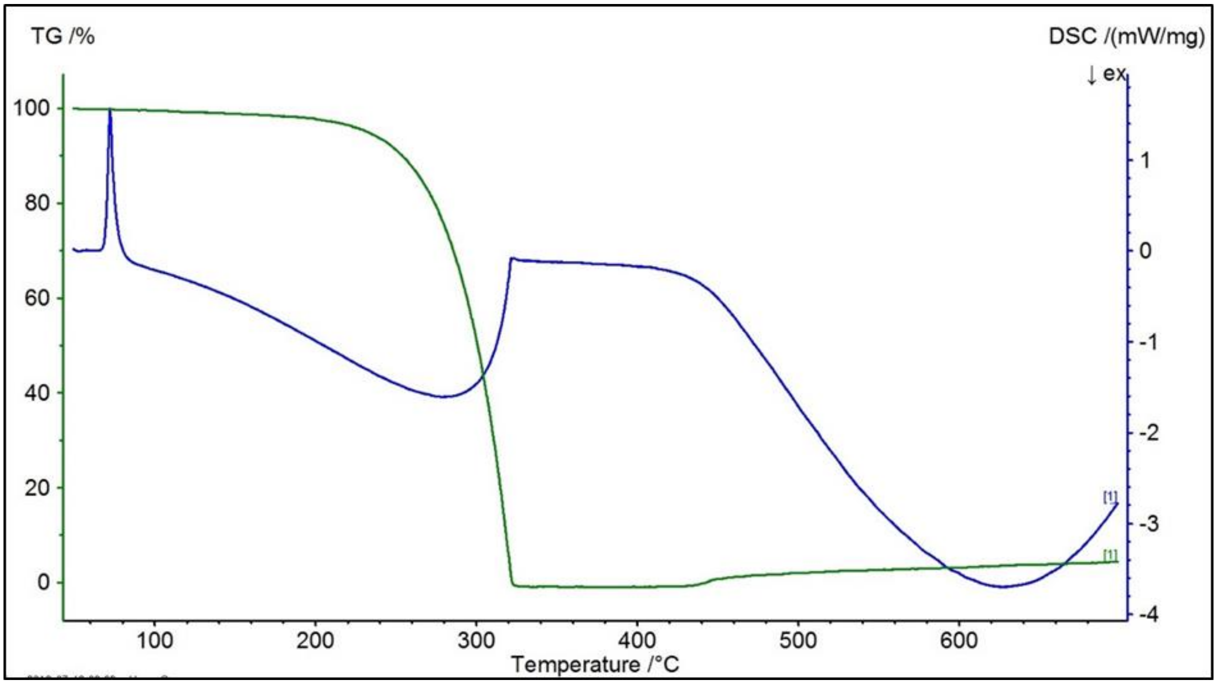

Figure S1. Thermogravimetric analysis (TGA), and differential scanning calorimetry (DSC) curves of **BFI-H** recorded at a heating rate 5 °C min^{-1} under a nitrogen atmosphere.

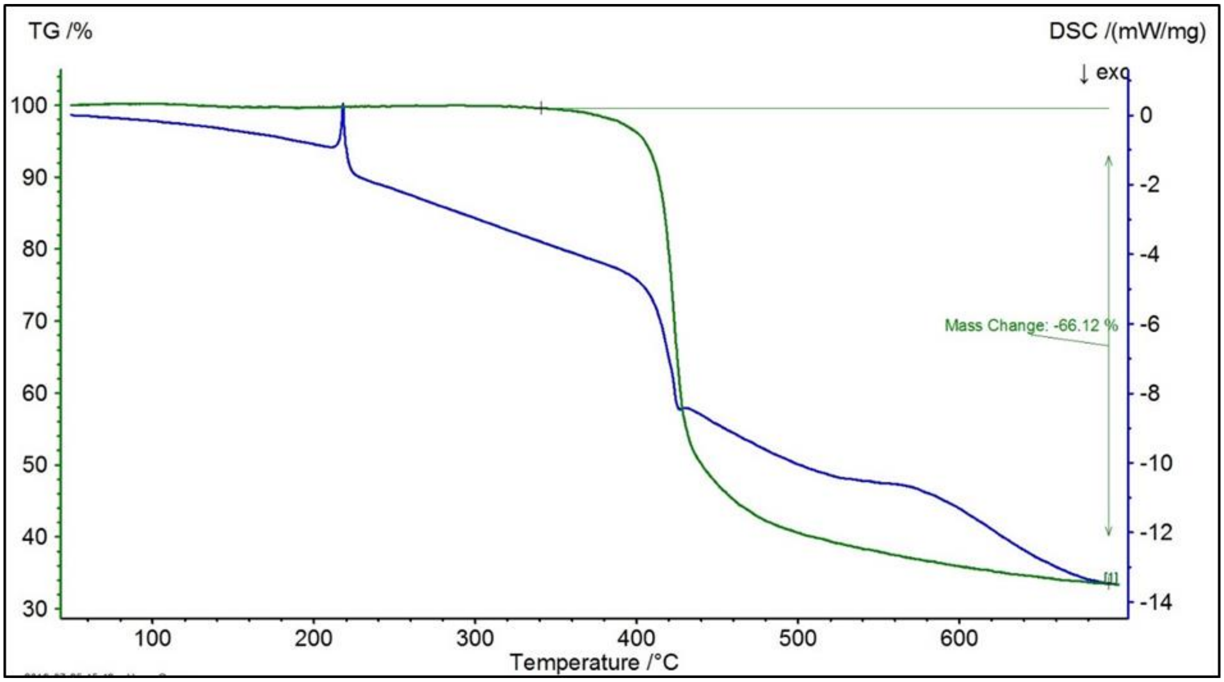

Figure S2. Thermogravimetric analysis (TGA), and differential scanning calorimetry (DSC) curves of **2BFI-H** recorded at a heating rate 5 °C min^{-1} under a nitrogen atmosphere.

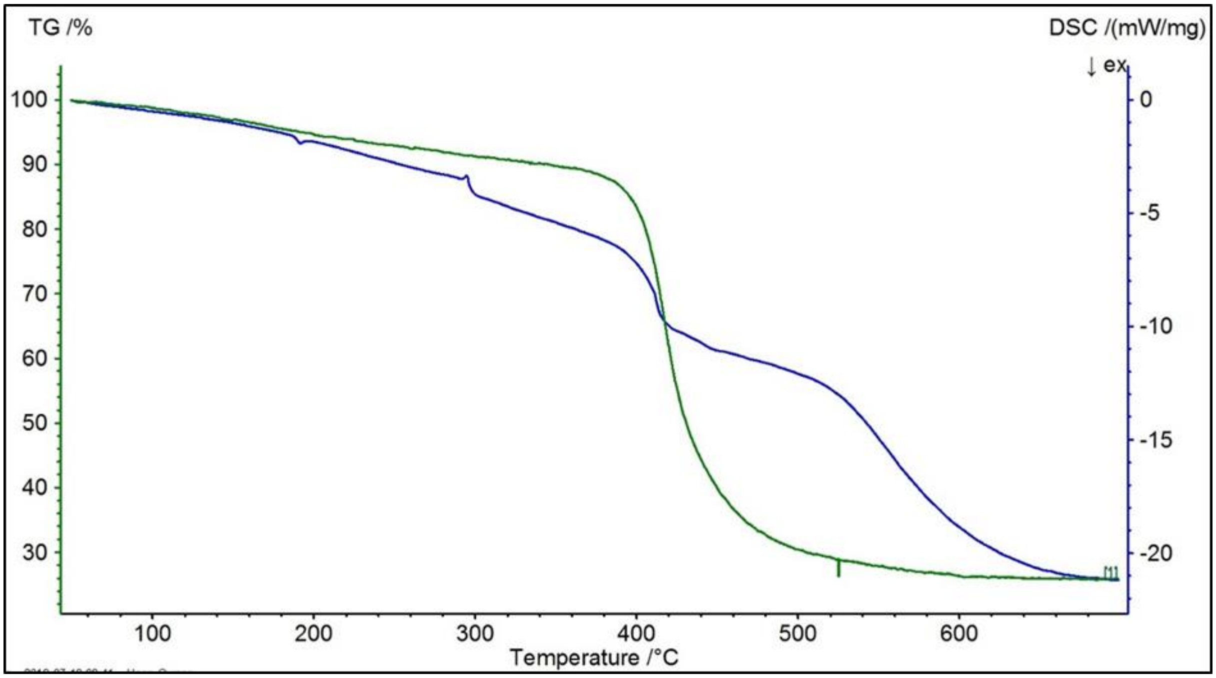

Figure S3. Thermogravimetric analysis (TGA), and differential scanning calorimetry (DSC) curves of **3BFI-H** recorded at a heating rate 5 °C min^{-1} under a nitrogen atmosphere.

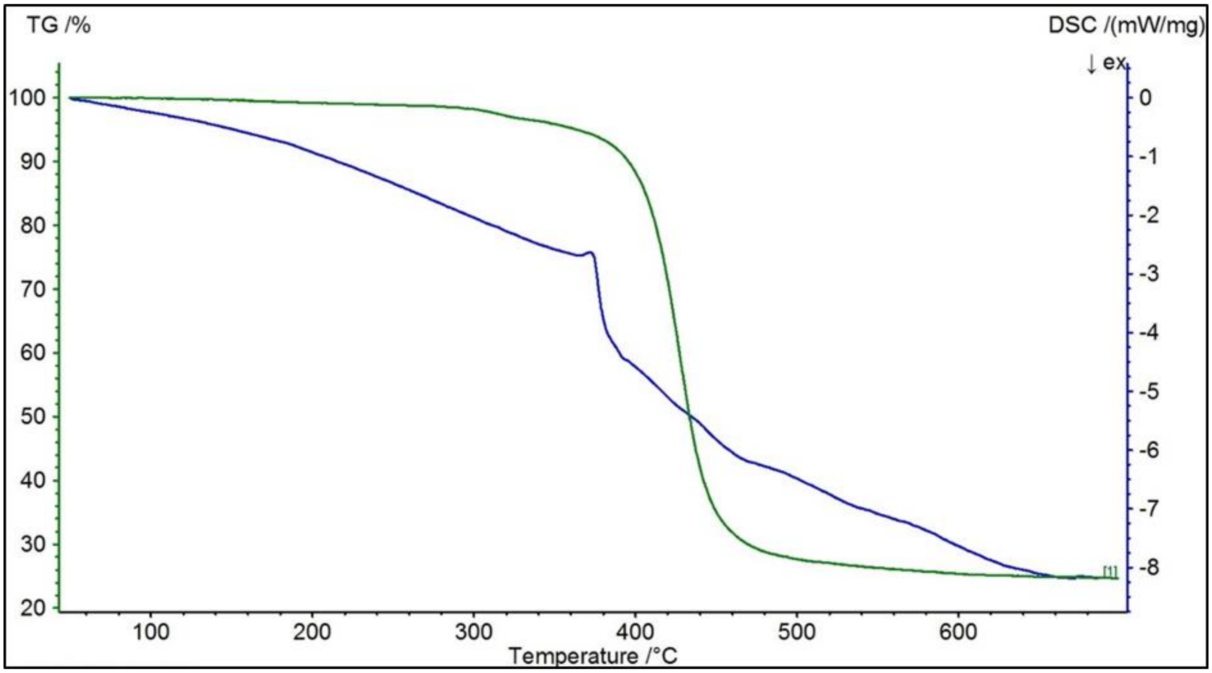

Figure S4. Thermogravimetric analysis (TGA), and differential scanning calorimetry (DSC) curves of **poly(BFI-OD)** recorded at a heating rate 5 °C min^{-1} under a nitrogen atmosphere.

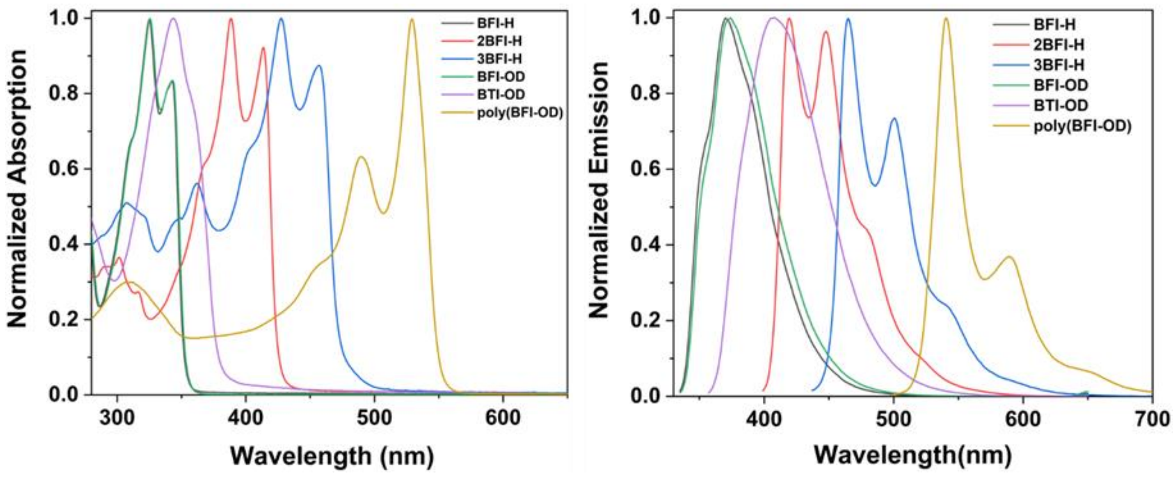

Figure S5. (*left*) Normalized absorbance spectra and (*right*) Normalized emission spectra measured at room temperature in hexane.

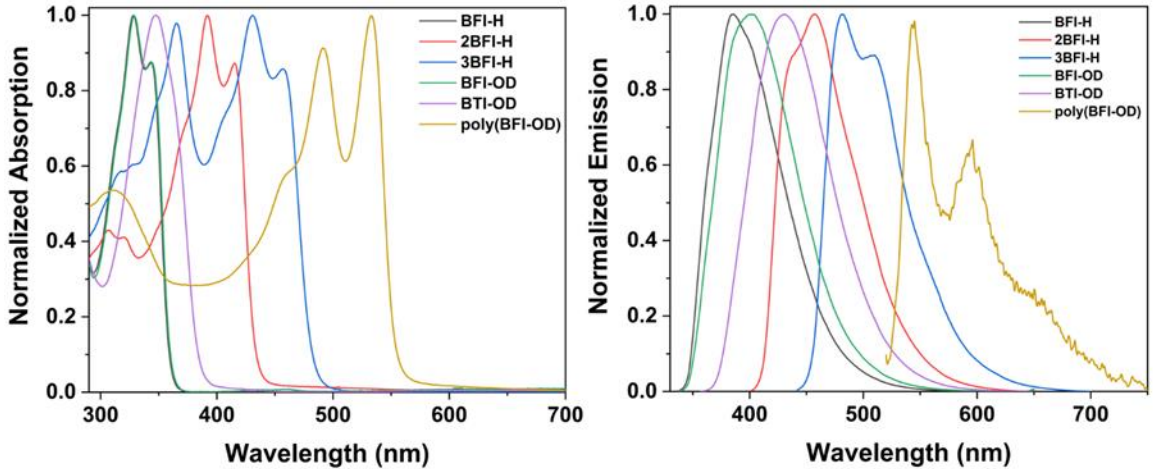

Figure S6. (*left*) Normalized absorbance spectra and (*right*) Normalized emission spectra measured at room temperature in CH_3CN.

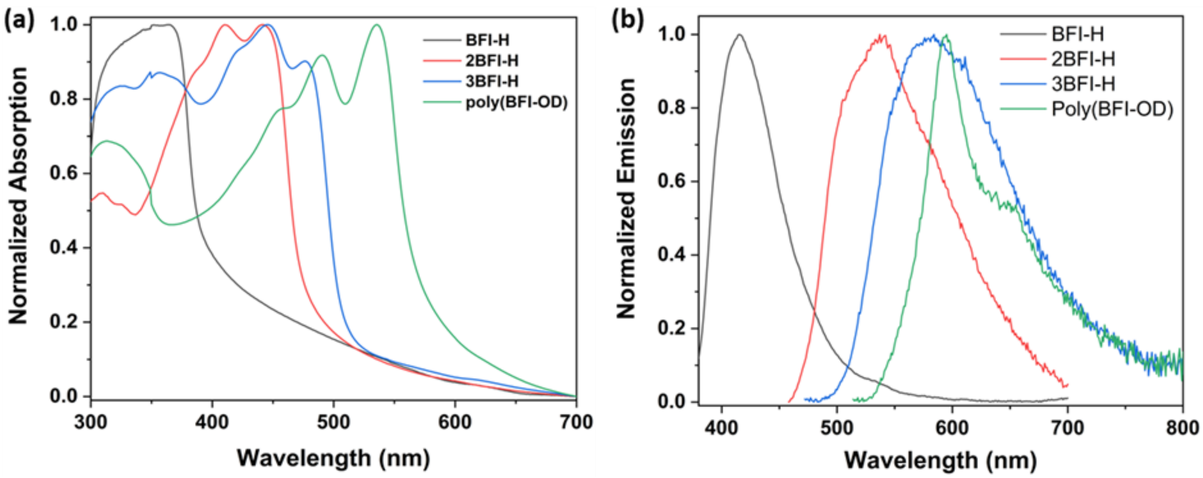

Figure S7. Thin film normalized absorbance and emission spectra measured at room temperature.

Table S1. Photophysical data measured in hexane and CH_3CN

Compounds	λ_{abs}[a] (nm)	λ_{em}[a] (nm)	Stokes shift[a] (eV)	Φ[a]	λ_{abs}[b] (nm)	λ_{em}[b] (nm)	Stokes shift[b] (eV)	Φ[b]	λ_{abs}[c] (nm)	λ_{em}[c] (nm)	Stokes shift[c] (eV)	$E_{g\ (opt)}$[d] (eV)
BFI-H	325	370	0.46	0.56	328	386	0.57	0.75	363	415	0.43	3.10
2BFI-H	389	419	0.16	0.76	392	458	0.46	0.60	410	537	0.72	2.59
3BFI-H	427	465	0.24	0.51	431	481	0.30	0.58	446	584	0.66	2.43
BFI-OD	326	374	0.49	0.31	329	401	0.67	0.65	-	-	-	-
BTI-OD	344	408	0.57	0.62	348	430	0.68	0.71	-	-	-	-
poly(BFI-OD)	529	540	0.05	0.58	533	545	0.05	-	536	595	0.23	2.16

[a] Measured in hexane, [b] Measured in CH_3CN, [c] Measured as a thin by drop casting with $CHCl_3$ solution, [d] $E_{gap} = 1242/\lambda_{onset}$.

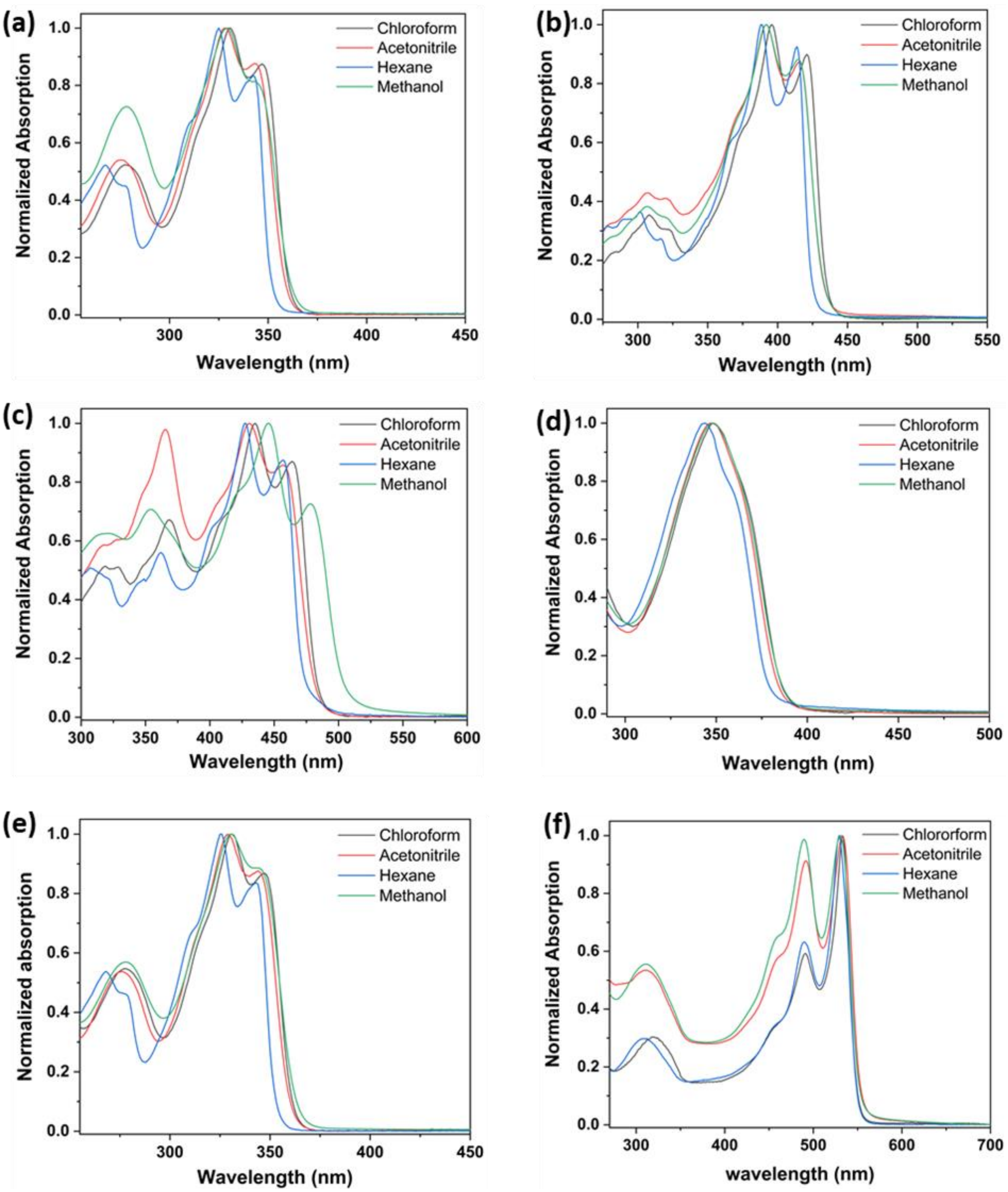

Figure S8. Normalized absorbance spectra of (a) **BFI-H**, (b) **2BFI-H**, (c) **3BFI-H**, (d) **BTI-OD**, (e) **BFI-OD**, and (f) **poly(BFI-OD** room temperature in $CHCl_3$, CH_3CN, Hexane and MeOH.

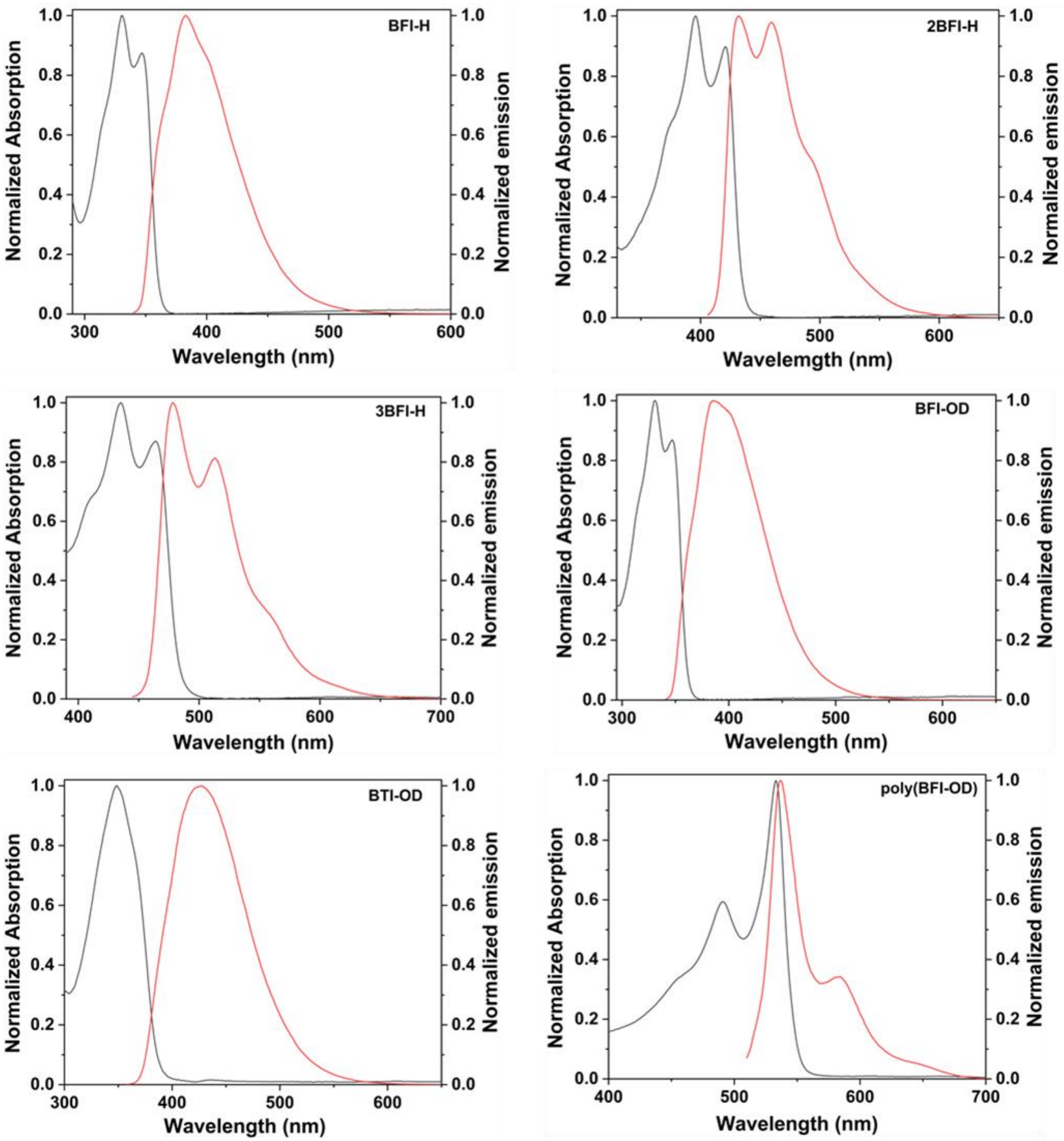

Figure S9. Normalized absorbance spectra and emission spectra measured at room temperature in $CHCl_3$.

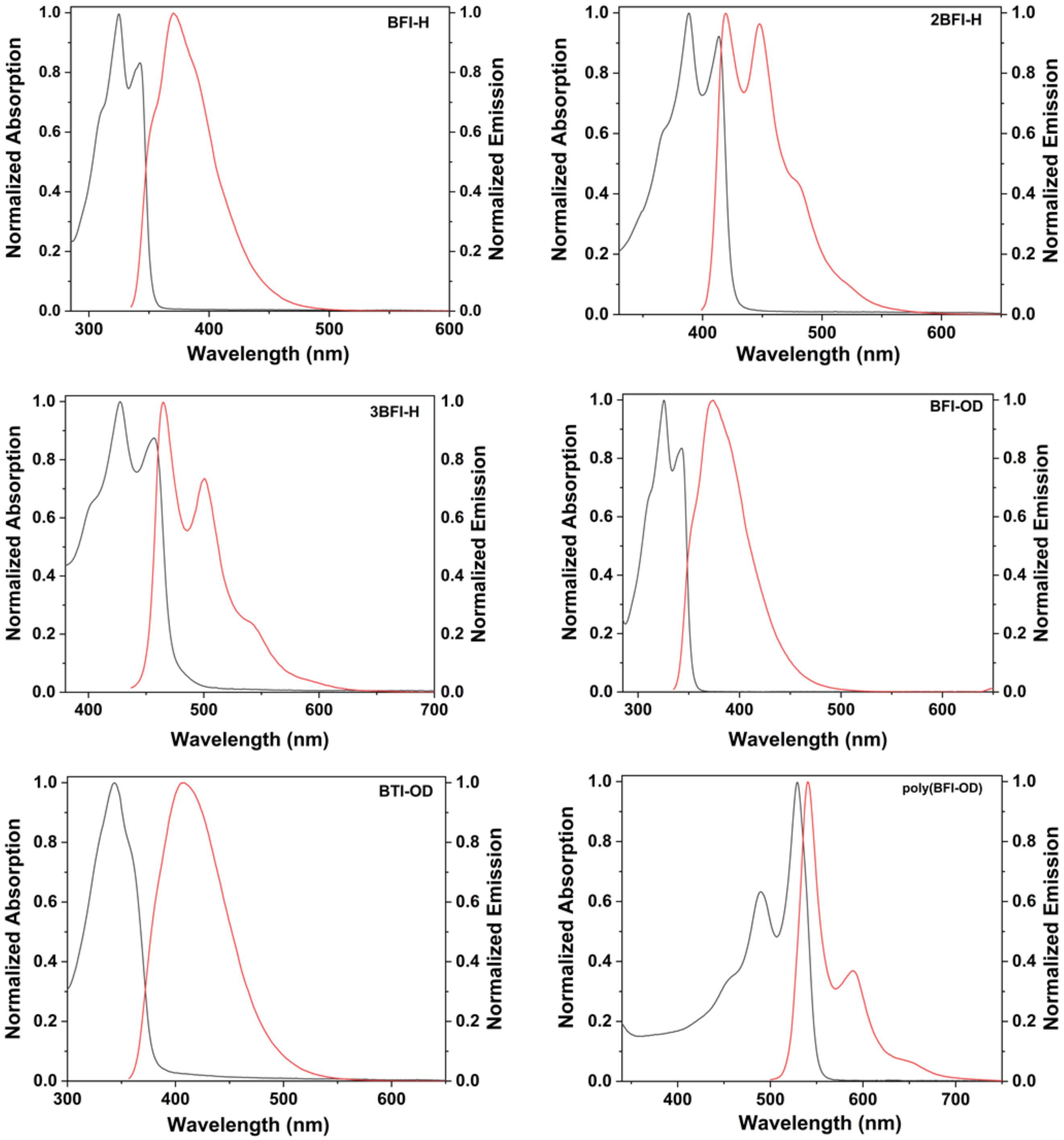

Figure S10. Normalized absorbance spectra and emission spectra measured at room temperature in hexane.

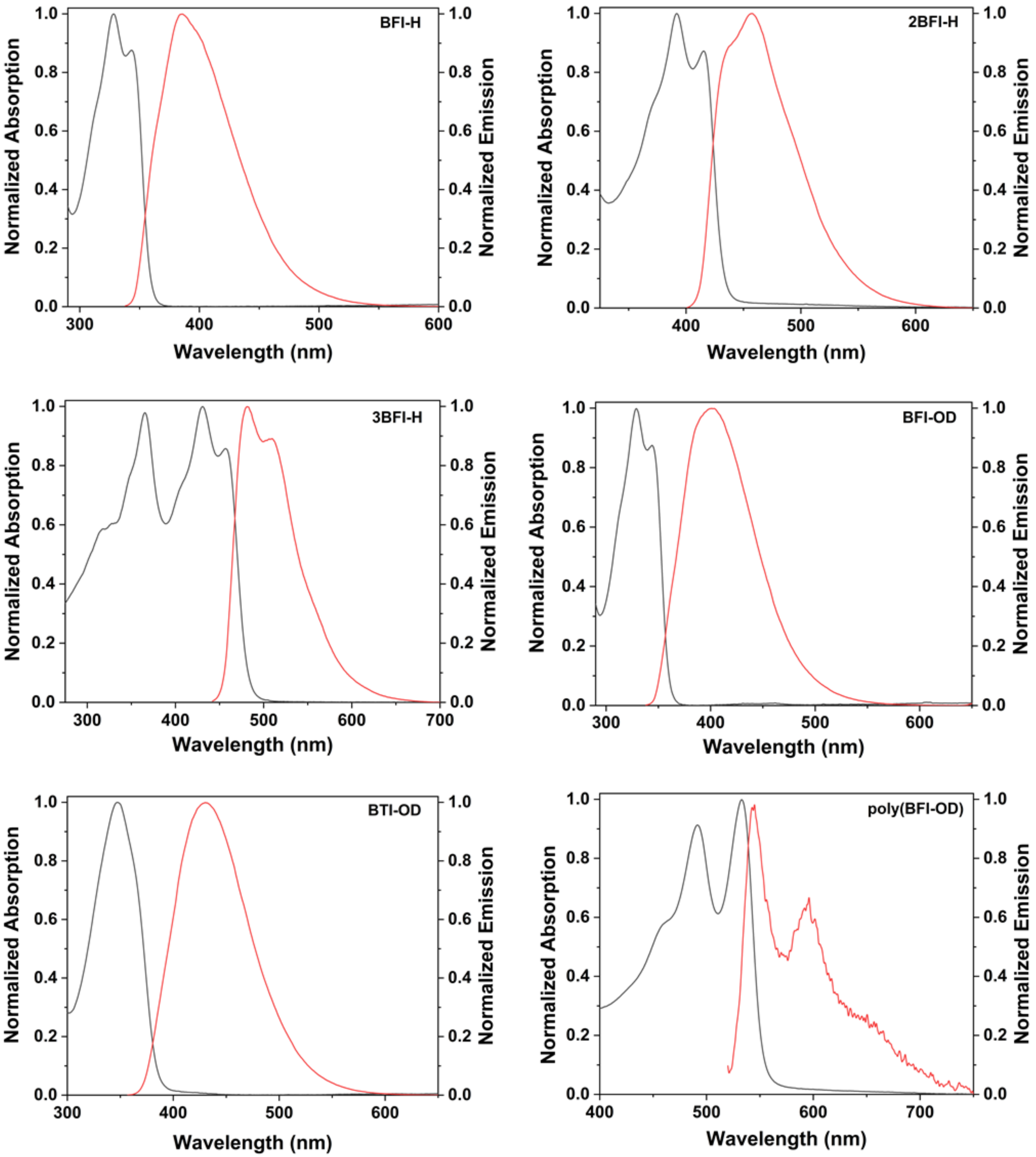

Figure S11. Normalized absorbance spectra and emission spectra measured at room temperature in CH_3CN.

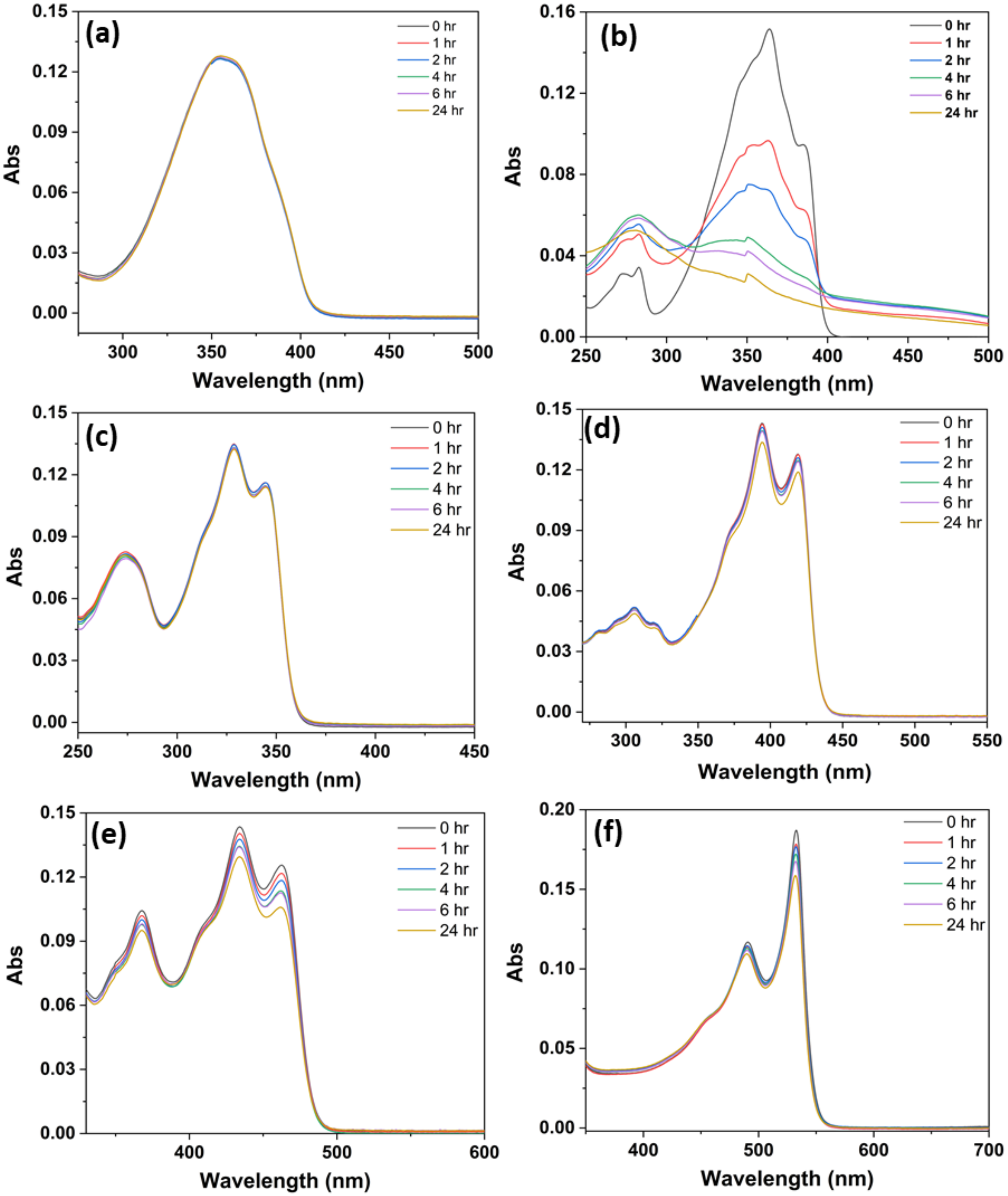

Figure S12. Photostability at normal light in 1,4-dioxane at room temperature a) *ter*-thiophene (**3T**); b) *tetra*-furan (**4F**); c) **BFI-H**; d) **2BFI-H**; e) **3BFI-H**; f) **poly(BFI-OD)**.

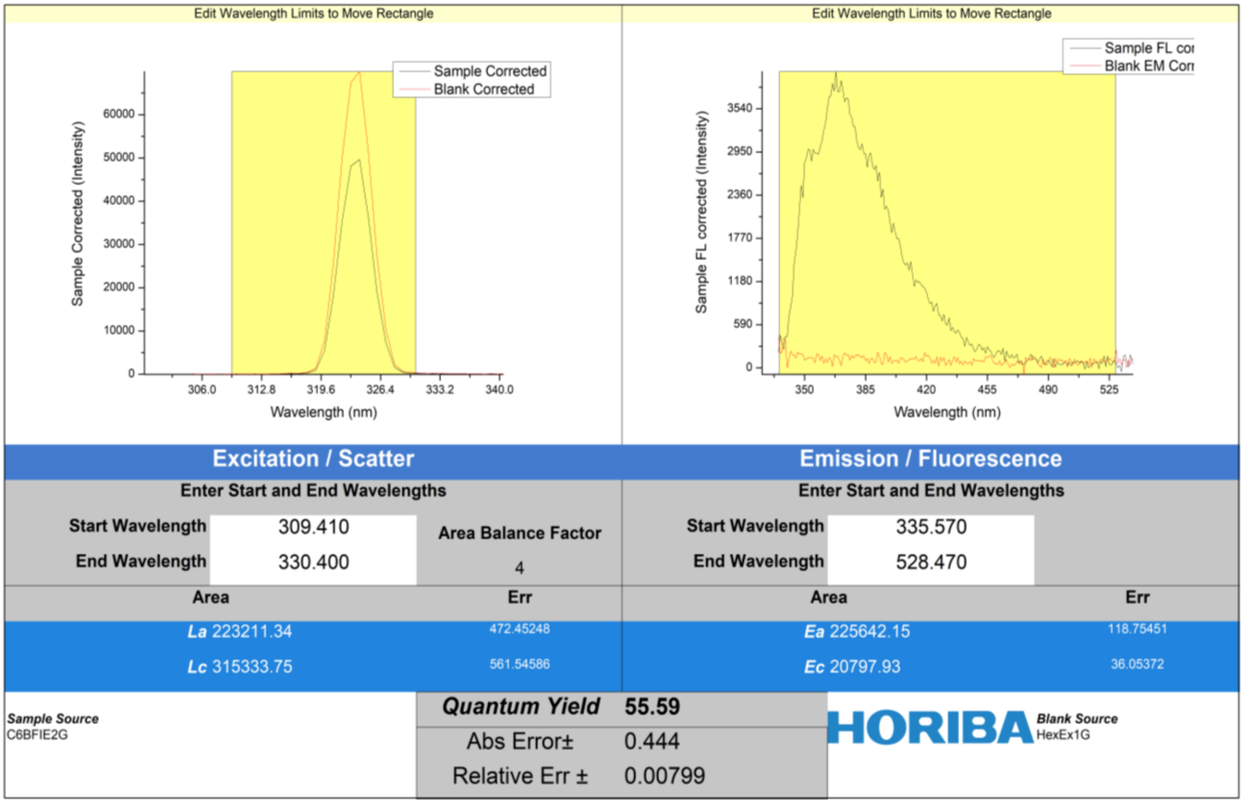

Excitation / Scatter

Enter Start and End Wavelengths

Start Wavelength 309.410

End Wavelength 330.400

Area Balance Factor 4

Area	Err
La 223211.34	472.45248
Lc 315333.75	561.54586

Emission / Fluorescence

Enter Start and End Wavelengths

Start Wavelength 335.570

End Wavelength 528.470

Area	Err
Ea 225642.15	118.75451
Ec 20797.93	36.05372

Sample Source
C6BFIE2G

Quantum Yield	55.59
Abs Error±	0.444
Relative Err ±	0.00799

Blank Source
HexEx1G

Figure S13. Quantum yield of **BFI-H** measured in the hexane at room temperature.

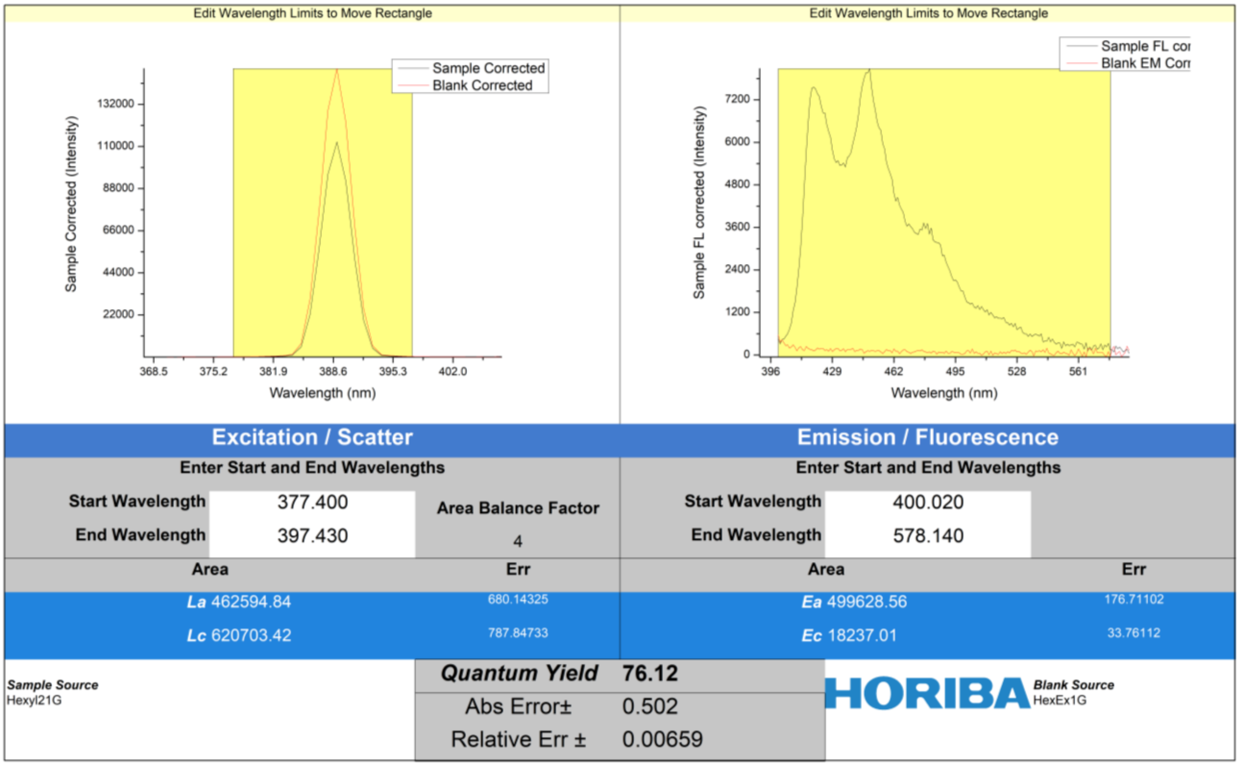

Excitation / Scatter

Enter Start and End Wavelengths

Start Wavelength 377.400

End Wavelength 397.430

Area Balance Factor 4

Area	Err
La 462594.84	680.14325
Lc 620703.42	787.84733

Emission / Fluorescence

Enter Start and End Wavelengths

Start Wavelength 400.020

End Wavelength 578.140

Area	Err
Ea 499628.56	176.71102
Ec 18237.01	33.76112

Sample Source
Hexyl21G

Quantum Yield	76.12
Abs Error±	0.502
Relative Err ±	0.00659

Blank Source
HexEx1G

Figure S14. Quantum yield of **2BFI-H** measured in the hexane at room temperature.

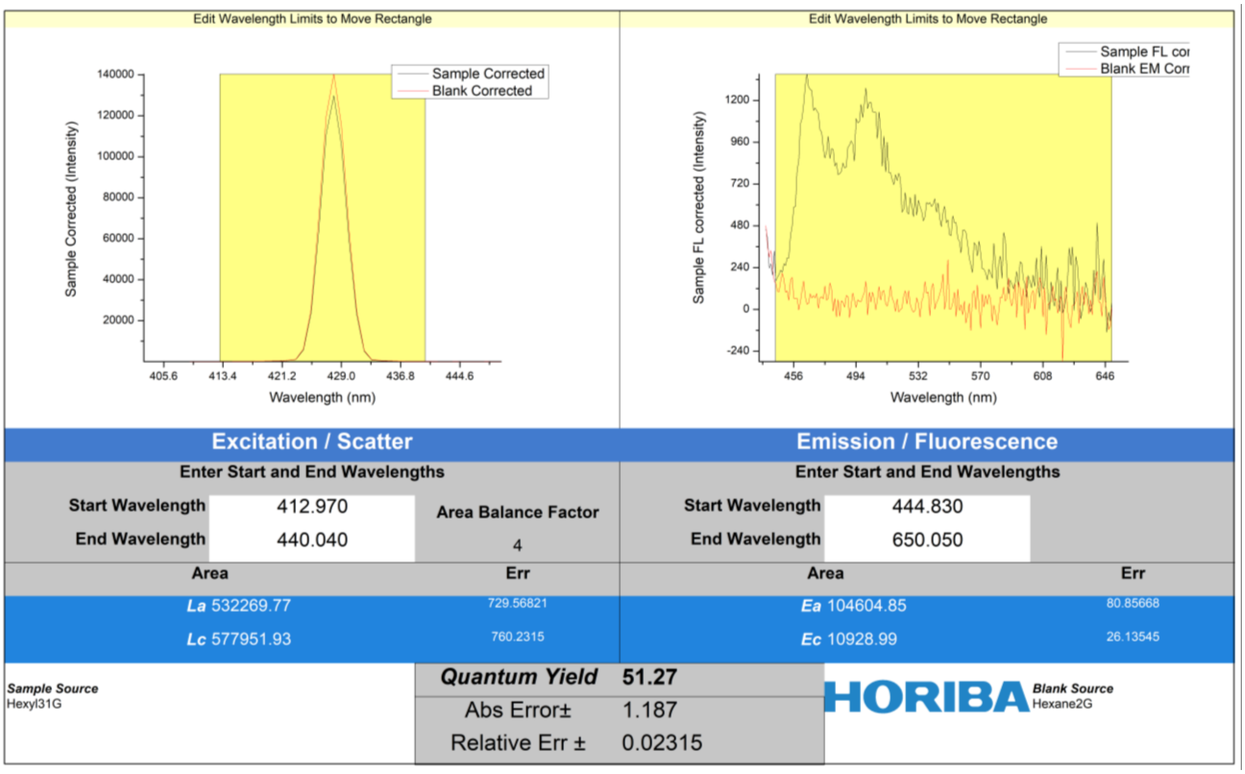

Excitation / Scatter

Enter Start and End Wavelengths

Start Wavelength	412.970	Area Balance Factor
End Wavelength	440.040	4
Area		Err
La 532269.77		729.56821
Lc 577951.93		760.2315

Emission / Fluorescence

Enter Start and End Wavelengths

Start Wavelength	444.830
End Wavelength	650.050
Area	Err
Ea 104604.85	80.85668
Ec 10928.99	26.13545

Sample Source
Hexyl31G

Quantum Yield	**51.27**
Abs Error±	1.187
Relative Err ±	0.02315

HORIBA ***Blank Source***
Hexane2G

Figure S15. Quantum yield of **3BFI-H** measured in the hexane at room temperature.

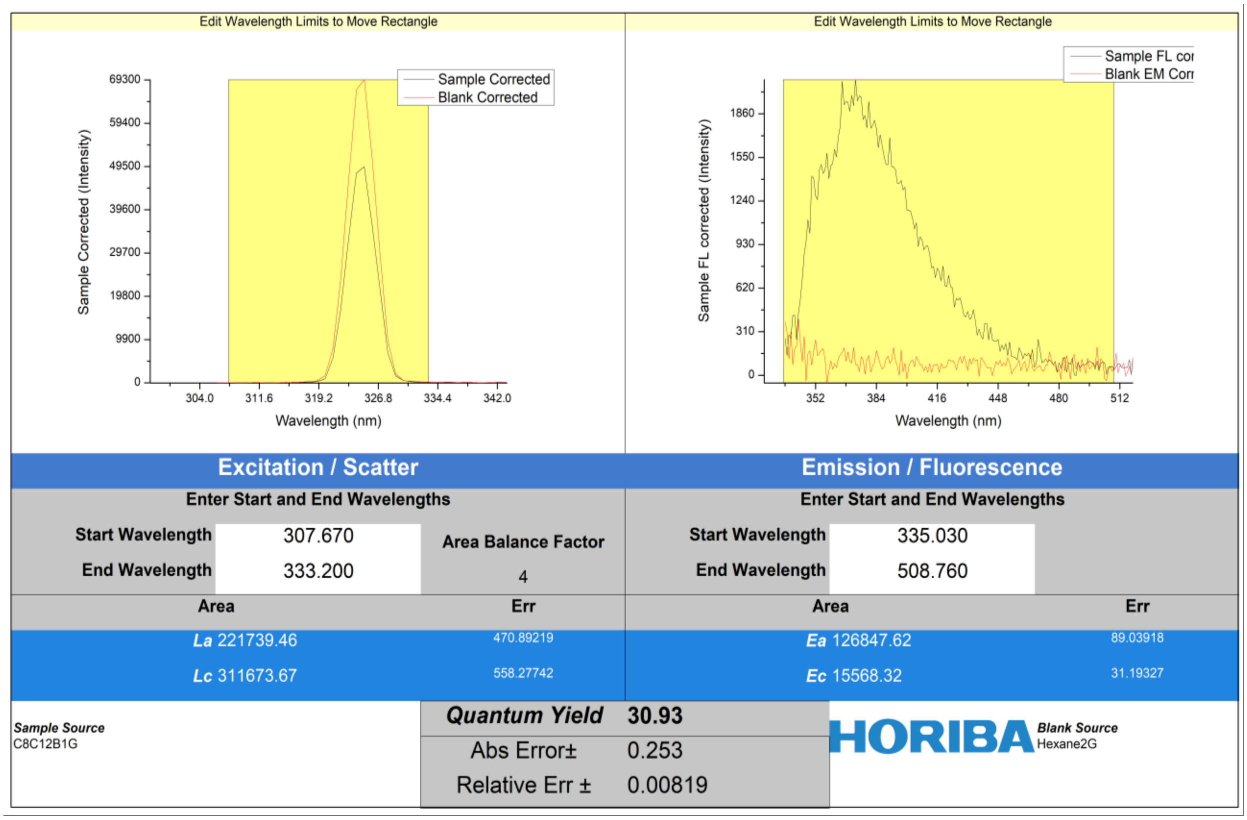

Excitation / Scatter

Enter Start and End Wavelengths

Start Wavelength	307.670	Area Balance Factor
End Wavelength	333.200	4
Area		Err
La 221739.46		470.89219
Lc 311673.67		558.27742

Emission / Fluorescence

Enter Start and End Wavelengths

Start Wavelength	335.030
End Wavelength	508.760
Area	Err
Ea 126847.62	89.03918
Ec 15568.32	31.19327

Sample Source
C8C12B1G

Quantum Yield	**30.93**
Abs Error±	0.253
Relative Err ±	0.00819

HORIBA ***Blank Source***
Hexane2G

Figure S16. Quantum yield of **BFI-OD** measured in the hexane at room temperature.

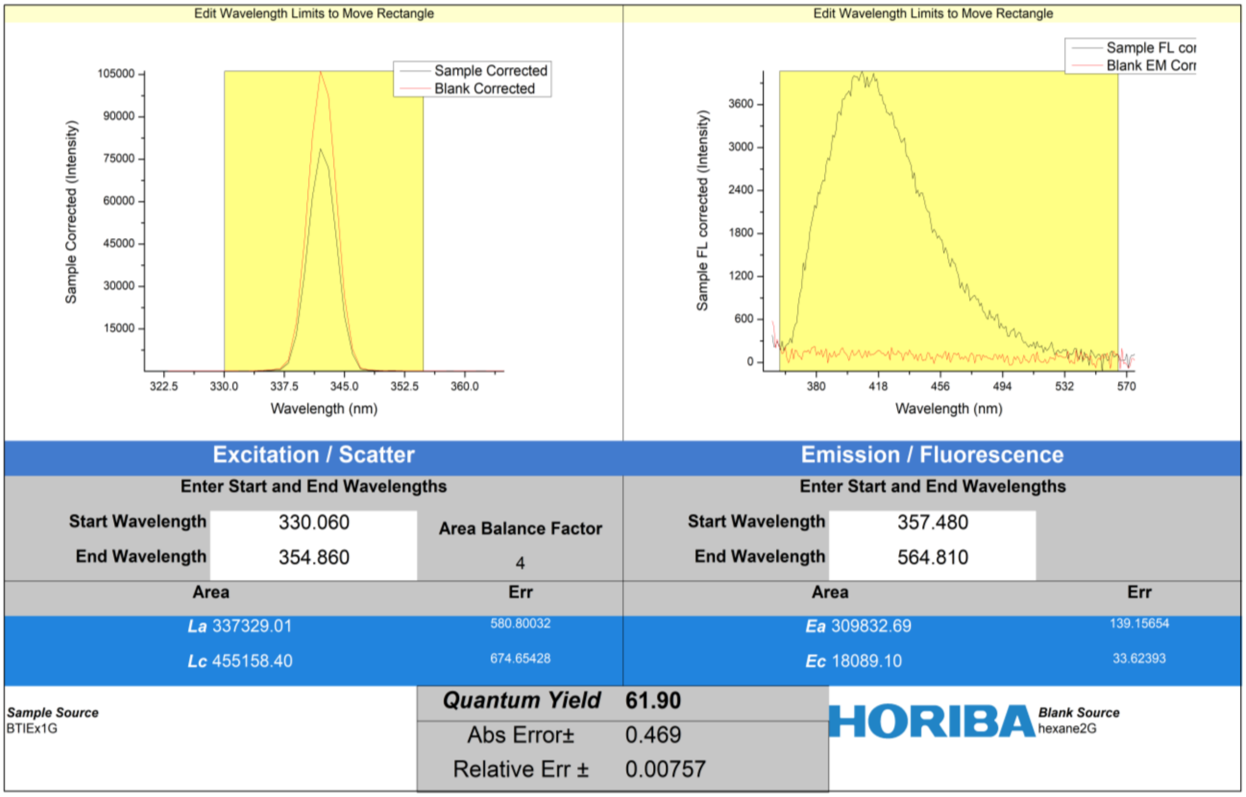

Excitation / Scatter

Enter Start and End Wavelengths

Start Wavelength	330.060	**Area Balance Factor**
End Wavelength	354.860	4

Area	Err
La 337329.01	580.80032
Lc 455158.40	674.65428

Emission / Fluorescence

Enter Start and End Wavelengths

Start Wavelength	357.480
End Wavelength	564.810

Area	Err
Ea 309832.69	139.15654
Ec 18089.10	33.62393

Sample Source
BTIEx1G

Quantum Yield	**61.90**
Abs Error±	0.469
Relative Err ±	0.00757

Blank Source
hexane2G

Figure S17. Quantum yield of **BTI-OD** measured in the hexane at room temperature.

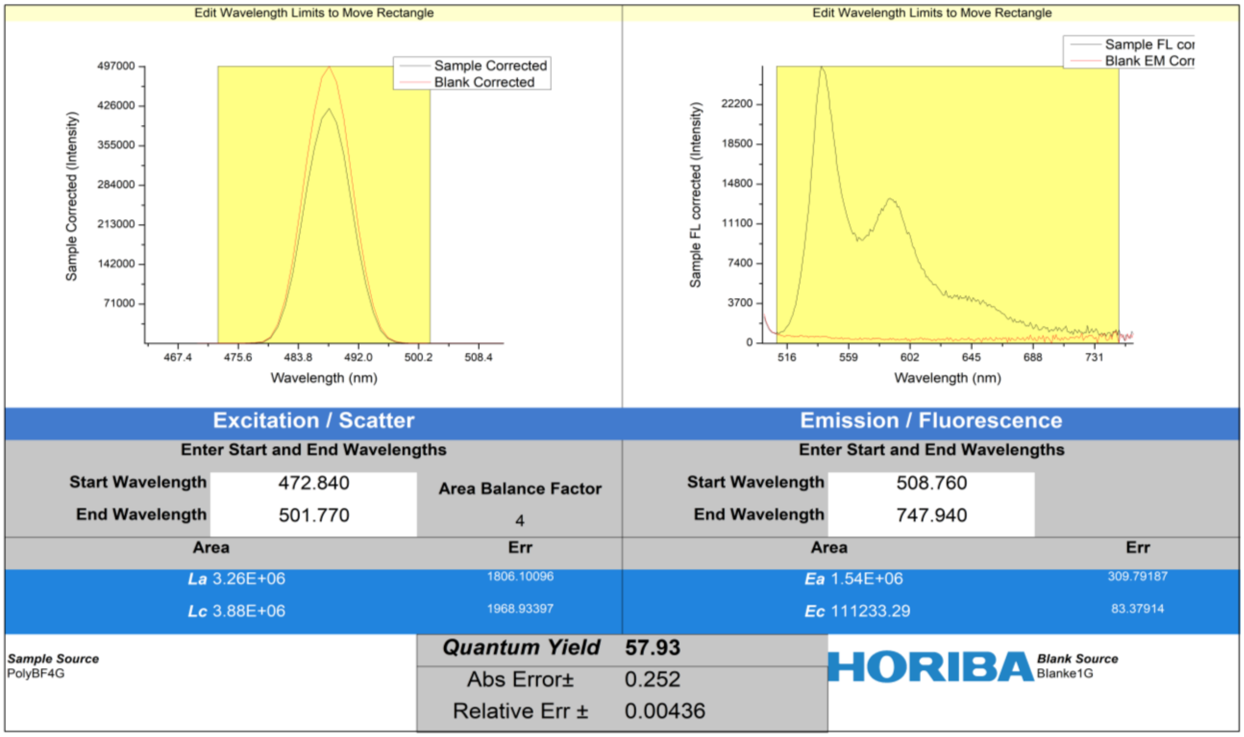

Excitation / Scatter

Enter Start and End Wavelengths

Start Wavelength	472.840	**Area Balance Factor**
End Wavelength	501.770	4

Area	Err
La 3.26E+06	1806.10096
Lc 3.88E+06	1968.93397

Emission / Fluorescence

Enter Start and End Wavelengths

Start Wavelength	508.760
End Wavelength	747.940

Area	Err
Ea 1.54E+06	309.79187
Ec 111233.29	83.37914

Sample Source
PolyBF4G

Quantum Yield	**57.93**
Abs Error±	0.252
Relative Err ±	0.00436

Blank Source
Blanke1G

Figure S18. Quantum yield of **poly(BFI-OD**) measured in the hexane at room temperature.

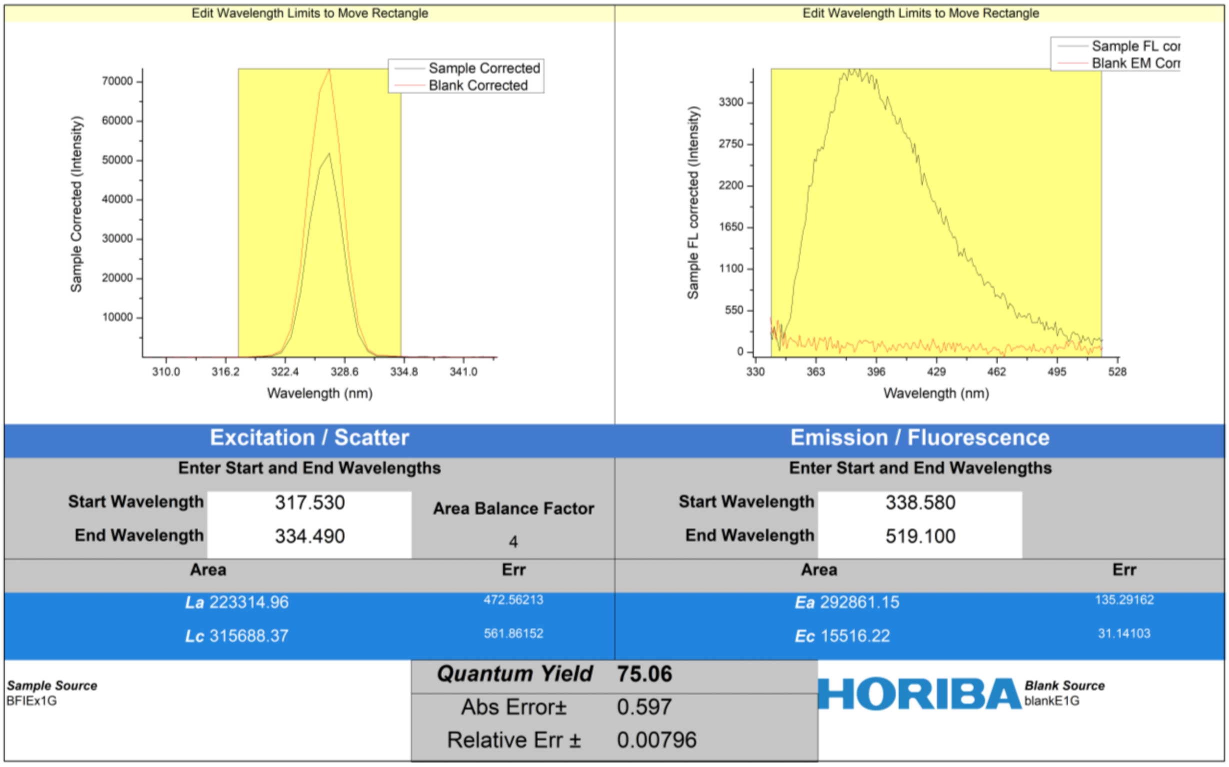

Excitation / Scatter

Enter Start and End Wavelengths

Start Wavelength 317.530

End Wavelength 334.490

Area Balance Factor 4

Area	Err
La 223314.96	472.56213
Lc 315688.37	561.86152

Emission / Fluorescence

Enter Start and End Wavelengths

Start Wavelength 338.580

End Wavelength 519.100

Area	Err
Ea 292861.15	135.29162
Ec 15516.22	31.14103

Sample Source
BFIEx1G

Quantum Yield	75.06
Abs Error±	0.597
Relative Err ±	0.00796

Blank Source
blankE1G

Figure S19. Quantum yield of **BFI-H** measured in the CH_3CN at room temperature.

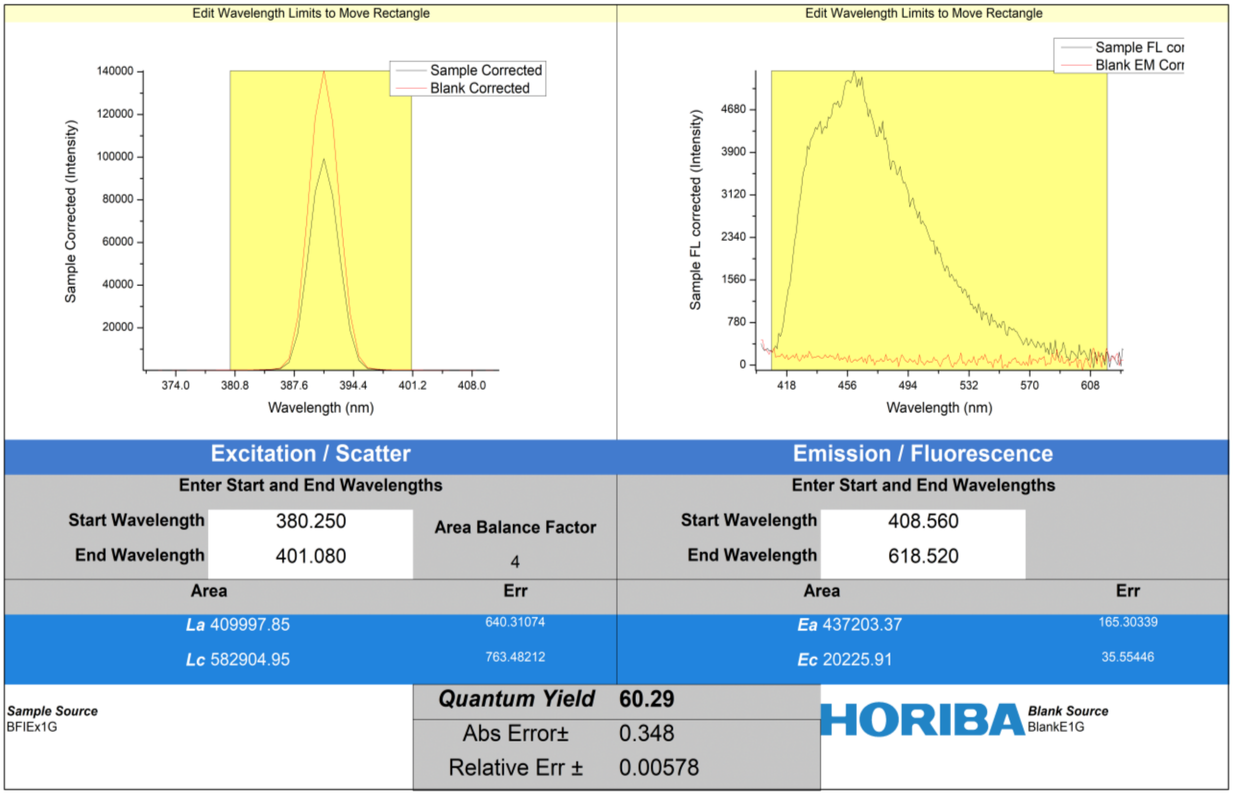

Excitation / Scatter

Enter Start and End Wavelengths

Start Wavelength 380.250

End Wavelength 401.080

Area Balance Factor 4

Area	Err
La 409997.85	640.31074
Lc 582904.95	763.48212

Emission / Fluorescence

Enter Start and End Wavelengths

Start Wavelength 408.560

End Wavelength 618.520

Area	Err
Ea 437203.37	165.30339
Ec 20225.91	35.55446

Sample Source
BFIEx1G

Quantum Yield	60.29
Abs Error±	0.348
Relative Err ±	0.00578

Blank Source
BlankE1G

Figure S20. Quantum yield of **2BFI-H** measured in the CH_3CN at room temperature.

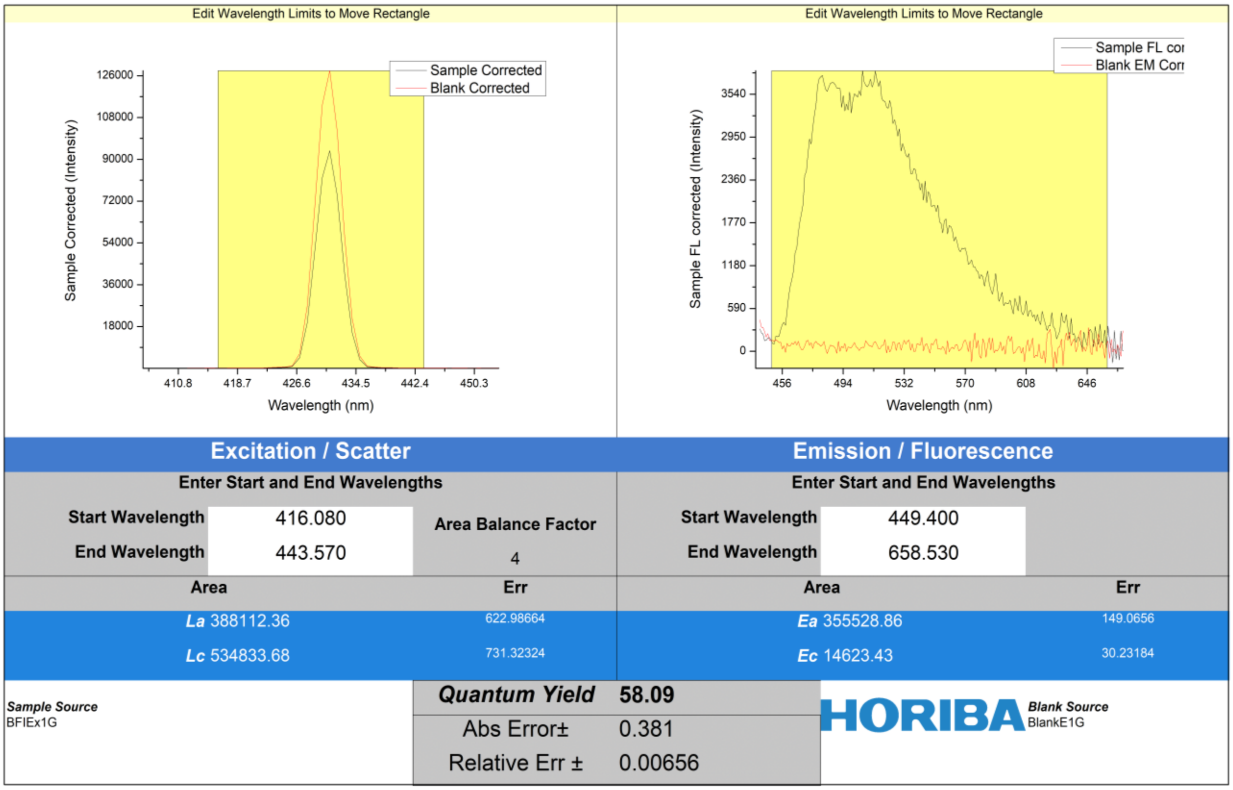

Excitation / Scatter

Enter Start and End Wavelengths

Start Wavelength 416.080

End Wavelength 443.570

Area Balance Factor 4

Area	Err
La 388112.36	622.98664
Lc 534833.68	731.32324

Emission / Fluorescence

Enter Start and End Wavelengths

Start Wavelength 449.400

End Wavelength 658.530

Area	Err
Ea 355528.86	149.0656
Ec 14623.43	30.23184

Sample Source
BFIEx1G

Quantum Yield	**58.09**
Abs Error±	0.381
Relative Err ±	0.00656

Blank Source
BlankE1G

Figure S21. Quantum yield of **2BFI-H** measured in the CH_3CN at room temperature.

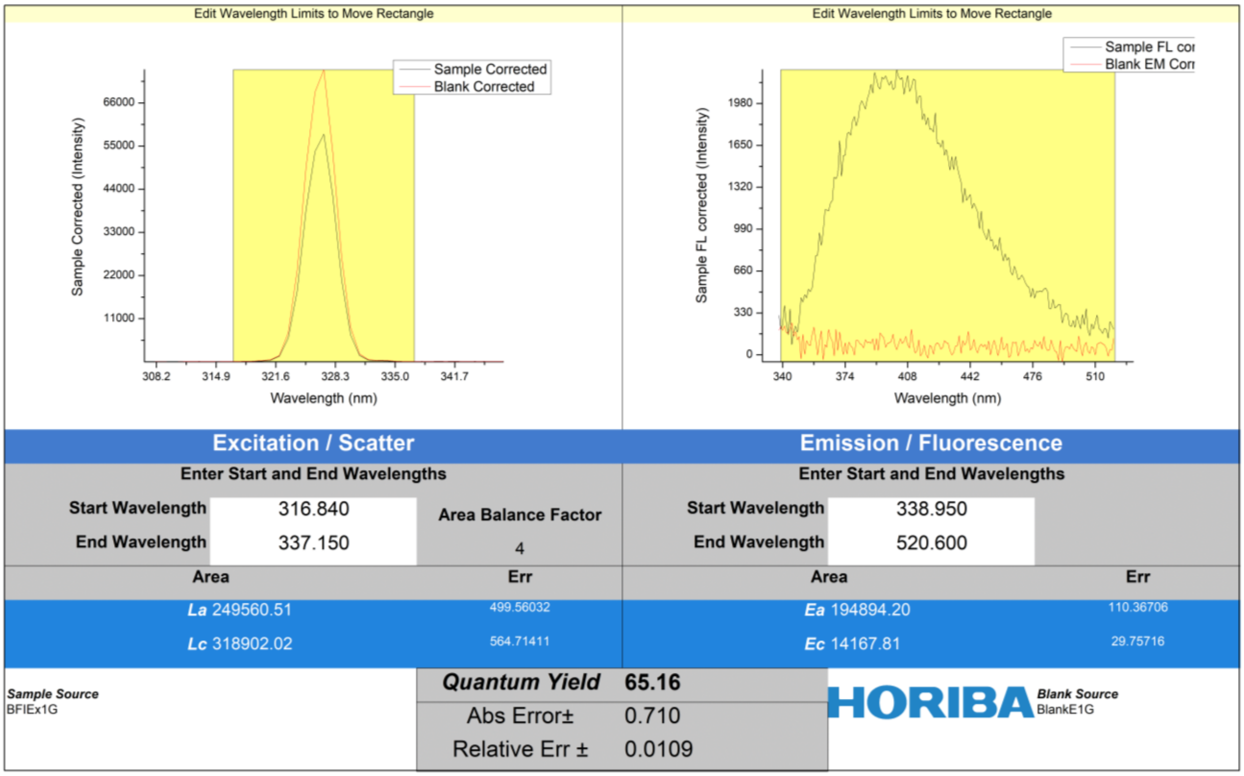

Excitation / Scatter

Enter Start and End Wavelengths

Start Wavelength 316.840

End Wavelength 337.150

Area Balance Factor 4

Area	Err
La 249560.51	499.56032
Lc 318902.02	564.71411

Emission / Fluorescence

Enter Start and End Wavelengths

Start Wavelength 338.950

End Wavelength 520.600

Area	Err
Ea 194894.20	110.36706
Ec 14167.81	29.75716

Sample Source
BFIEx1G

Quantum Yield	**65.16**
Abs Error±	0.710
Relative Err ±	0.0109

Blank Source
BlankE1G

Figure S22. Quantum yield of **BFI-OD** measured in the CH_3CN at room temperature.

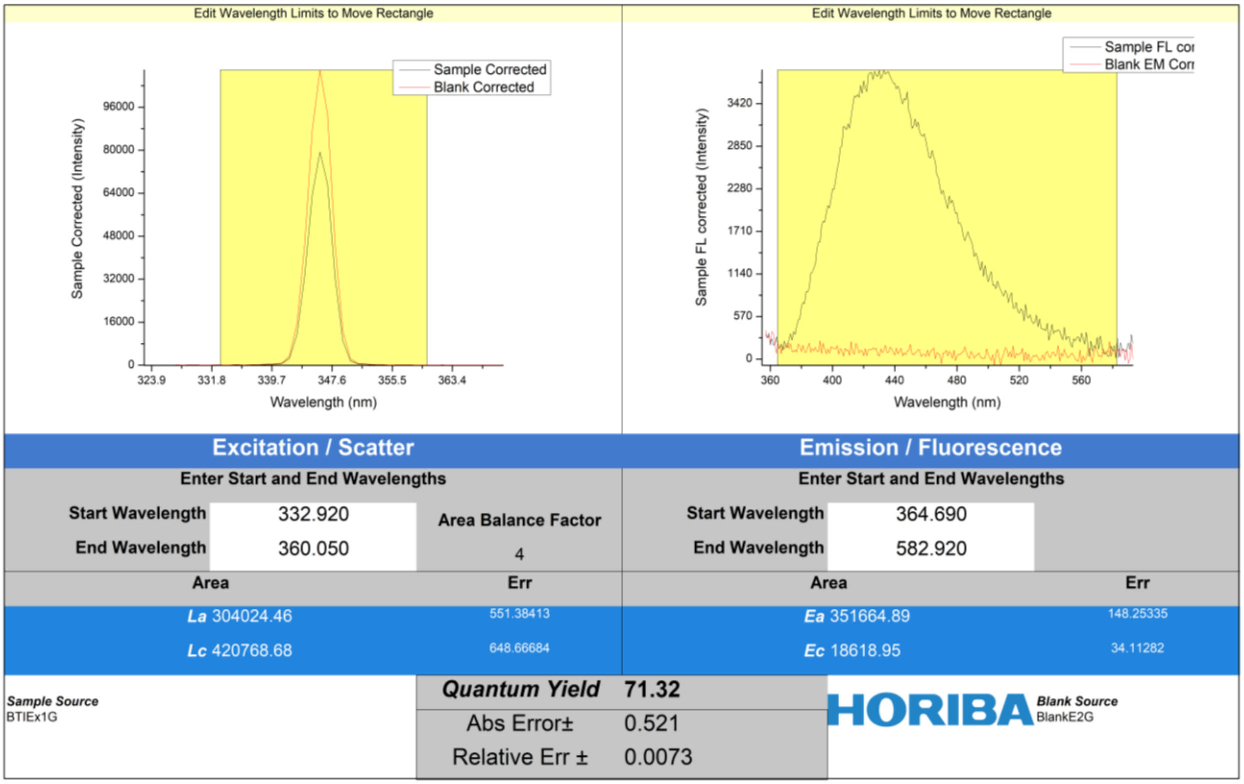

Excitation / Scatter

Enter Start and End Wavelengths

Start Wavelength 332.920
End Wavelength 360.050

Area Balance Factor 4

Area	Err
La 304024.46	551.38413
Lc 420768.68	648.66684

Emission / Fluorescence

Enter Start and End Wavelengths

Start Wavelength 364.690
End Wavelength 582.920

Area	Err
Ea 351664.89	148.25335
Ec 18618.95	34.11282

Sample Source
BTIEx1G

Quantum Yield	**71.32**
Abs Error±	0.521
Relative Err ±	0.0073

Blank Source
BlankE2G

Figure S23. Quantum yield of **BTI-OD** measured in the CH_3CN at room temperature.

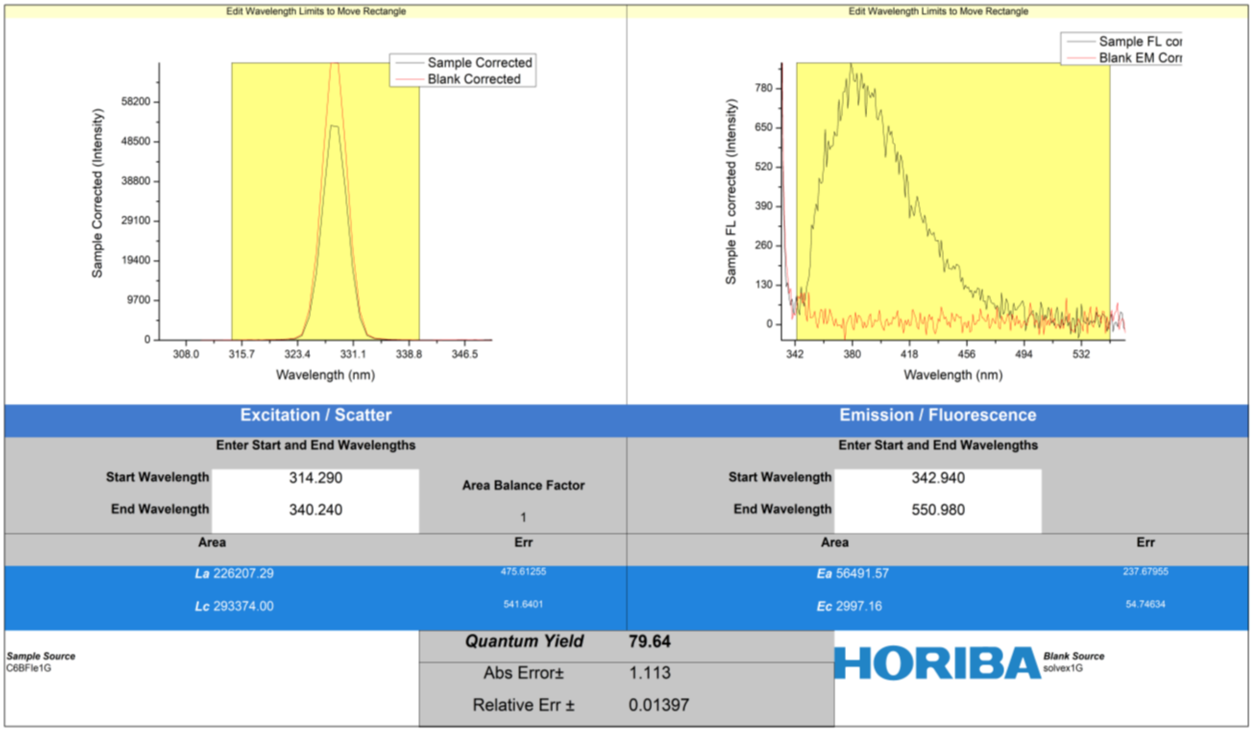

Excitation / Scatter

Enter Start and End Wavelengths

Start Wavelength 314.290
End Wavelength 340.240

Area Balance Factor 1

Area	Err
La 226207.29	475.61255
Lc 293374.00	541.6401

Emission / Fluorescence

Enter Start and End Wavelengths

Start Wavelength 342.940
End Wavelength 550.980

Area	Err
Ea 56491.57	237.67955
Ec 2997.16	54.74634

Sample Source
C6BFle1G

Quantum Yield	**79.64**
Abs Error±	1.113
Relative Err ±	0.01397

Blank Source
solvex1G

Figure S24. Quantum yield of **BFI-H** measured in the $CHCl_3$ at room temperature.

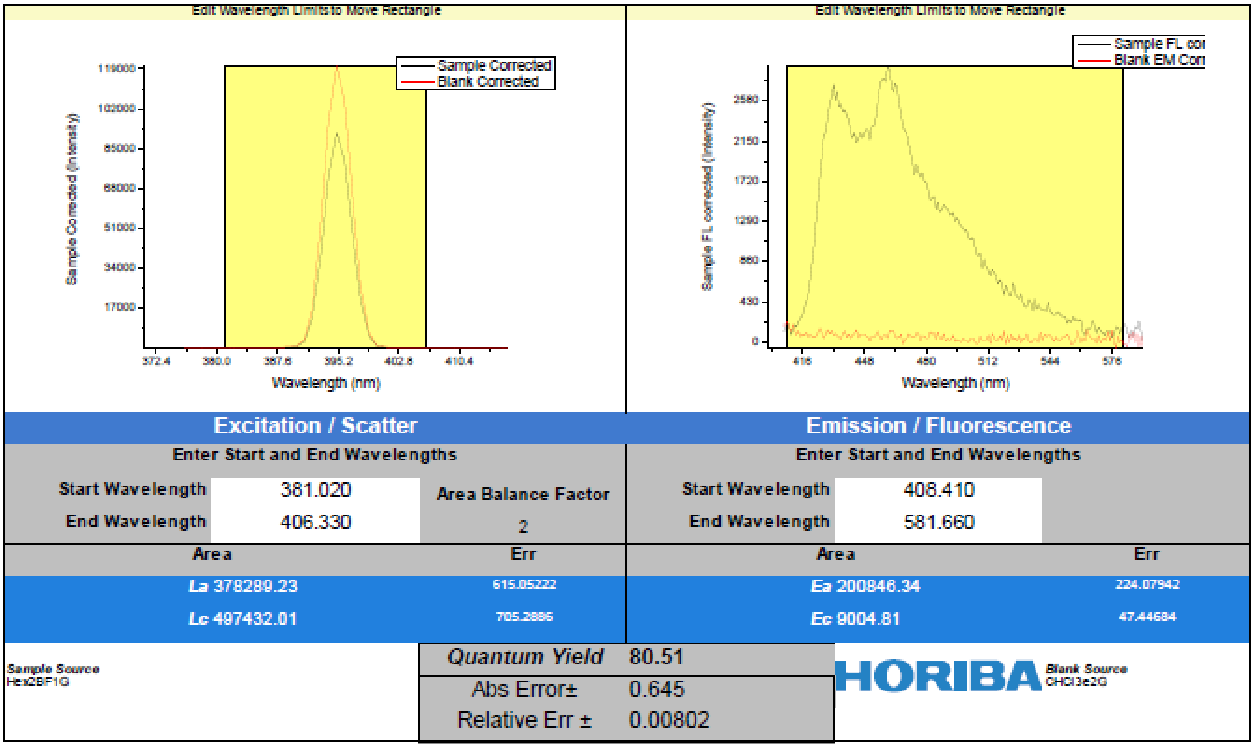

Excitation / Scatter			Emission / Fluorescence	
Enter Start and End Wavelengths			Enter Start and End Wavelengths	
Start Wavelength	381.020	Area Balance Factor	Start Wavelength	408.410
End Wavelength	406.330	2	End Wavelength	581.660
Area		Err	Area	Err
La 378289.23		615.05222	Ea 200846.34	224.07942
Lc 497432.01		705.2886	Ec 9004.81	47.44684

Sample Source
Hex2BF1G

Quantum Yield	80.51
Abs Error±	0.645
Relative Err ±	0.00802

Blank Source
CHCl3e2G

Figure S25. Quantum yield of **2BFI-H** measured in the $CHCl_3$ at room temperature.

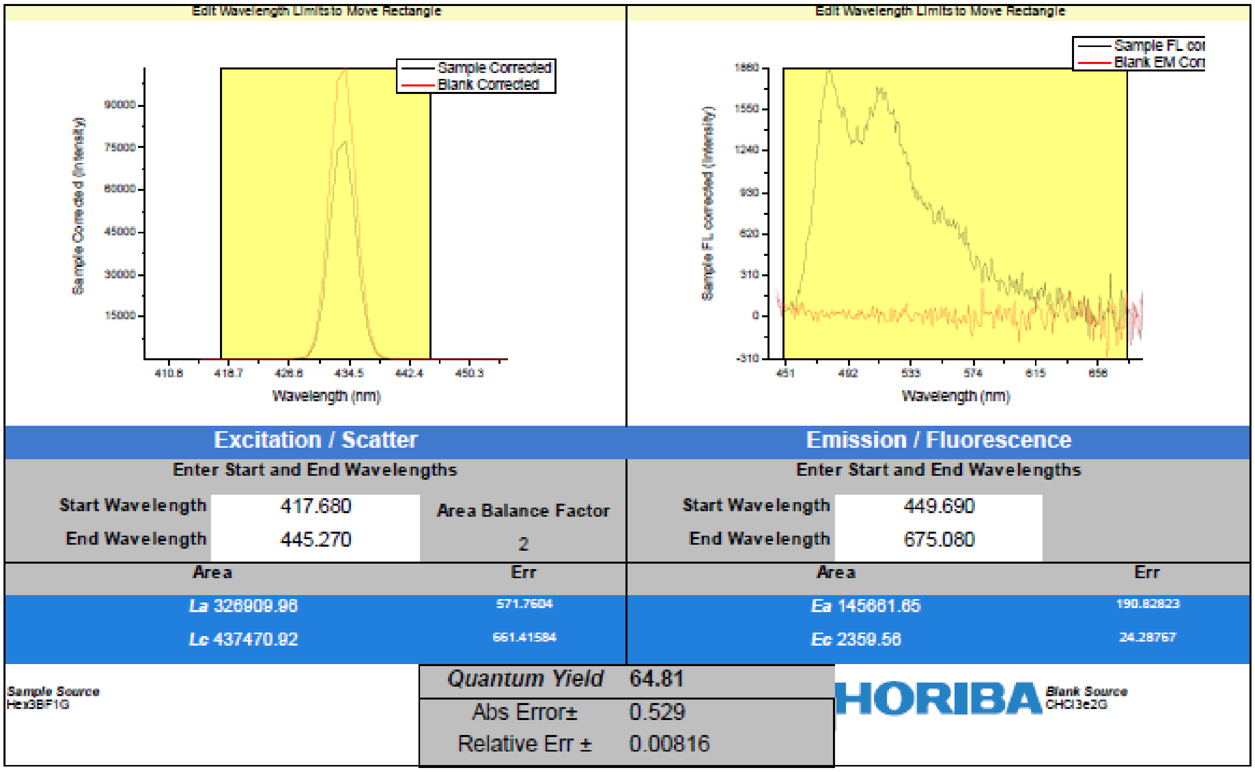

Excitation / Scatter			Emission / Fluorescence	
Enter Start and End Wavelengths			Enter Start and End Wavelengths	
Start Wavelength	417.680	Area Balance Factor	Start Wavelength	449.690
End Wavelength	445.270	2	End Wavelength	675.080
Area		Err	Area	Err
La 326909.96		571.7604	Ea 145661.65	190.82823
Lc 437470.92		661.41584	Ec 2359.56	24.28767

Sample Source
Hex3BF1G

Quantum Yield	64.81
Abs Error±	0.529
Relative Err ±	0.00816

Blank Source
CHCl3e2G

Figure S26. Quantum yield of **3BFI-H** measured in the $CHCl_3$ at room temperature.

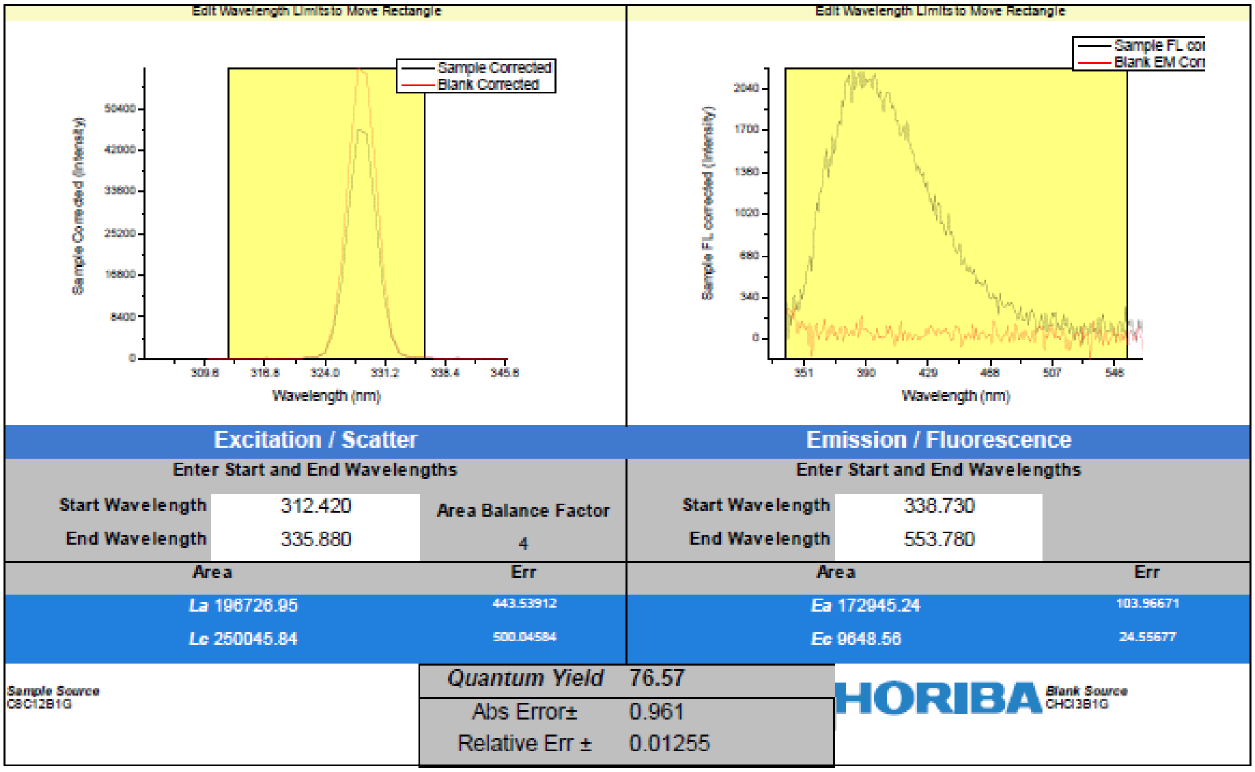

Excitation / Scatter			Emission / Fluorescence	
Enter Start and End Wavelengths			Enter Start and End Wavelengths	
Start Wavelength	312.420	Area Balance Factor	Start Wavelength	338.730
End Wavelength	335.880	4	End Wavelength	553.780
Area		Err	Area	Err
La 196726.95		443.53912	*Ea* 172945.24	103.96671
Lc 250045.84		500.04584	*Ec* 9648.56	24.55677

Sample Source
C8C12B1G

Quantum Yield	76.57
Abs Error±	0.961
Relative Err ±	0.01255

HORIBA ***Blank Source***
CHCl3B1G

Figure S27. Quantum yield of **BFI-OD** measured in the $CHCl_3$ at room temperature.

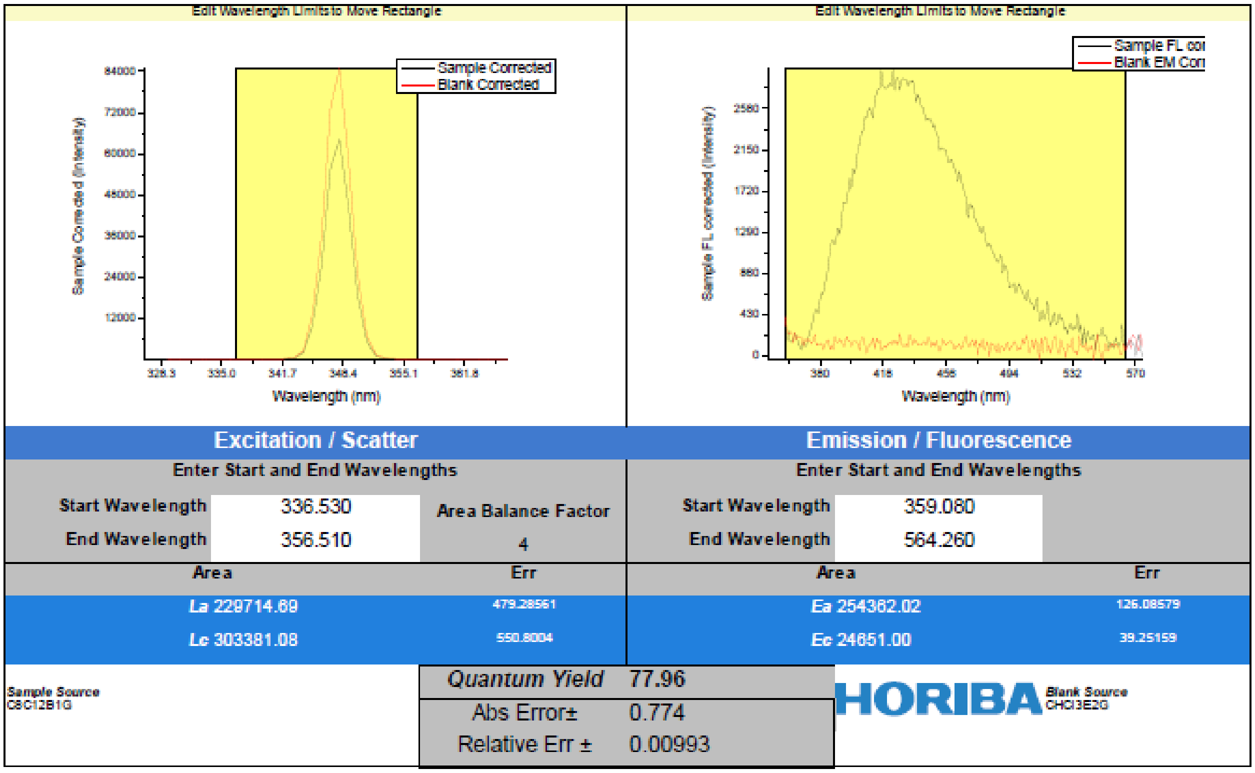

Excitation / Scatter			Emission / Fluorescence	
Enter Start and End Wavelengths			Enter Start and End Wavelengths	
Start Wavelength	336.530	Area Balance Factor	Start Wavelength	359.080
End Wavelength	356.510	4	End Wavelength	564.260
Area		Err	Area	Err
La 229714.69		479.28561	*Ea* 254362.02	126.08579
Lc 303381.08		550.8004	*Ec* 24651.00	39.25159

Sample Source
C8C12B1G

Quantum Yield	77.96
Abs Error±	0.774
Relative Err ±	0.00993

HORIBA ***Blank Source***
CHCl3E2G

Figure S28. Quantum yield of **BTI-OD** measured in the $CHCl_3$ at room temperature.

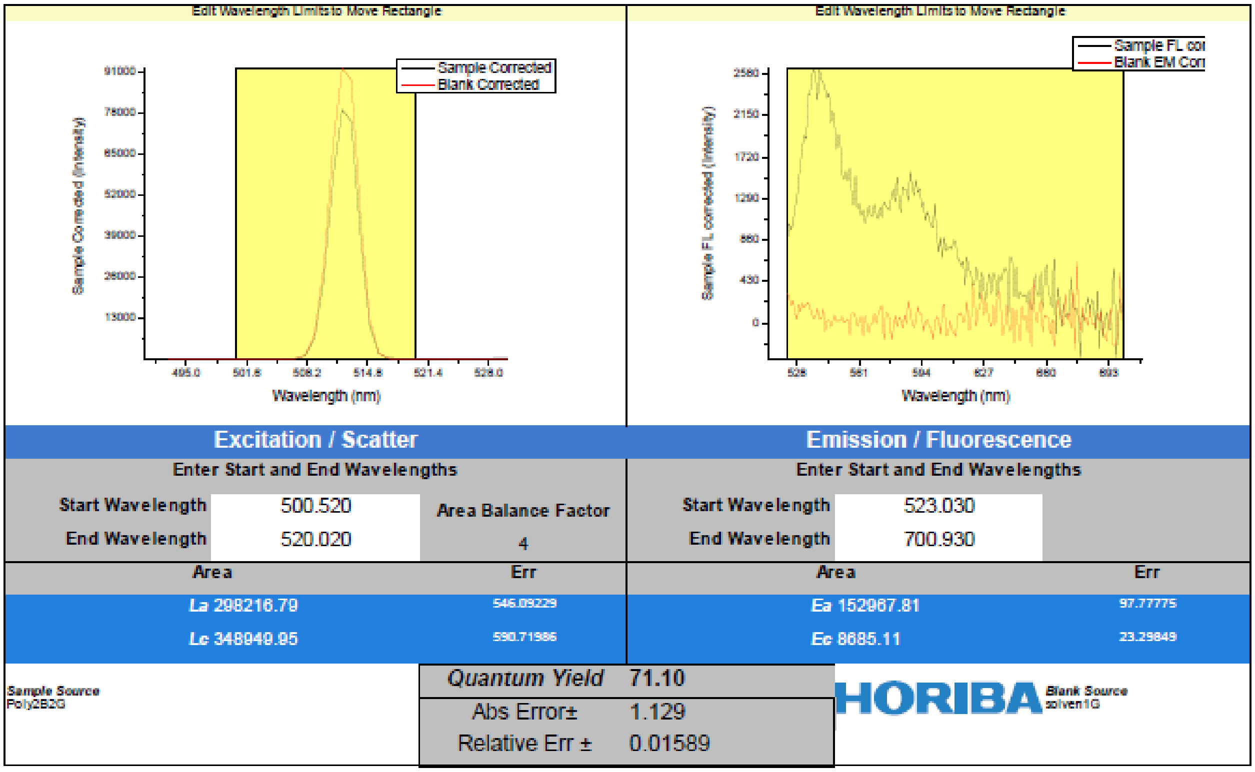

Excitation / Scatter

Enter Start and End Wavelengths

Start Wavelength	500.520	Area Balance Factor
End Wavelength	520.020	4

Area	Err
La 298216.79	546.09229
Lc 348949.95	590.71986

Emission / Fluorescence

Enter Start and End Wavelengths

Start Wavelength	523.030
End Wavelength	700.930

Area	Err
Ea 152967.81	97.77775
Ec 8685.11	23.29849

Sample Source
Poly2B2G

Quantum Yield	71.10
Abs Error±	1.129
Relative Err ±	0.01589

Blank Source
solven1G

Figure S29. Quantum yield of **poly(BFI-OD)** measured in the $CHCl_3$ at room temperature.

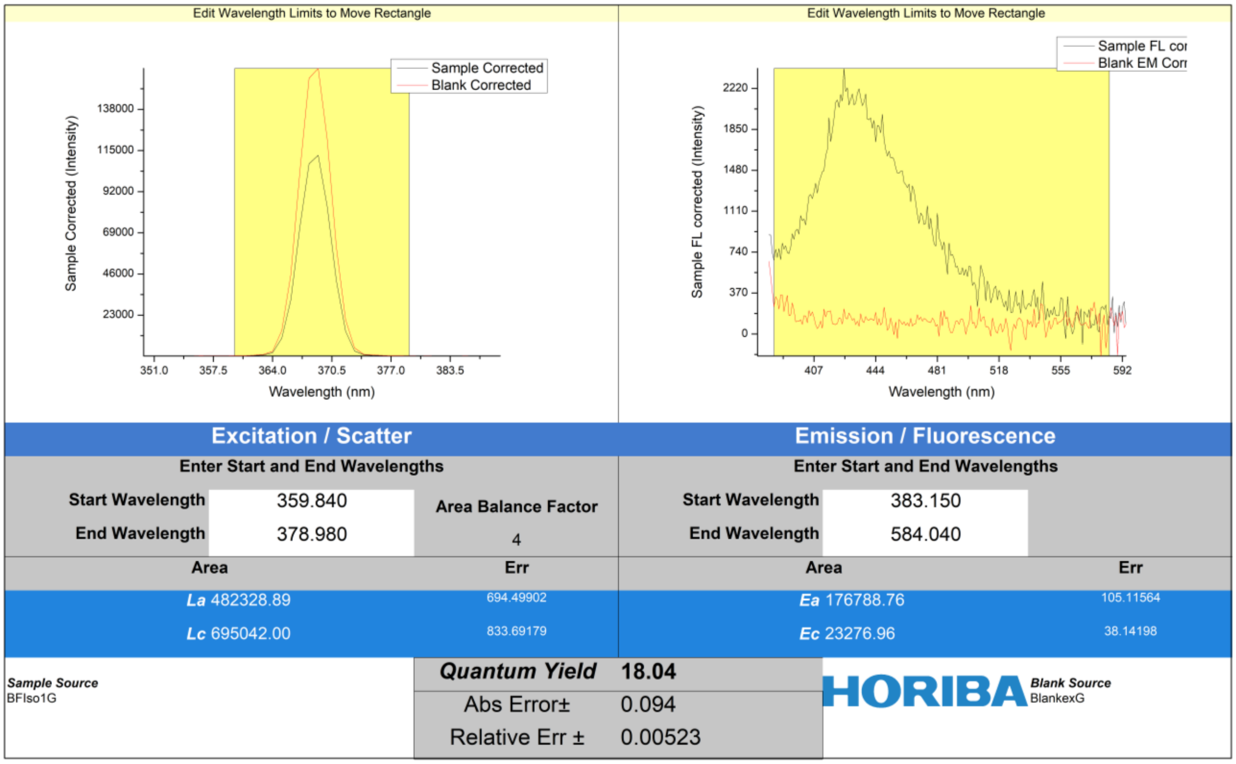

Excitation / Scatter

Enter Start and End Wavelengths

Start Wavelength	359.840	Area Balance Factor
End Wavelength	378.980	4

Area	Err
La 482328.89	694.49902
Lc 695042.00	833.69179

Emission / Fluorescence

Enter Start and End Wavelengths

Start Wavelength	383.150
End Wavelength	584.040

Area	Err
Ea 176788.76	105.11564
Ec 23276.96	38.14198

Sample Source
BFIso1G

Quantum Yield	**18.04**
Abs Error±	0.094
Relative Err ±	0.00523

Blank Source
BlankexG

Figure S30. Quantum yield of **BFI-H** measured in the solid state at room temperature.

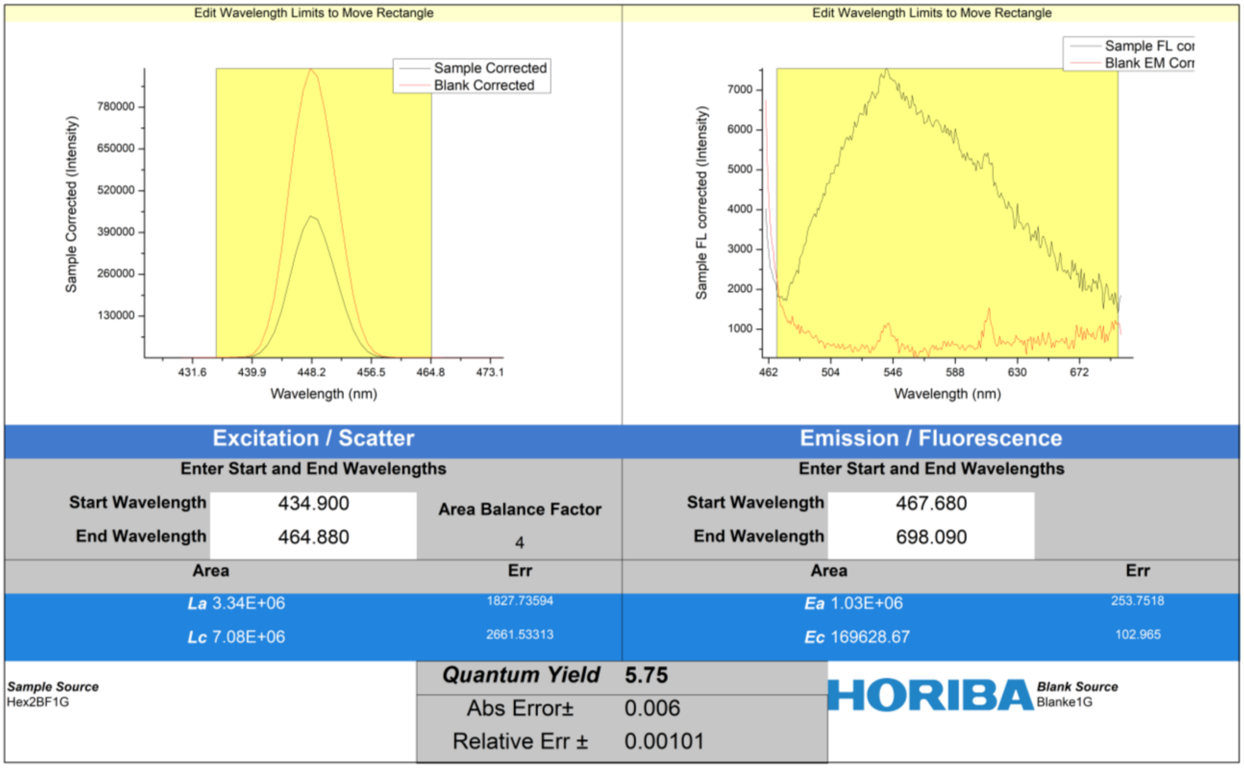

Excitation / Scatter

Enter Start and End Wavelengths

Start Wavelength 434.900

End Wavelength 464.880

Area Balance Factor 4

Area	Err
La 3.34E+06	1827.73594
Lc 7.08E+06	2661.53313

Emission / Fluorescence

Enter Start and End Wavelengths

Start Wavelength 467.680

End Wavelength 698.090

Area	Err
Ea 1.03E+06	253.7518
Ec 169628.67	102.965

Sample Source
Hex2BF1G

Quantum Yield 5.75
Abs Error± 0.006
Relative Err ± 0.00101

Blank Source
Blanke1G

Figure S31. Quantum yield of **2BFI-H** measured in the solid state at room temperature.

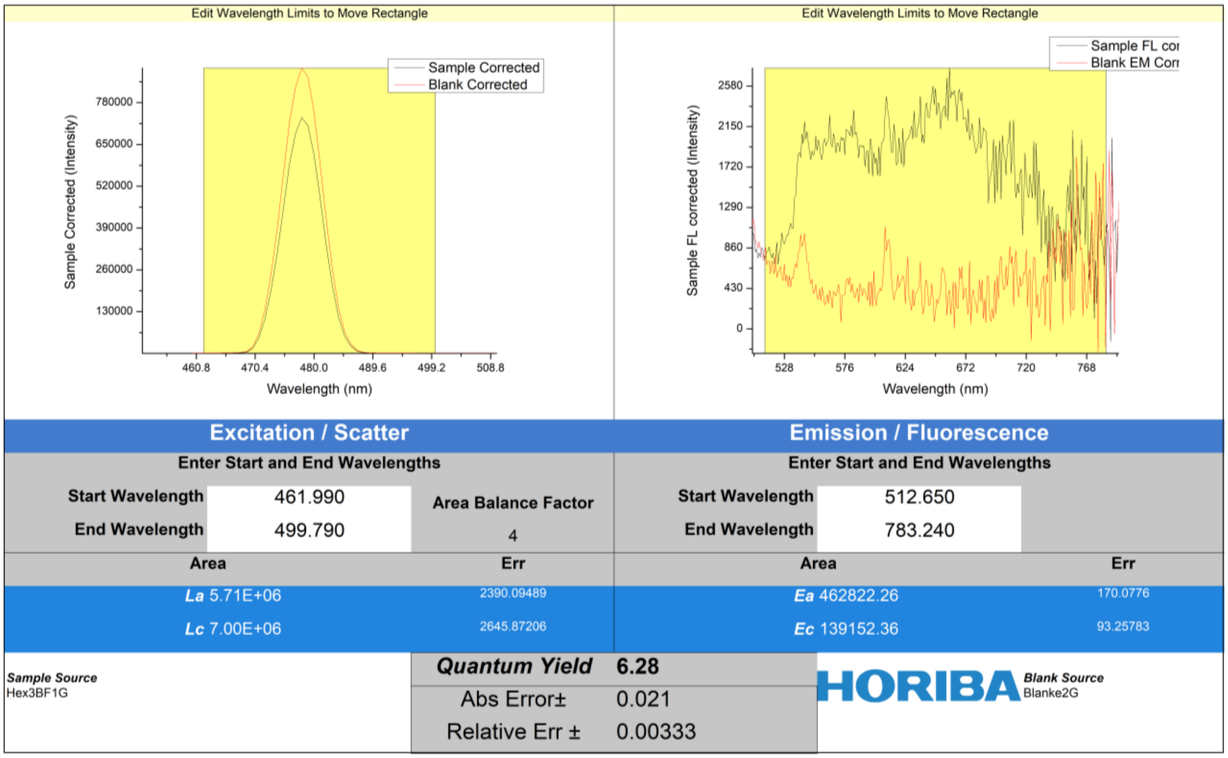

Excitation / Scatter

Enter Start and End Wavelengths

Start Wavelength 461.990

End Wavelength 499.790

Area Balance Factor 4

Area	Err
La 5.71E+06	2390.09489
Lc 7.00E+06	2645.87206

Emission / Fluorescence

Enter Start and End Wavelengths

Start Wavelength 512.650

End Wavelength 783.240

Area	Err
Ea 462822.26	170.0776
Ec 139152.36	93.25783

Sample Source
Hex3BF1G

Quantum Yield 6.28
Abs Error± 0.021
Relative Err ± 0.00333

Blank Source
Blanke2G

Figure S32. Quantum yield of **3BFI-H** measured in the solid state at room temperature.

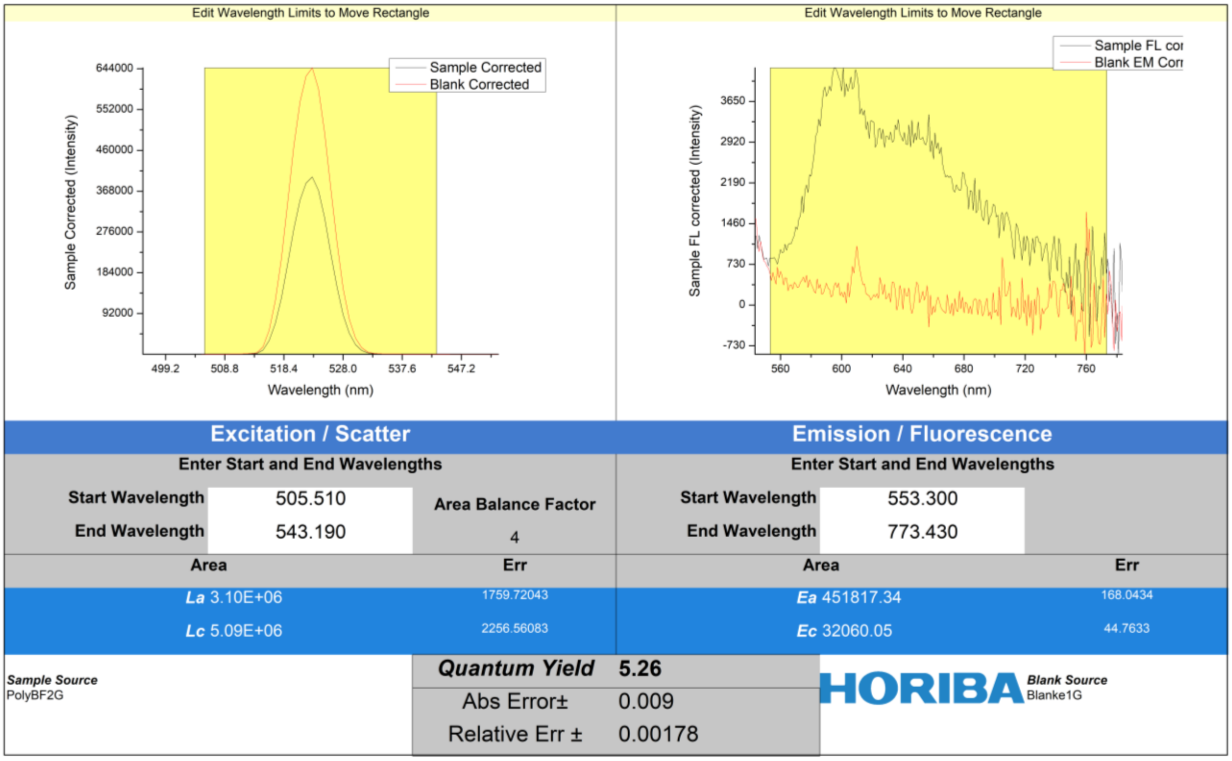

Excitation / Scatter

Enter Start and End Wavelengths

Start Wavelength	505.510	**Area Balance Factor**
End Wavelength	543.190	4

Area	**Err**
La 3.10E+06	1759.72043
Lc 5.09E+06	2256.56083

Emission / Fluorescence

Enter Start and End Wavelengths

Start Wavelength	553.300
End Wavelength	773.430

Area	**Err**
Ea 451817.34	168.0434
Ec 32060.05	44.7633

Sample Source
PolyBF2G

Quantum Yield	**5.26**
Abs Error±	0.009
Relative Err ±	0.00178

Blank Source
Blanke1G

Figure S33. Quantum yield of **poly(BFI-OD)** measured in the solid state at room temperature.

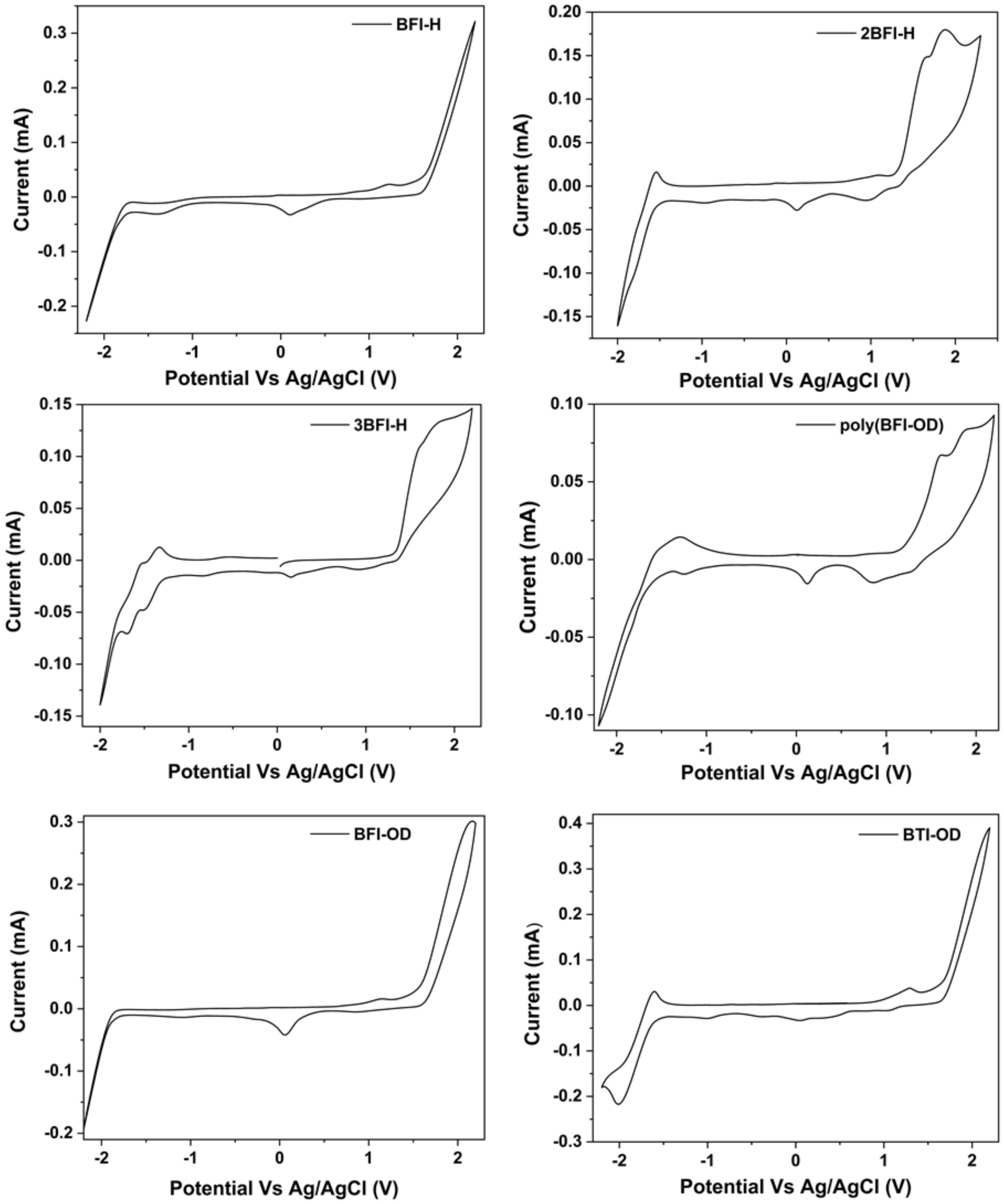

Figure S34. Cyclic voltammograms of **BFI-H**, **2BFI-H**, **3BFI-H**, **poly(BFI-OD)**, **BFI-OD**, and **BTI-OD** (1.5 mg/mL) in 0.1 M tetrabutylammonium perchlorate in dry dichloromethane as solvent using a Pt disk as the working electrode, a Pt-wire counter electrode, scan rate is 100 mV/s Vs Ag/AgCl.

Table S2. Electrochemical data of **BFI-H**, **2BFI-H**, **3BFI-H**, **poly(BFI-OD)**, **BFI-OD**, and **BTI-OD** (1.5 mg/mL) in 0.1 M tetrabutylammonium perchlorate in dry dichloromethane as solvent using a Pt disk as the working electrode, a Pt-wire counter electrode, scan rate is 100 mV/s Vs Ag/AgCl.

Compounds	E_{ox}(V)	$E_{ox(onset)}$(V)	$E_{1/2ox}$(V)
BFI-H	1.23	0.83	1.05
2BFI-H	1.65	1.30	1.29
3BFI-H	1.60	1.34	1.27
BFI-OD	1.15	0.71	1.00
BTI-OD	1.29	0.88	1.17
Poly(**BFI-OD**)	1.61	1.28	–

S4. NMR Spectra

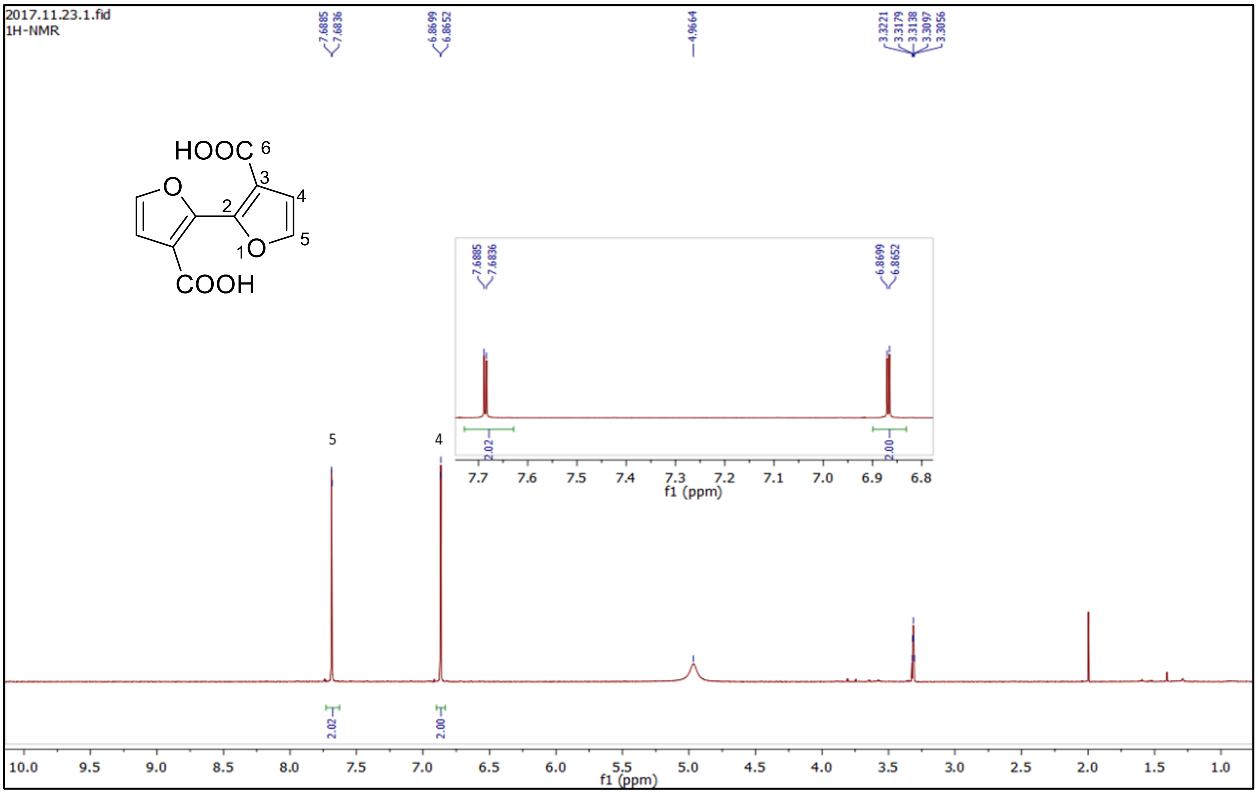

Figure S35. ^{1}H NMR spectrum of **2** in MeOD, measured at 298 K.

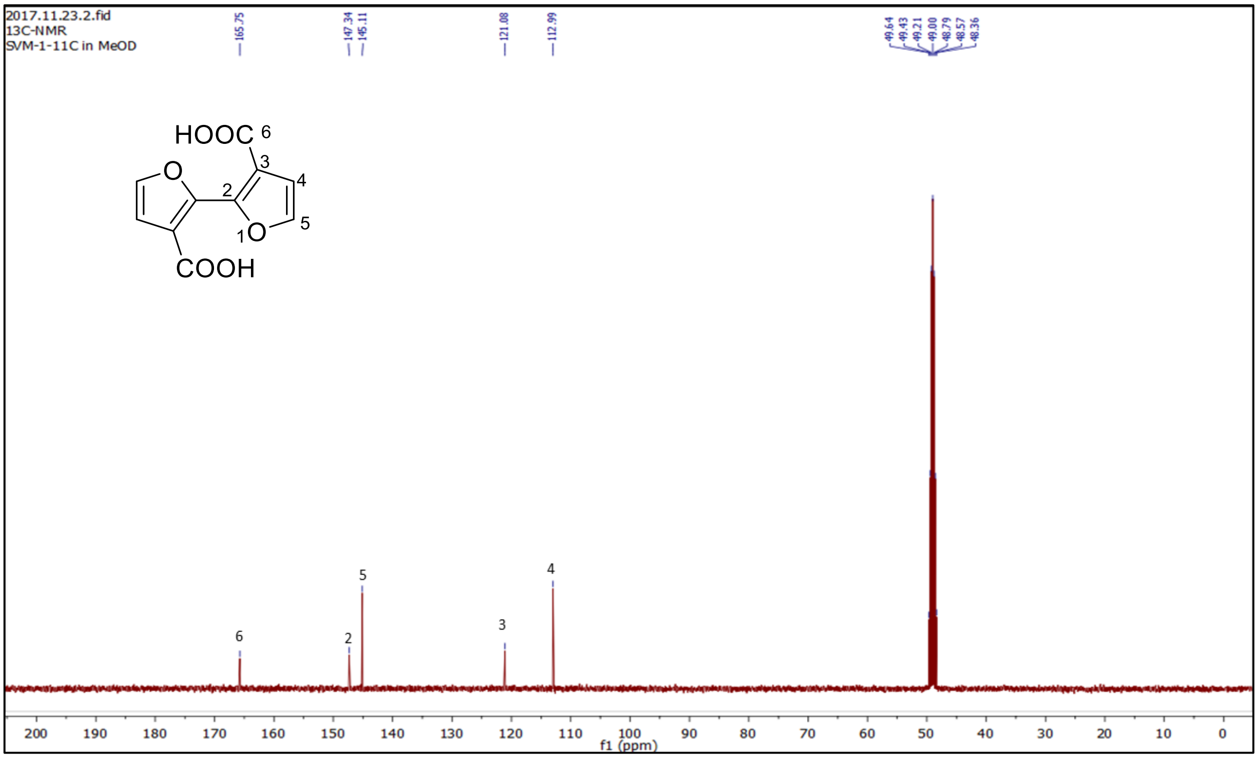

Figure S36. ^{13}C NMR spectrum of **2** in MeOD, measured at 298 K.

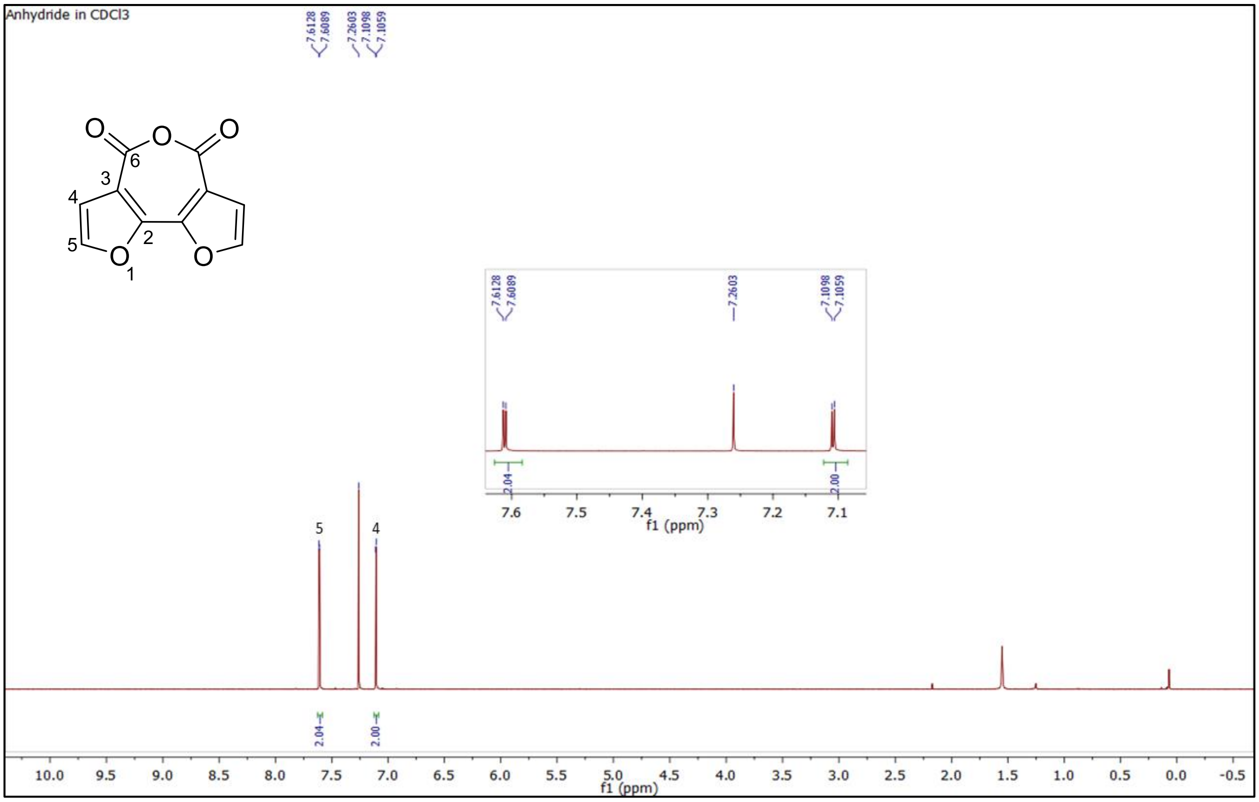

Figure S37. ^{1}H NMR spectrum of **3** in $CDCl_3$, measured at 298 K.

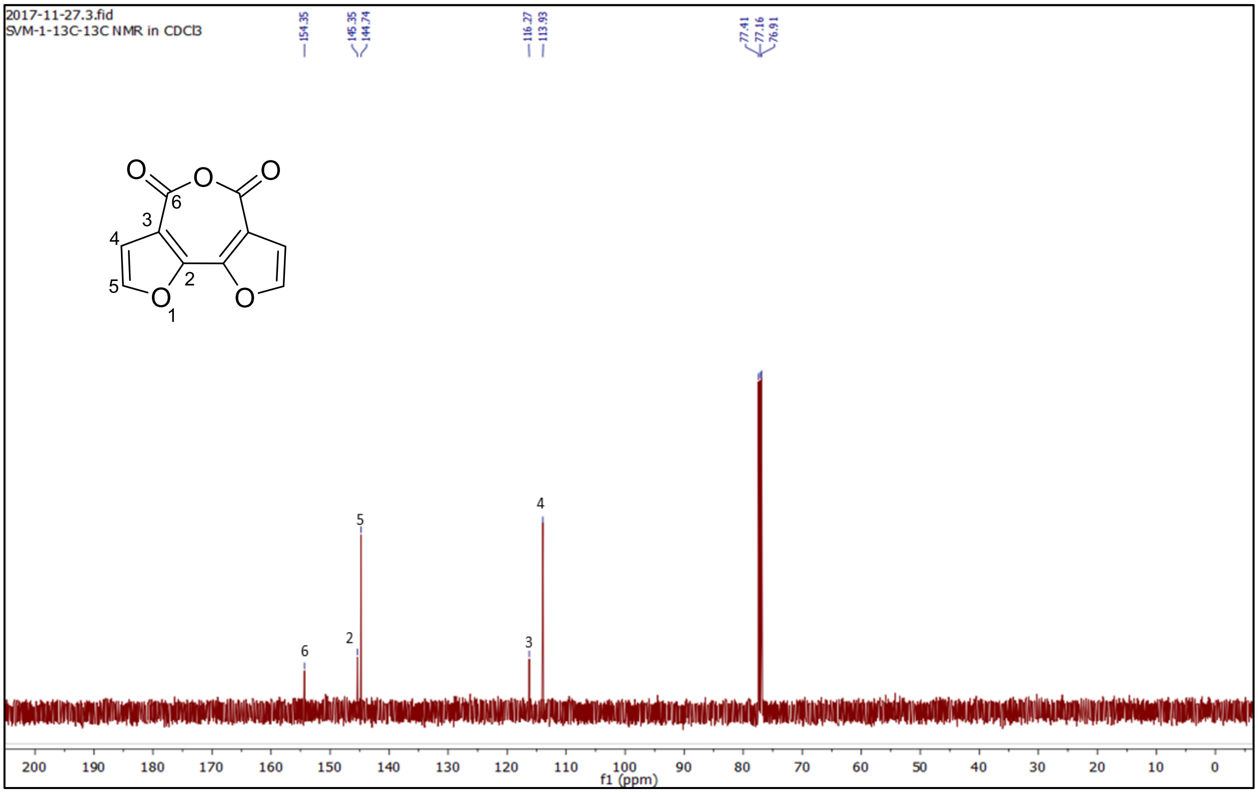

Figure S38. ^{13}C NMR spectrum of **3** in $CDCl_3$, measured at 298 K.

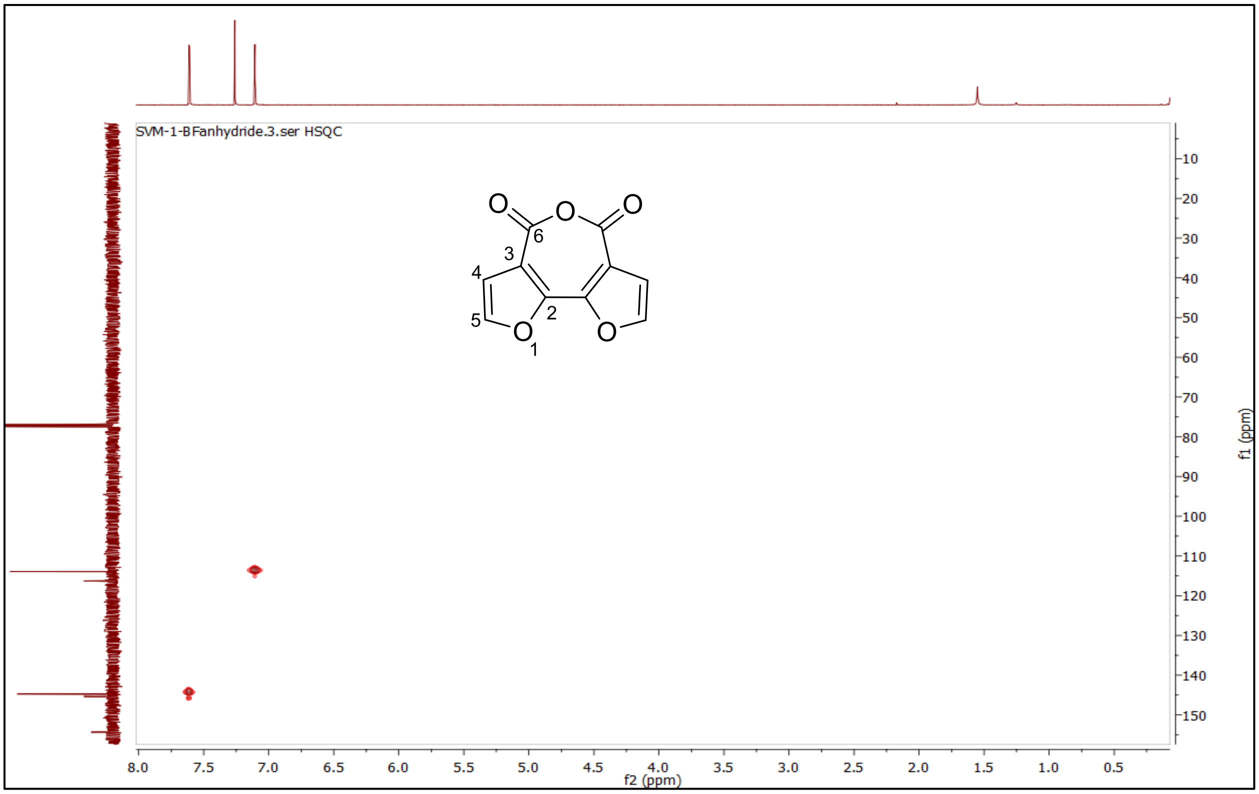

Figure S39. HSQC spectrum of **3** in $CDCl_3$, measured at 298 K.

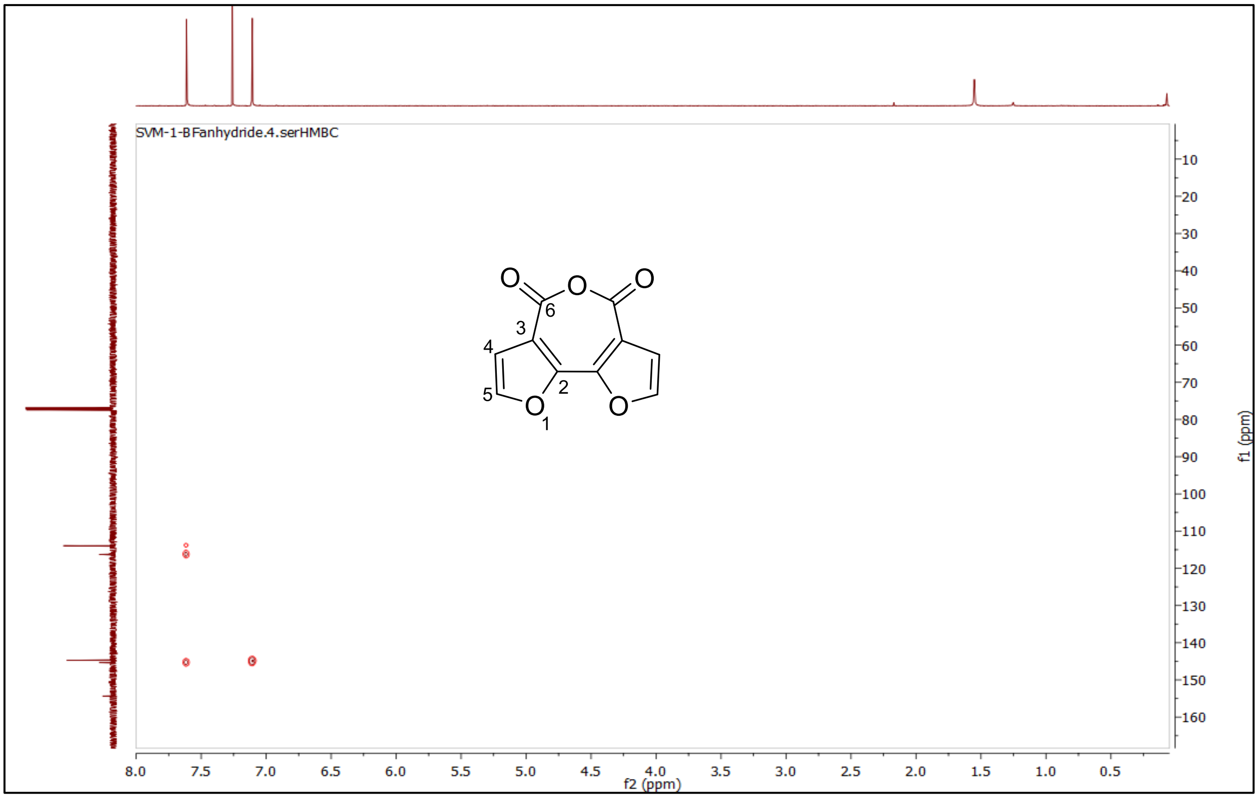

Figure S40. HMBC spectrum of **3** in $CDCl_3$, measured at 298 K.

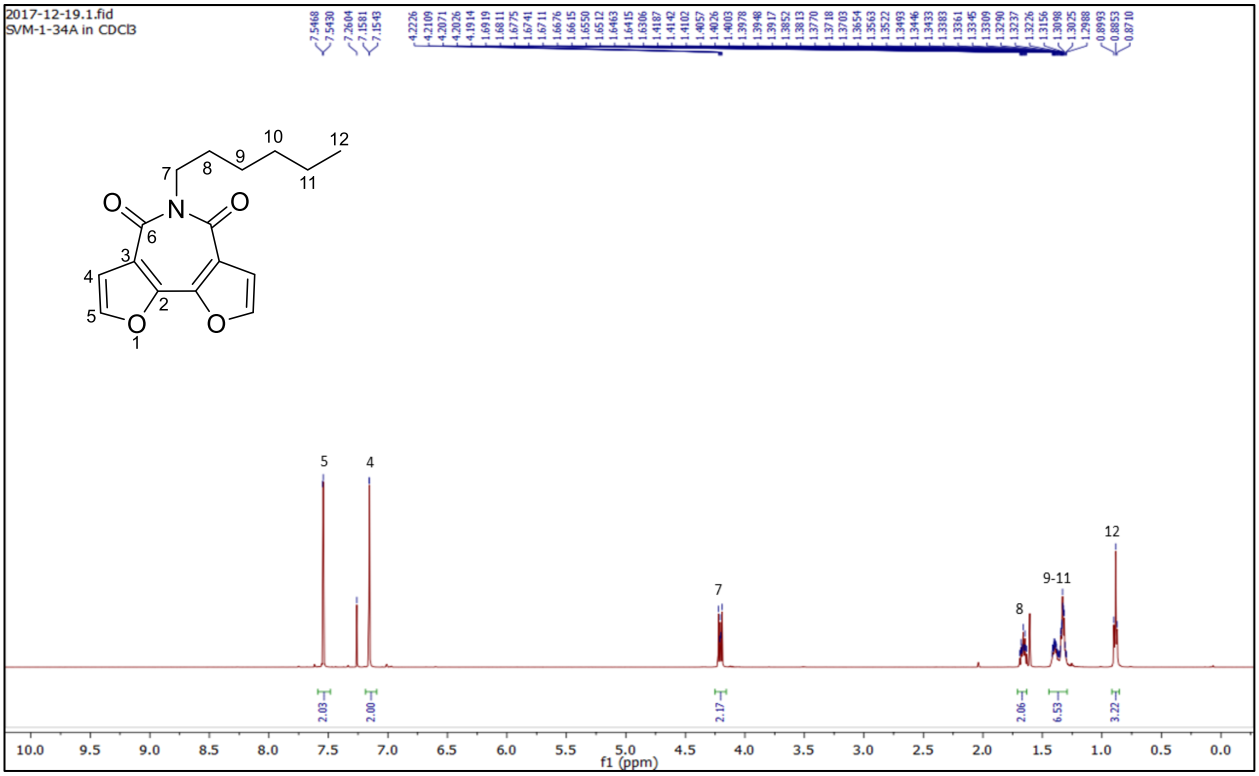

Figure S41. ^{1}H NMR spectrum of **BFI-H** in $CDCl_3$, measured at 298 K.

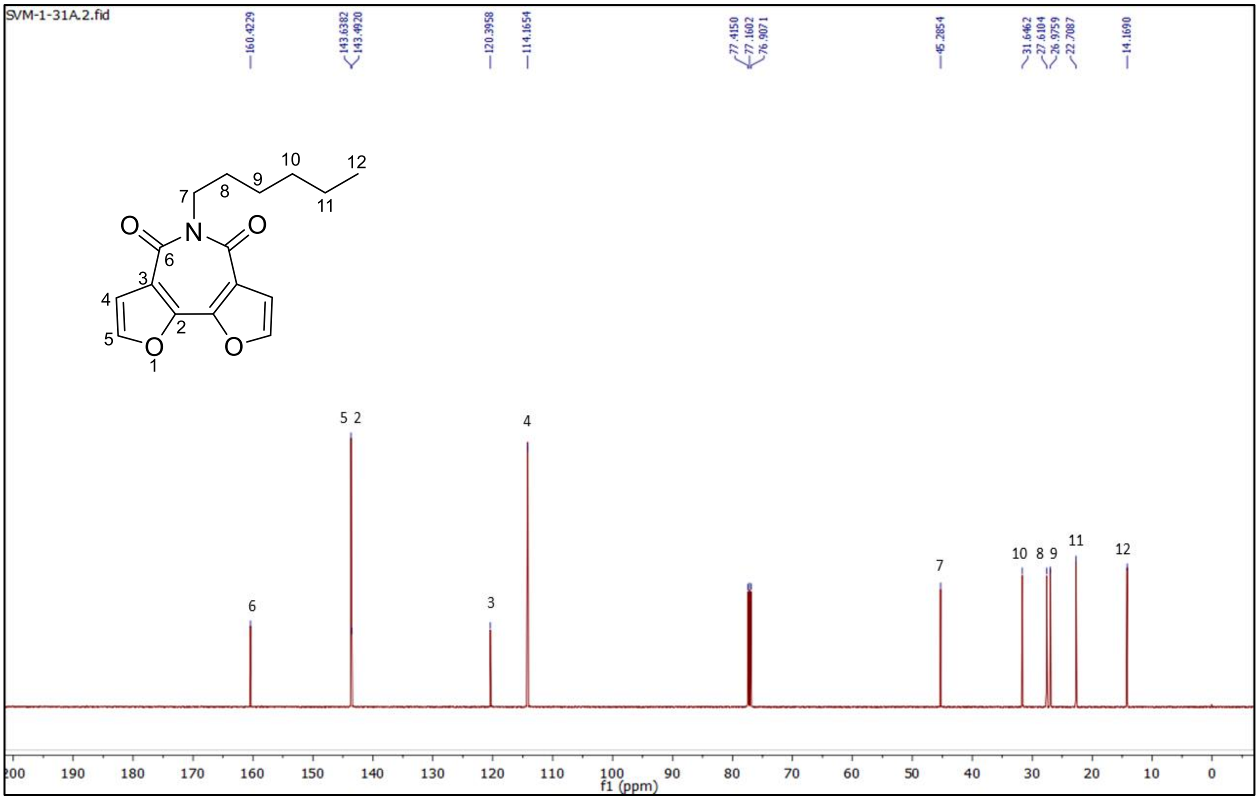

Figure S42. ^{13}C NMR spectrum of **BFI-H** in $CDCl_3$, measured at 298 K.

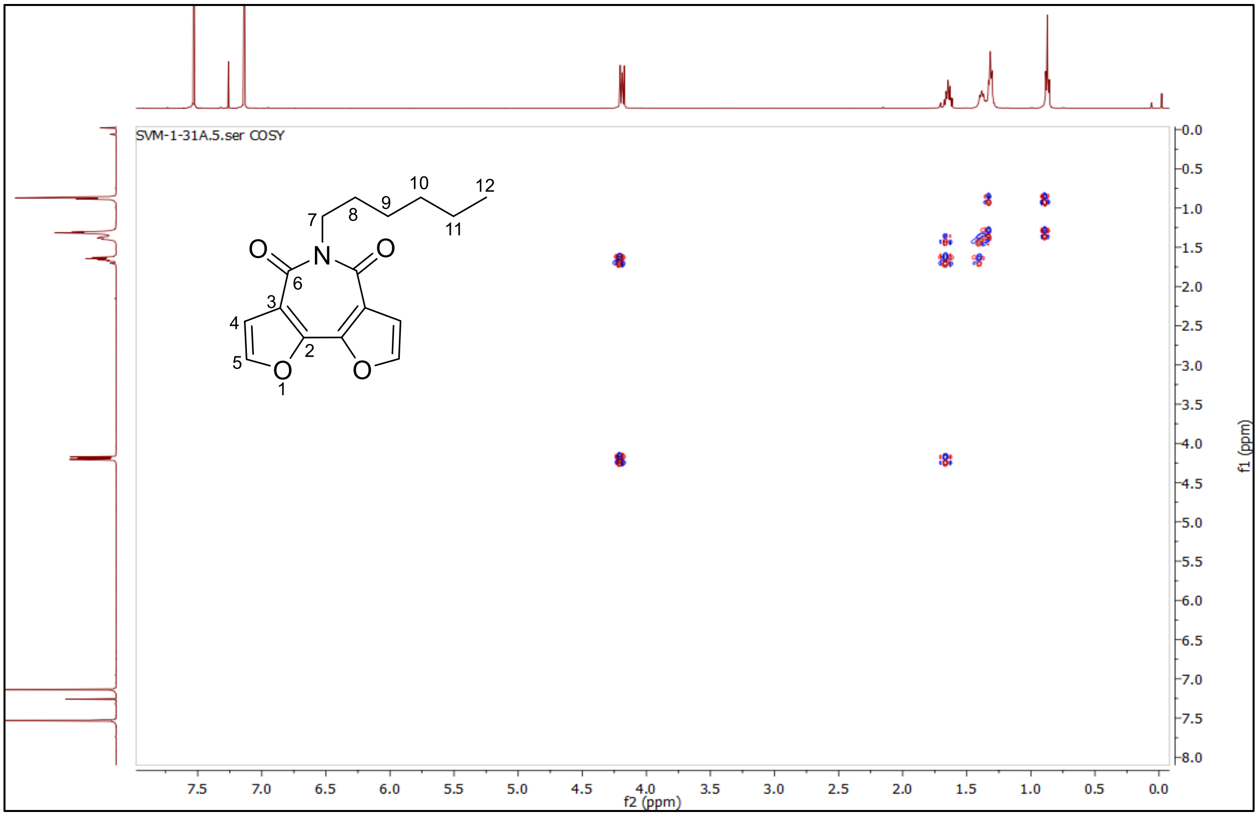

Figure S43. COSY spectrum of **BFI-H** in $CDCl_3$, measured at 298 K.

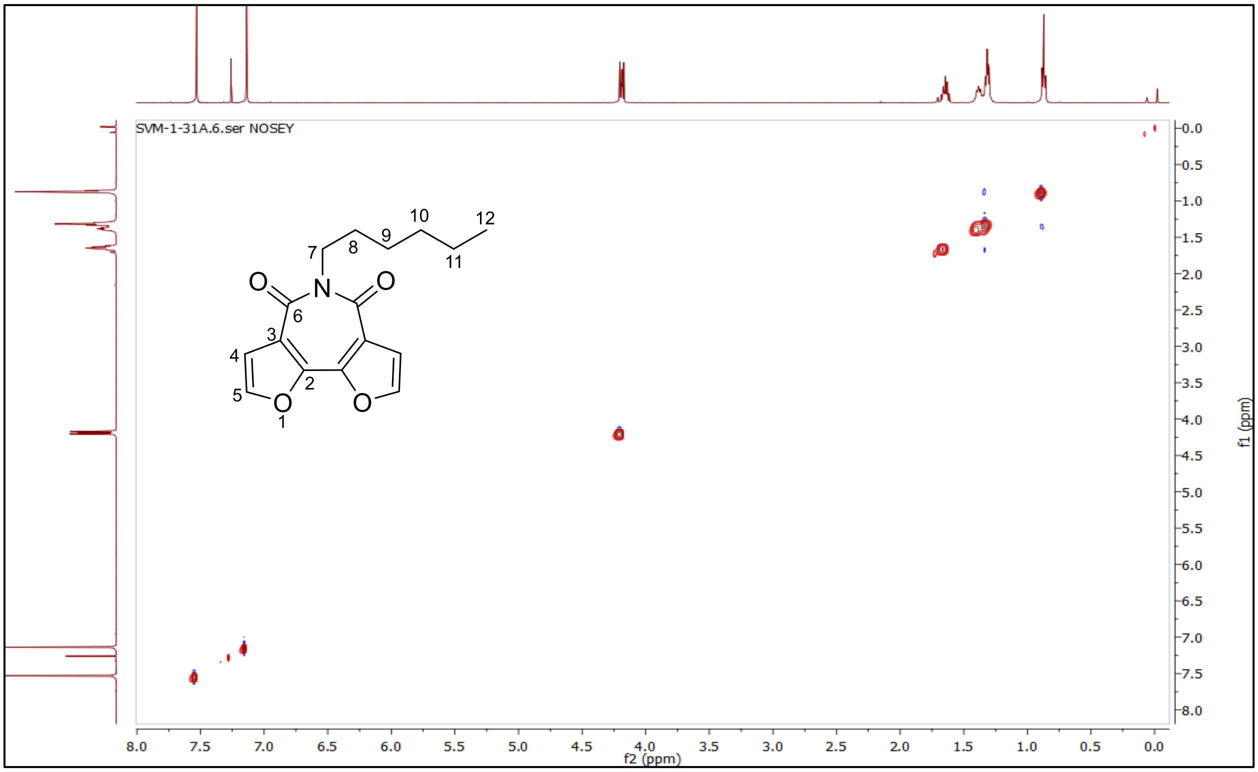

Figure S44. NOESY spectrum of **BFI-H** in $CDCl_3$, measured at 298 K.

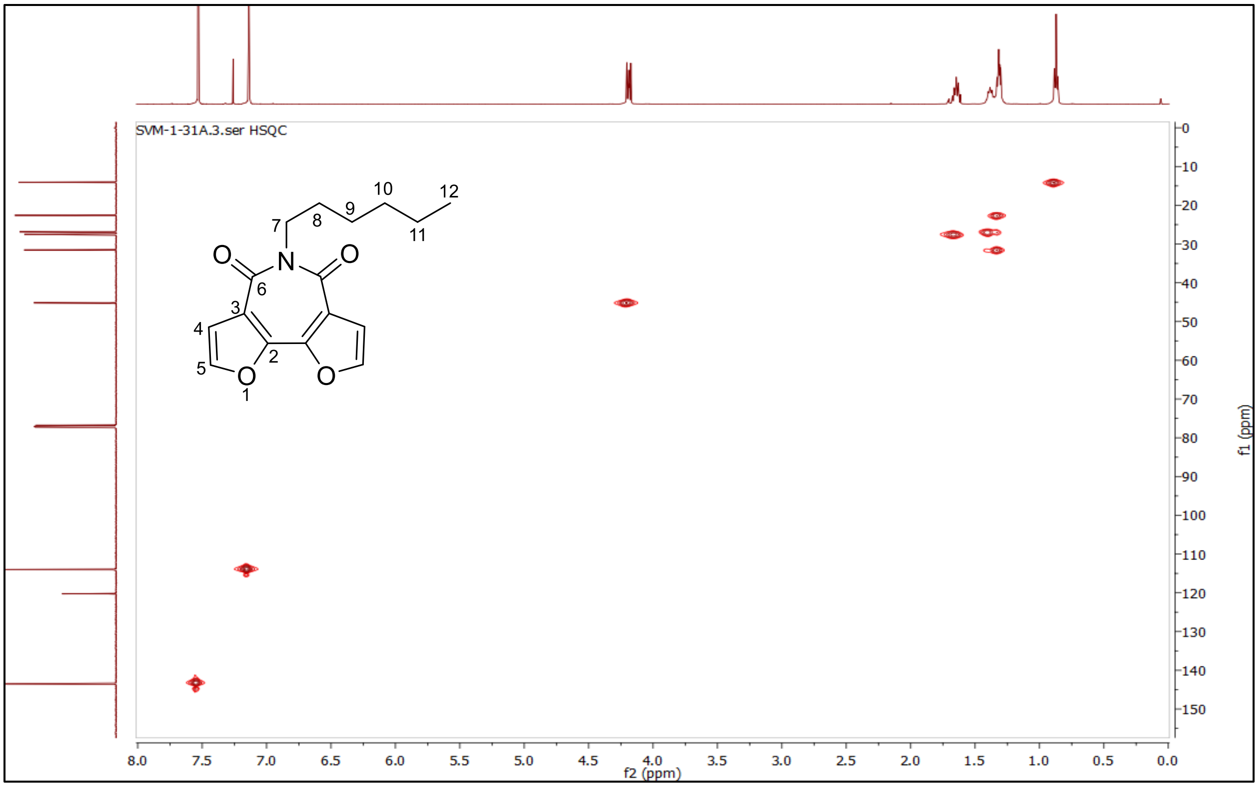

Figure S45. HSQC NMR spectrum of **BFI-H** in $CDCl_3$, measured at 298 K.

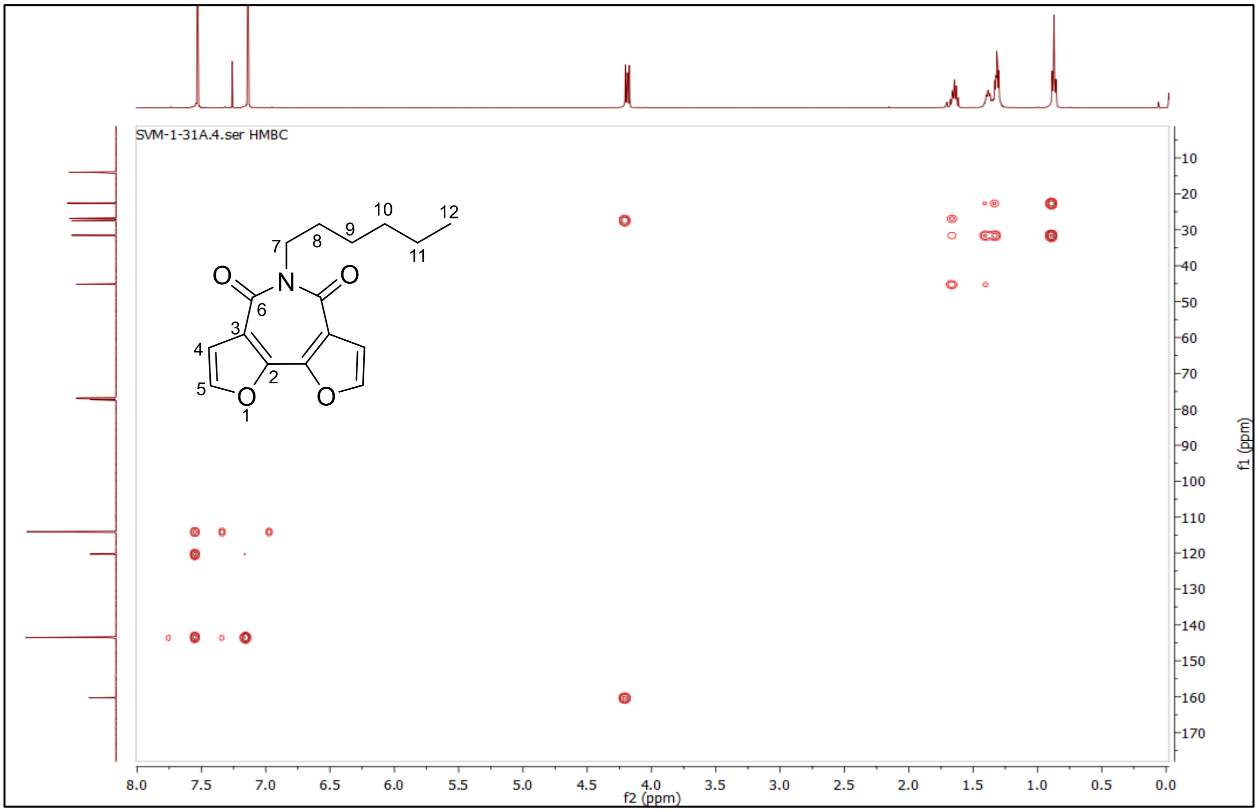

Figure S46. HMBC NMR spectrum of **BFI-H** in $CDCl_3$, measured at 298 K.

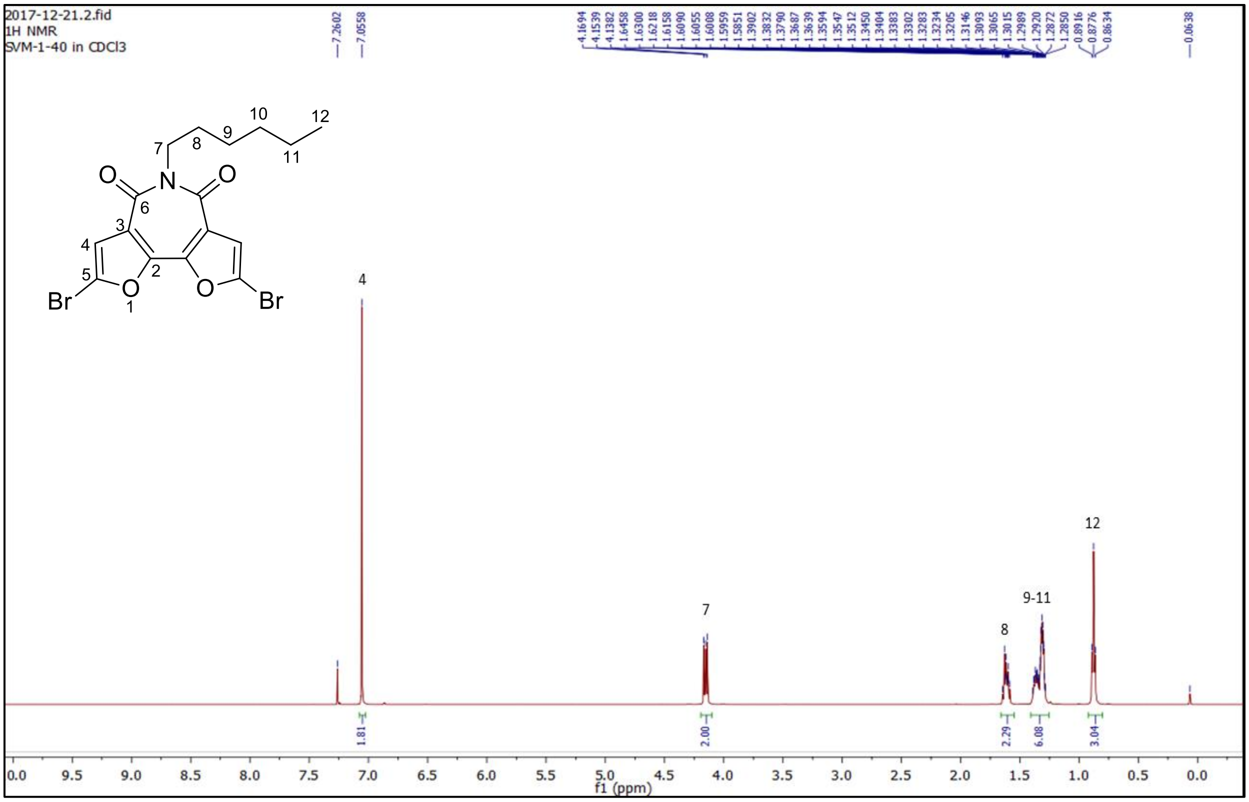

Figure S47. ^{1}H NMR spectrum of **4b** in CDCl$_3$, measured at 298 K.

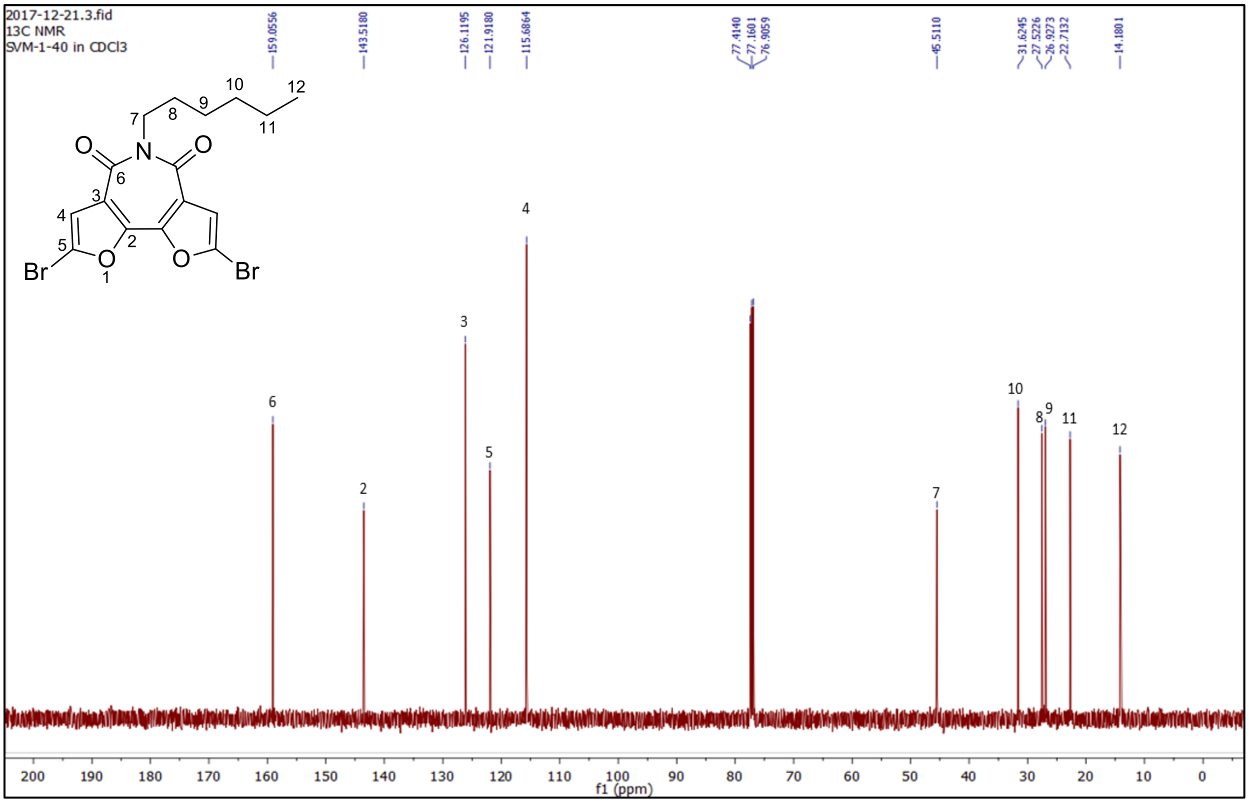

Figure S48. ^{13}C NMR spectrum of **4b** in CDCl$_3$, measured at 298 K.

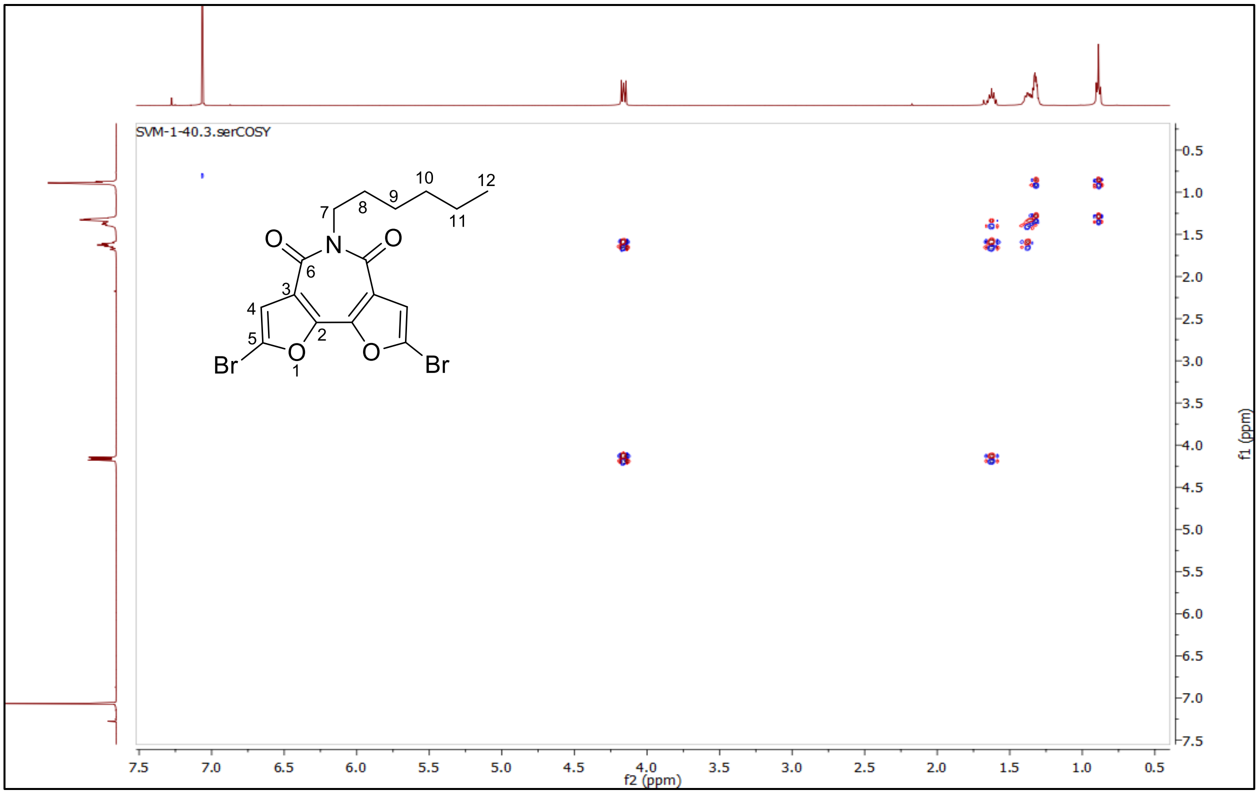

Figure S49. COSY spectrum of **4b** in $CDCl_3$, measured at 298 K.

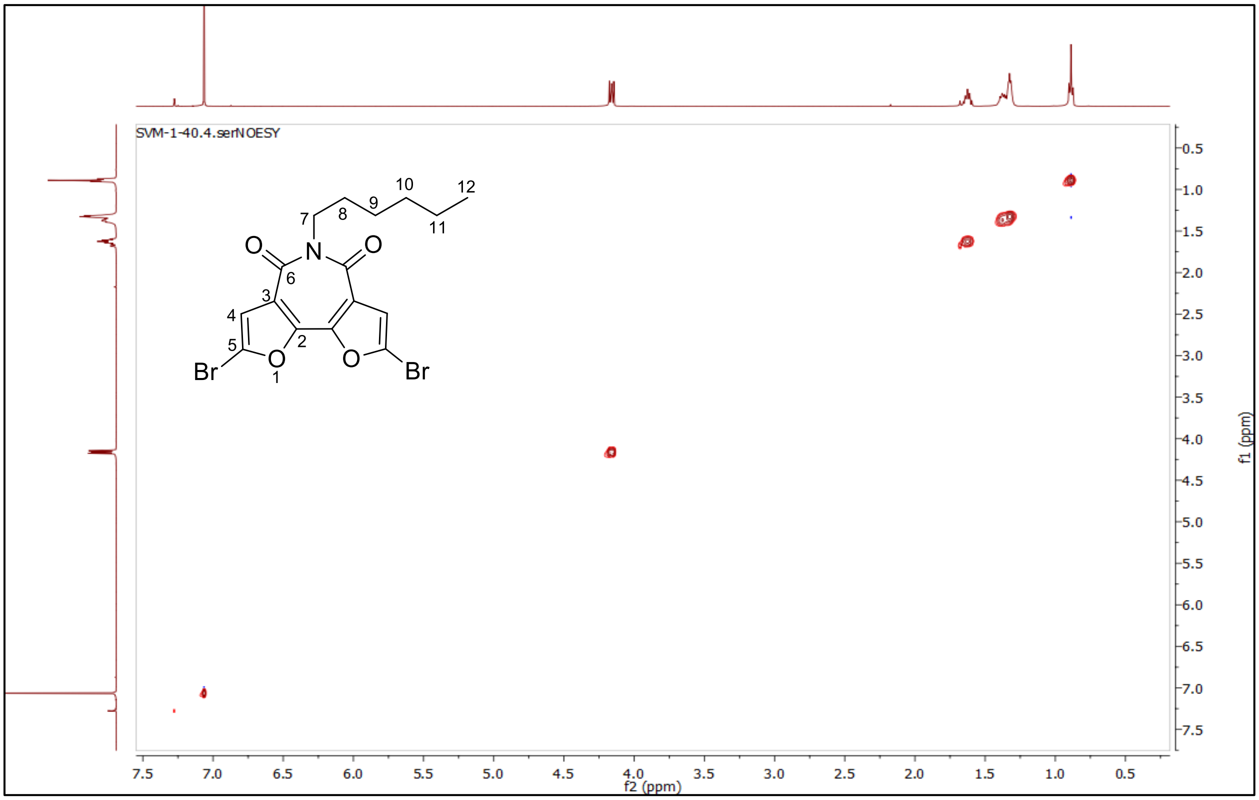

Figure S50. NOESY spectrum of **4b** in $CDCl_3$, measured at 298 K.

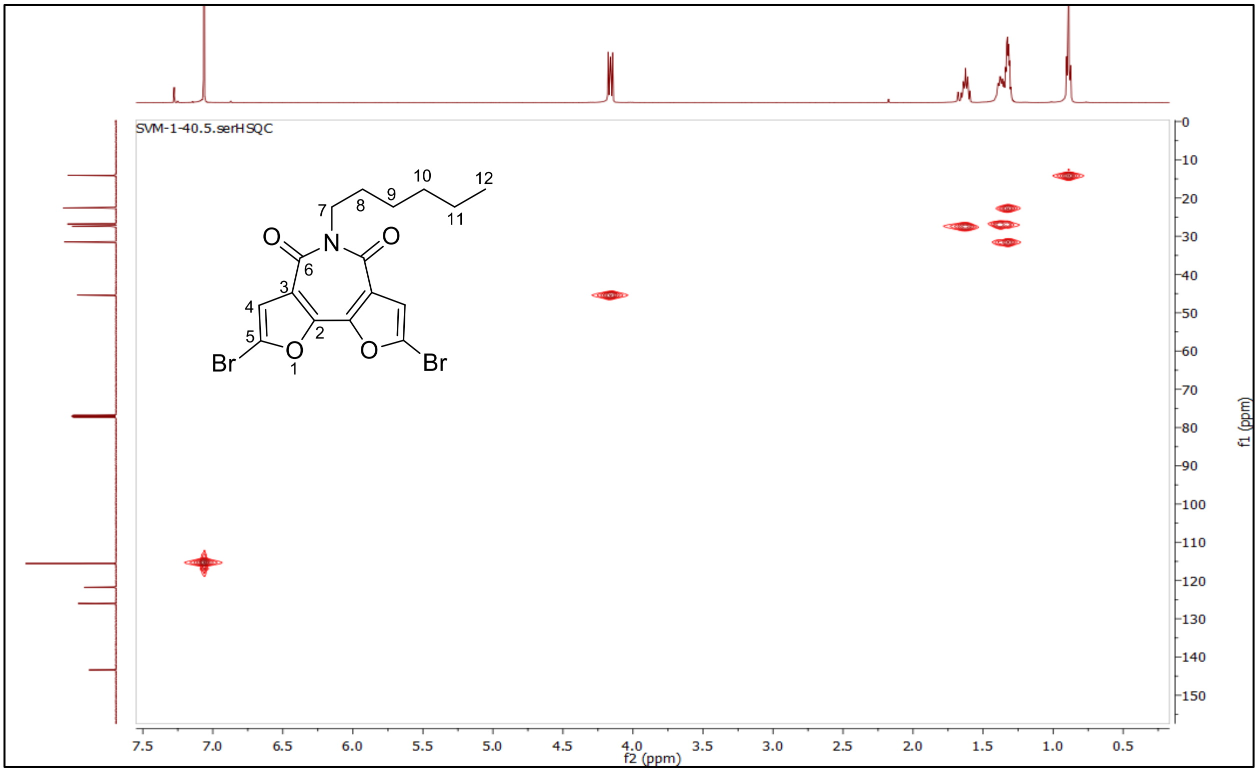

Figure S51. HSQC NMR spectrum of **4b** in $CDCl_3$, measured at 298 K.

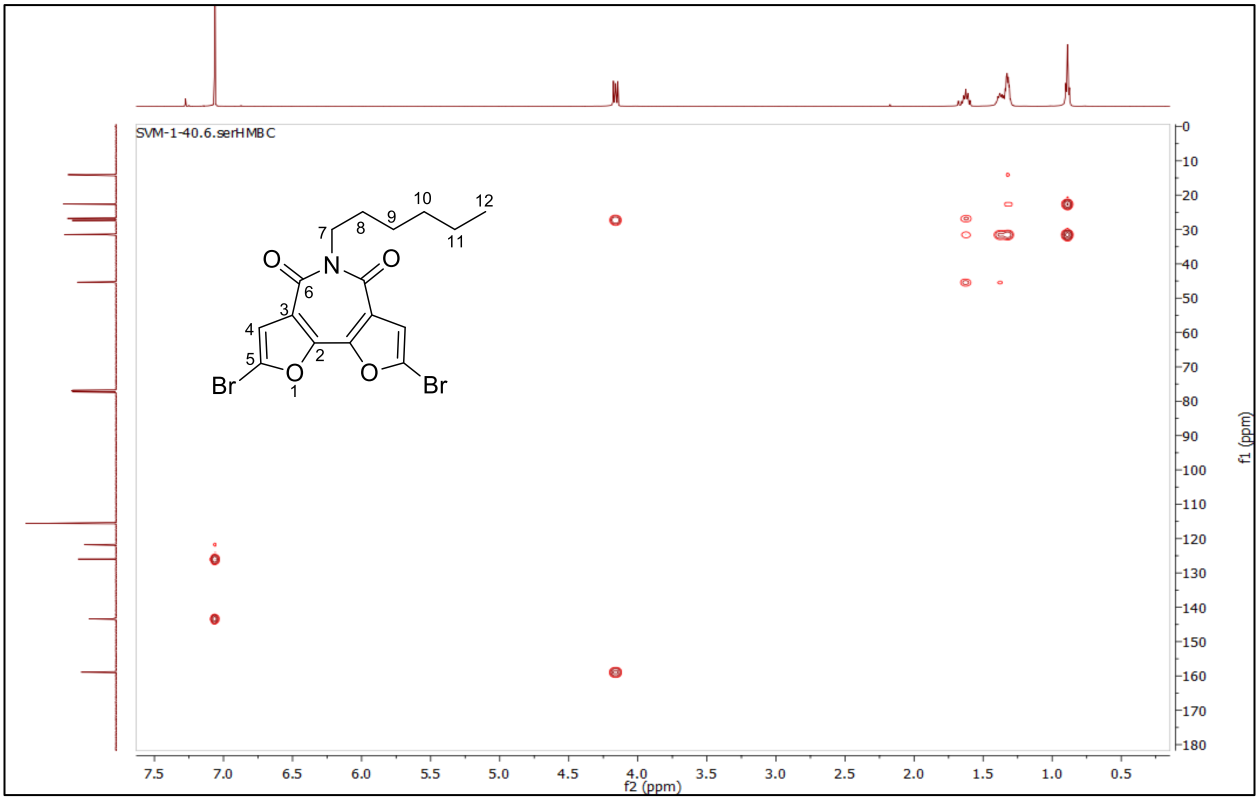

Figure S52. HMBC NMR spectrum of **4b** in $CDCl_3$, measured at 298 K.

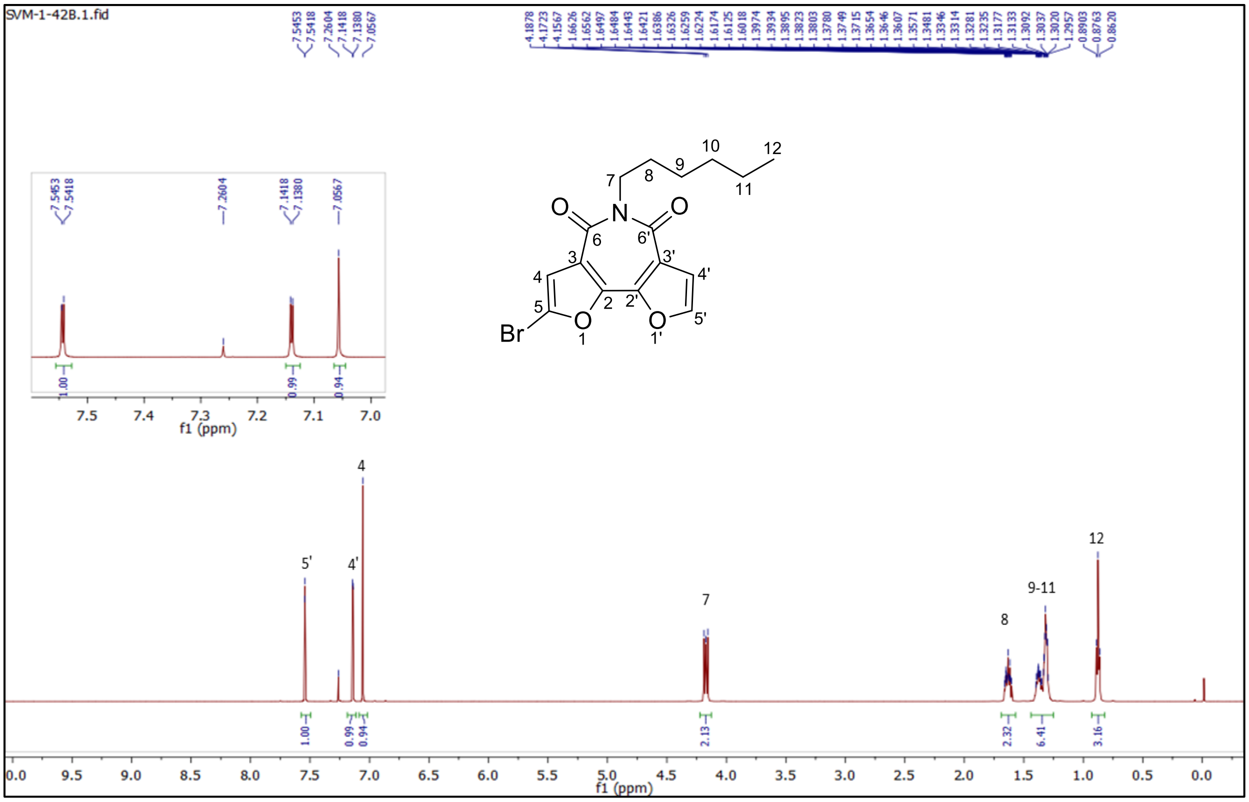

Figure S53. ^{1}H NMR spectrum of **4a** in $CDCl_3$, measured at 298 K.

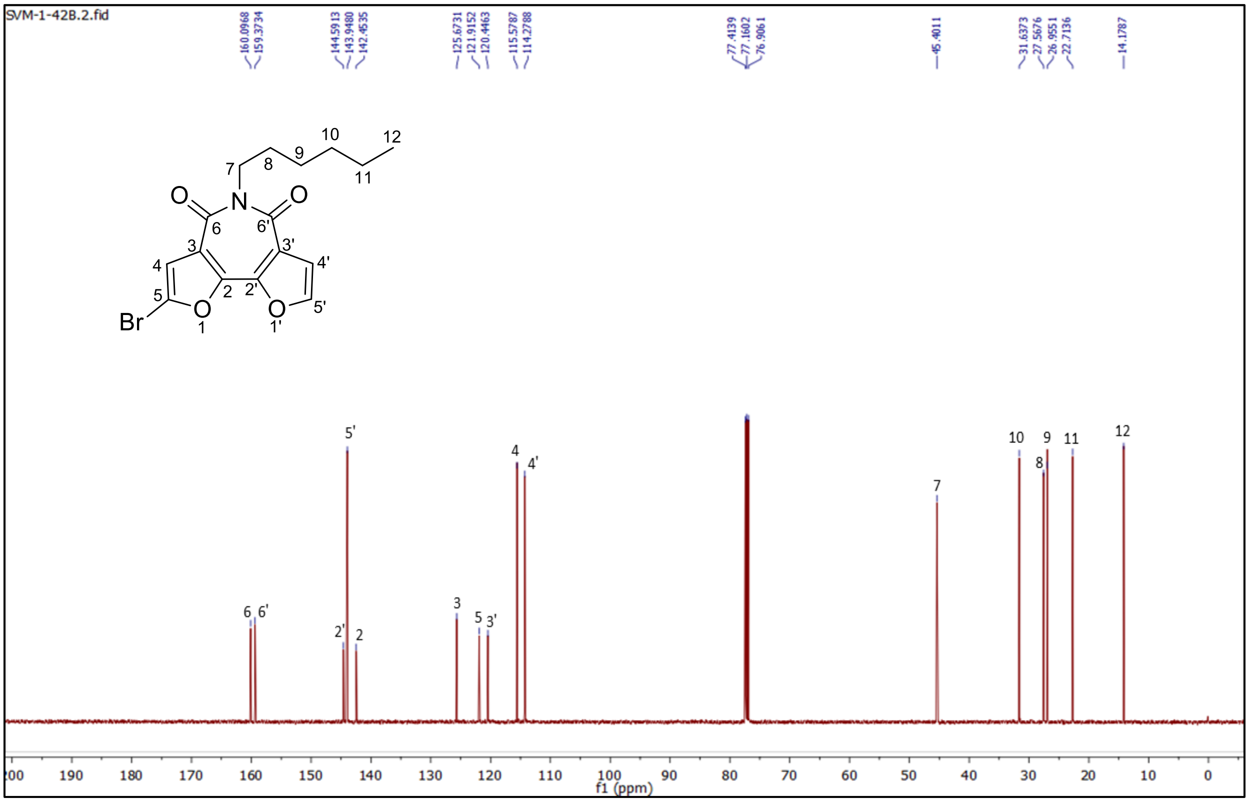

Figure S54. ^{13}C NMR spectrum of **4a**in $CDCl_3$, measured at 298 K.

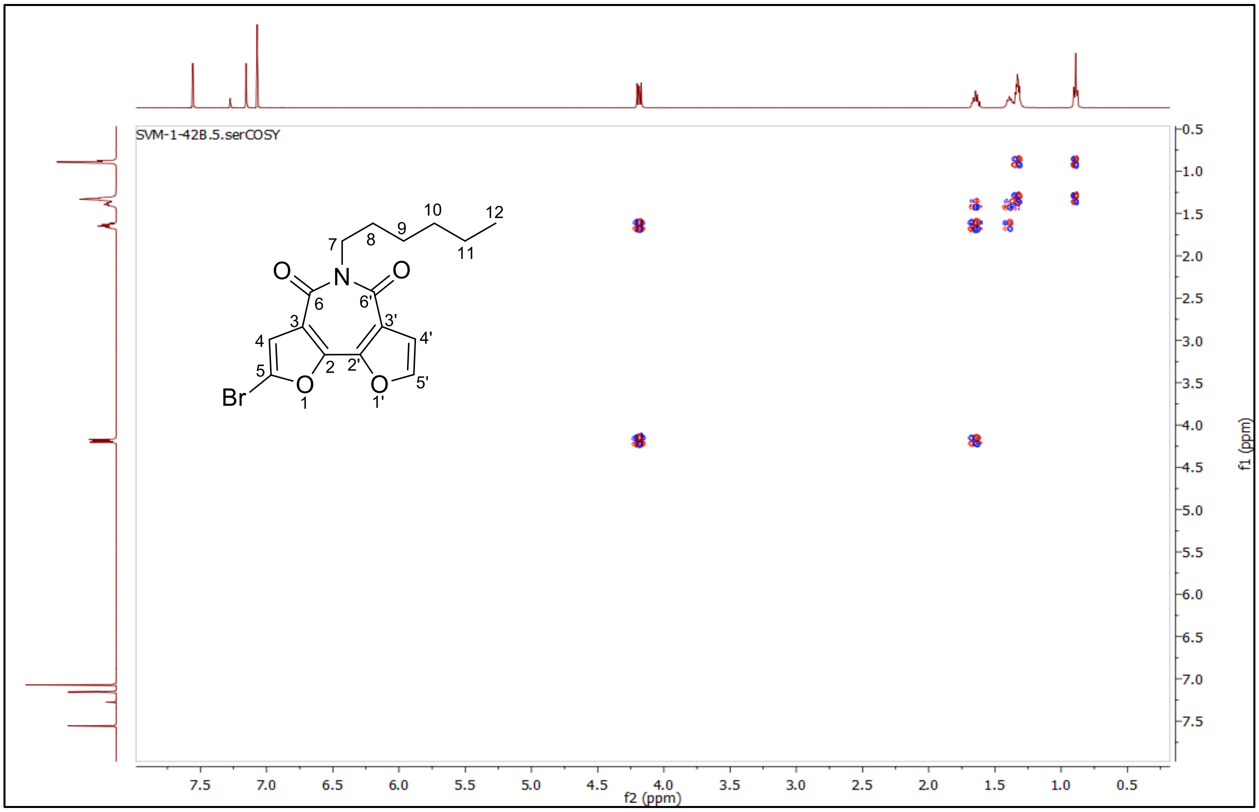

Figure S55. COSY spectrum of **4a** in $CDCl_3$, measured at 298 K.

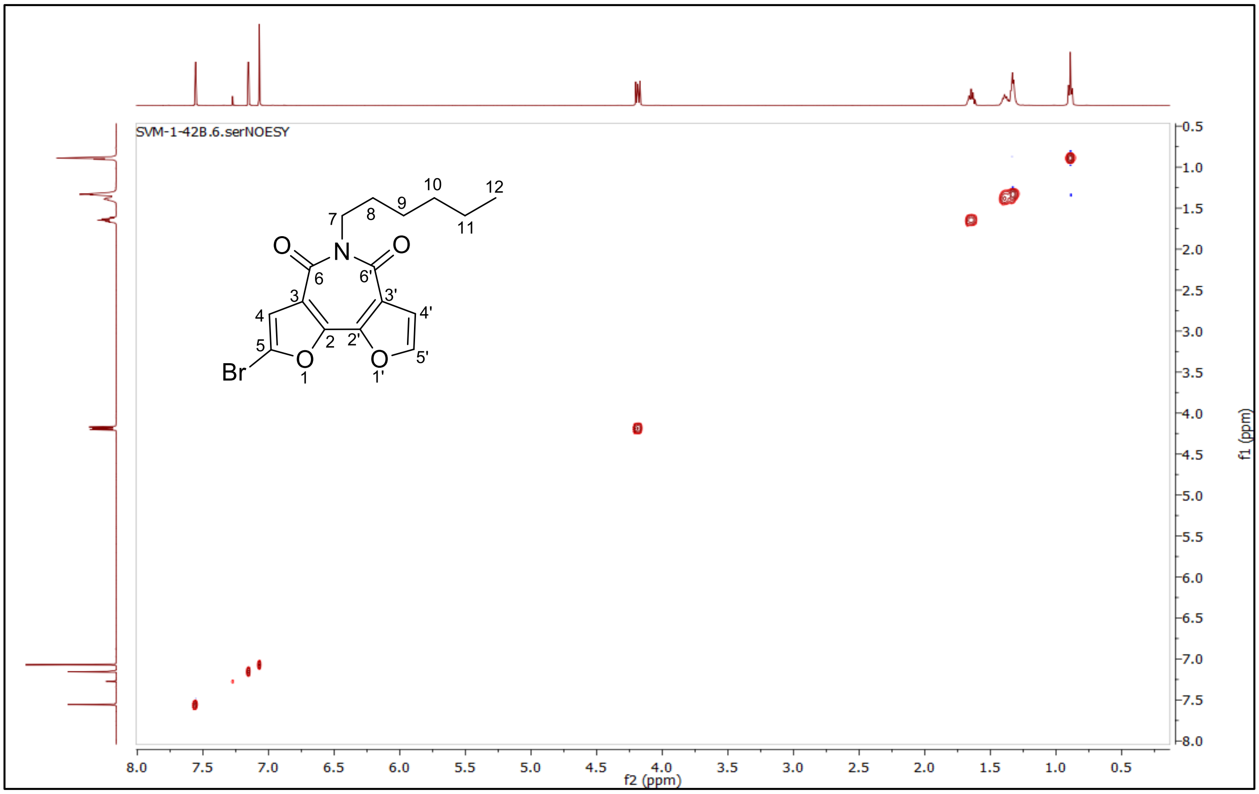

Figure S56. NOESY spectrum of **4a** in $CDCl_3$, measured at 298 K.

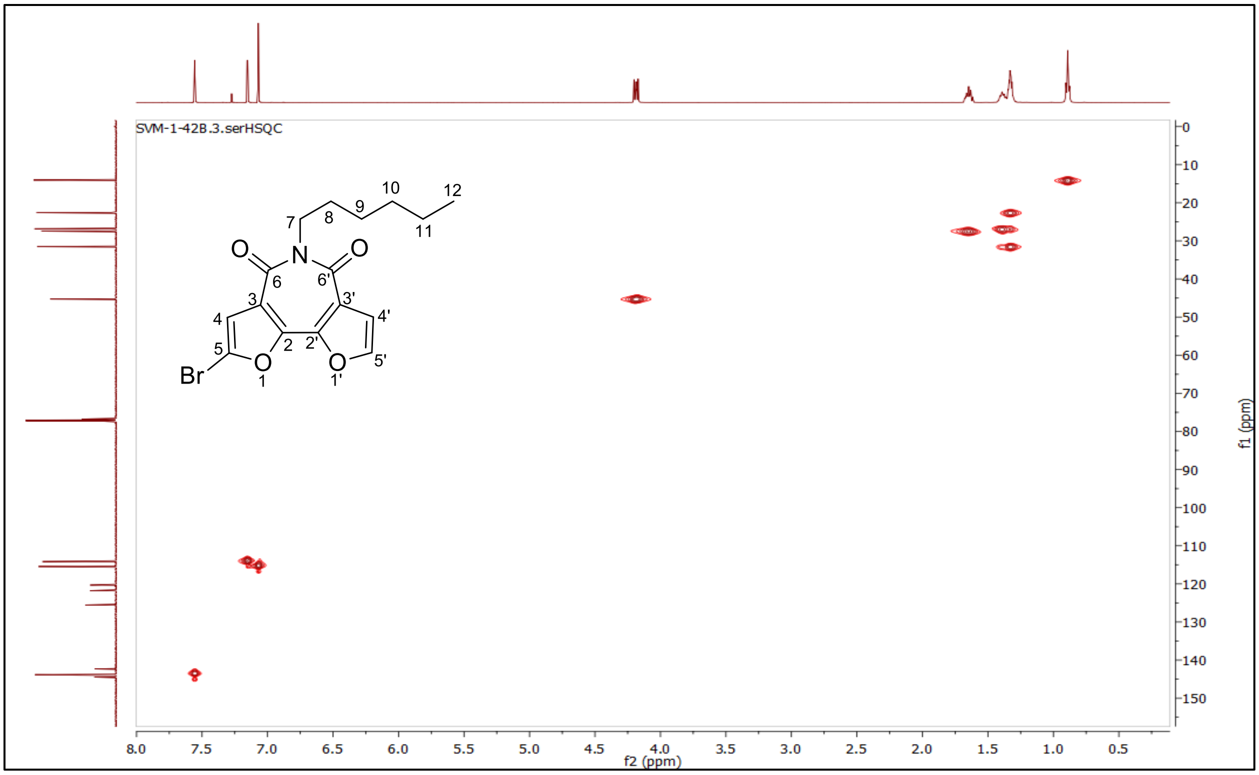

Figure S57. HSQC NMR spectrum of **4a** in $CDCl_3$, measured at 298 K.

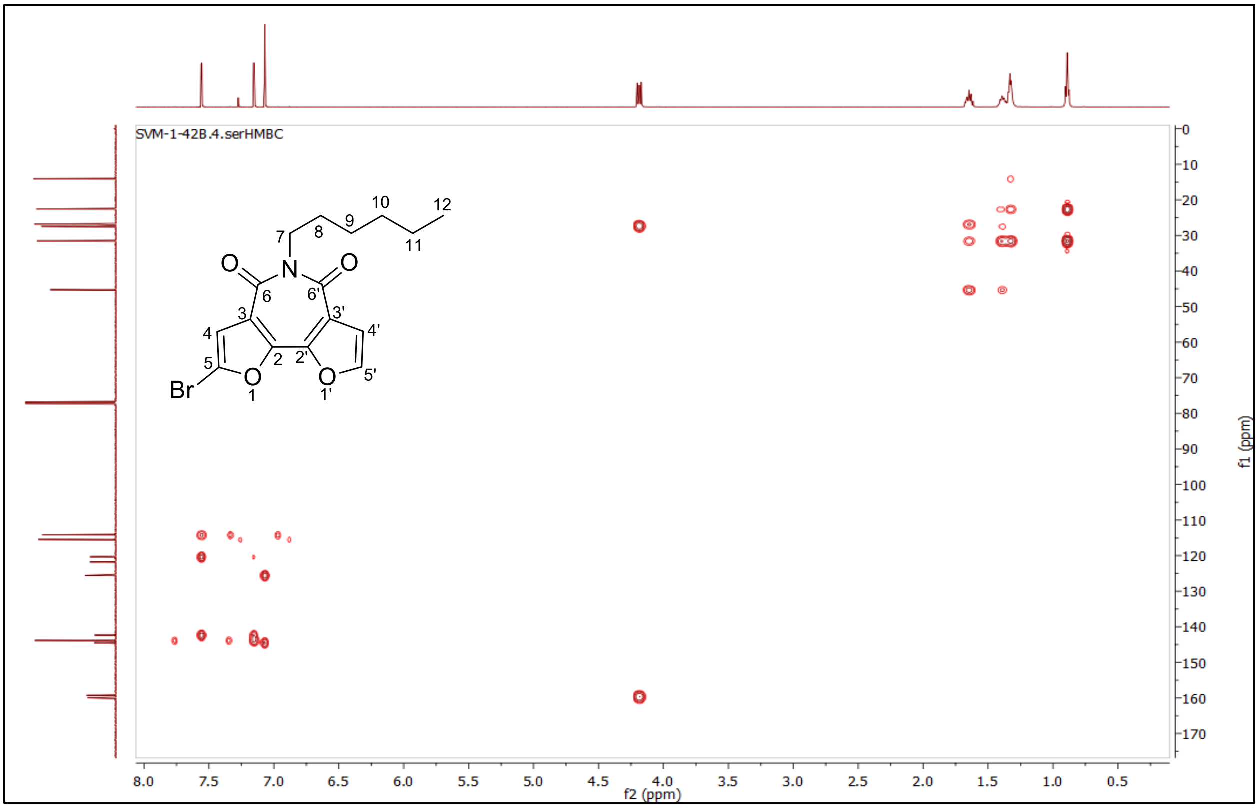

Figure S58. HMBC NMR spectrum of **4a** in $CDCl_3$, measured at 298 K.

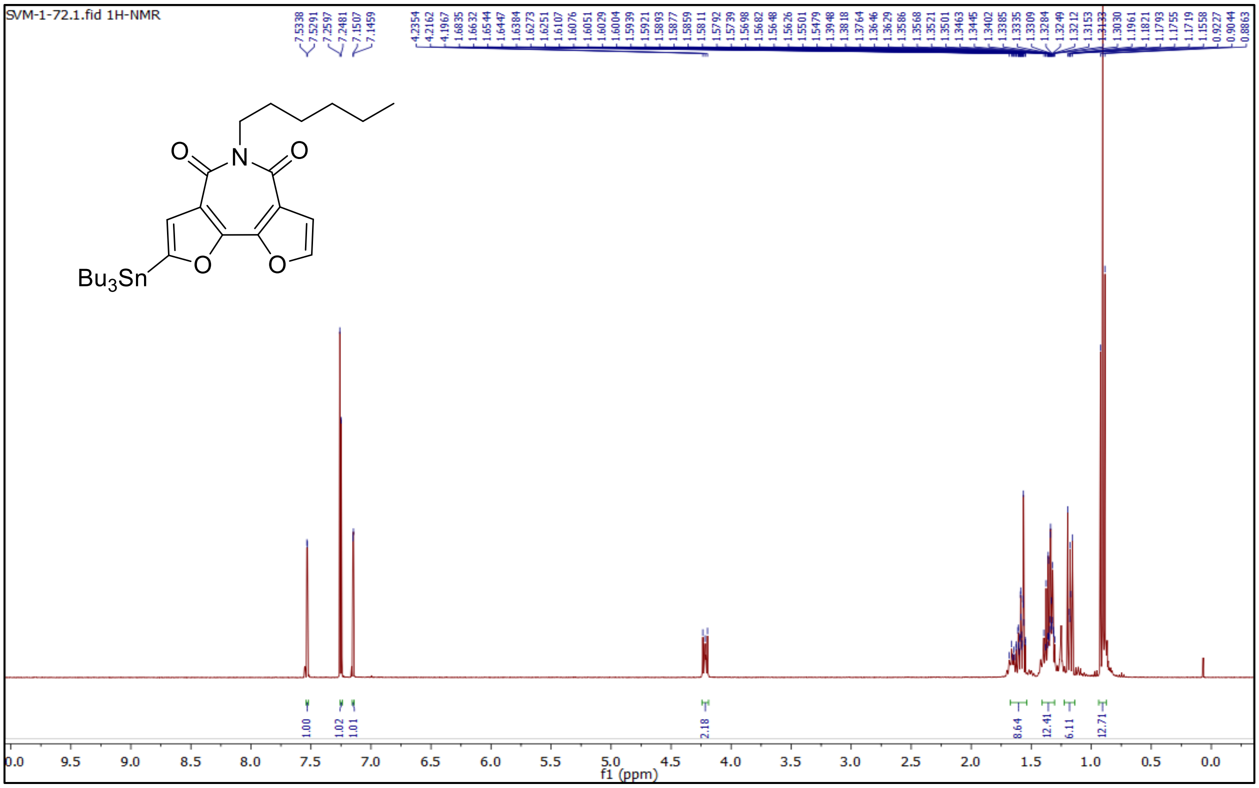

Figure S59. ^{1}H NMR spectrum of **5** in $CDCl_3$, measured at 298 K.

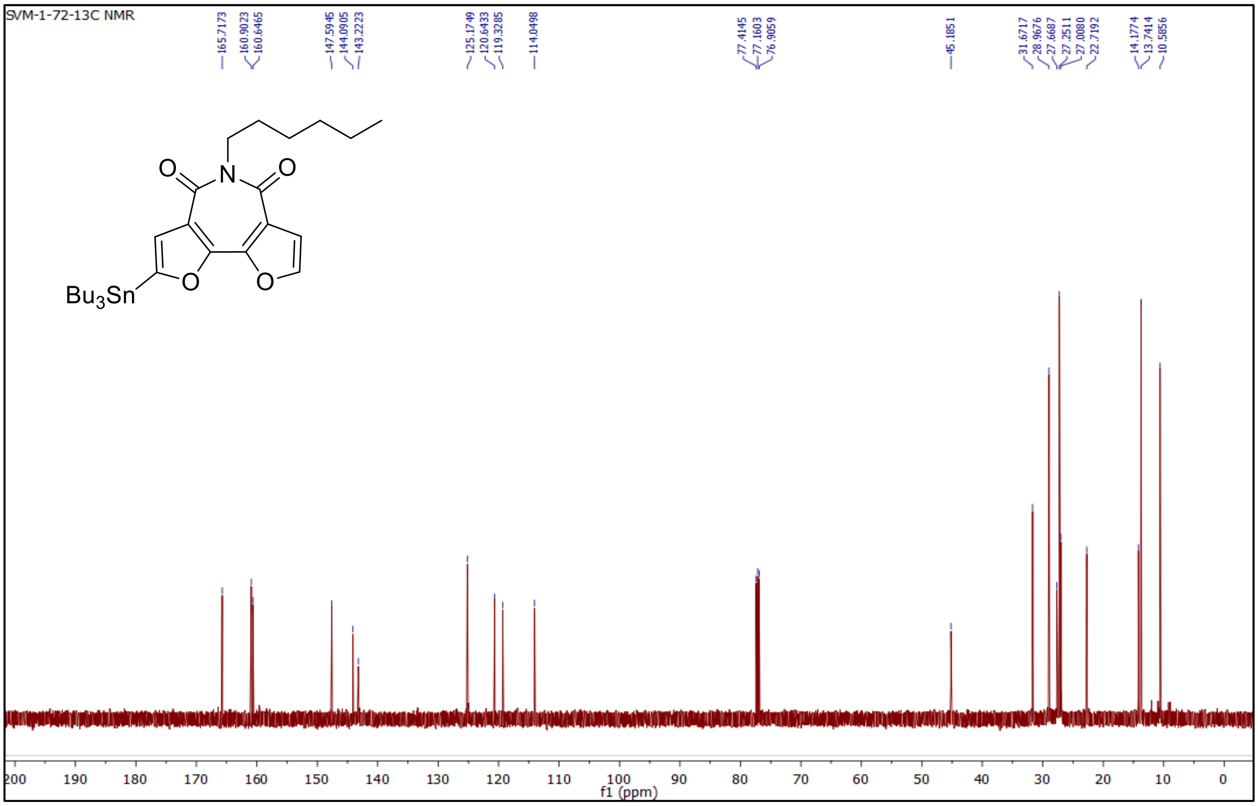

Figure S60. ^{13}C NMR spectrum of **5** in $CDCl_3$, measured at 298 K.

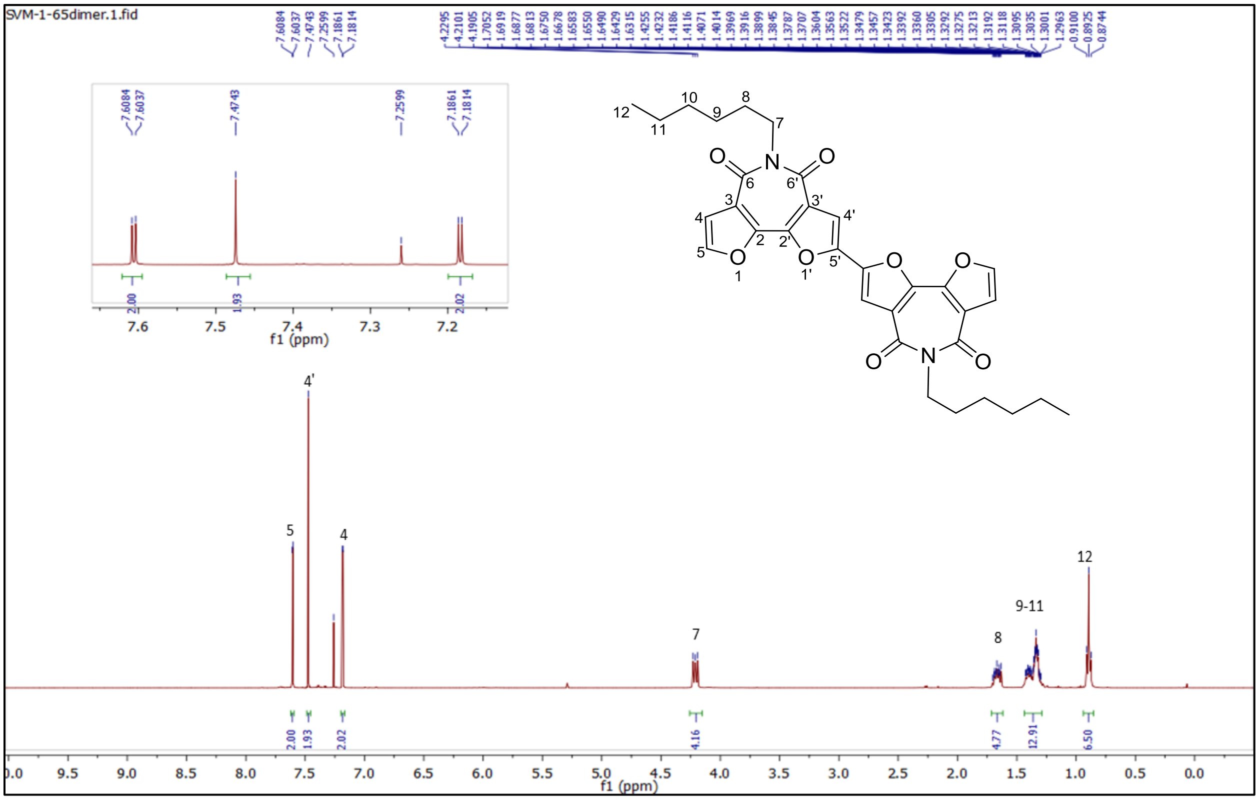

Figure S61. ^{1}H NMR spectrum of **2BFI-H** in $CDCl_3$, measured at 298 K.

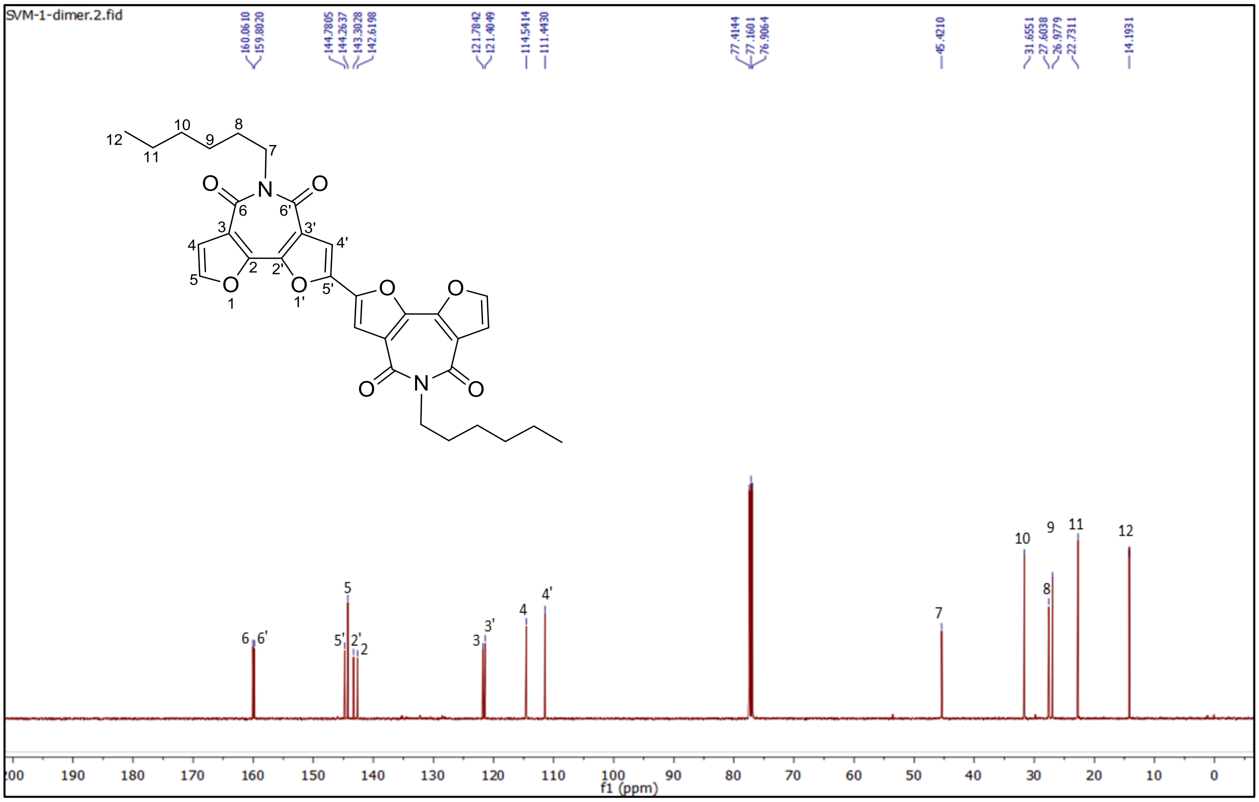

Figure S62. ^{13}C NMR spectrum of **2BFI-H** in $CDCl_3$, measured at 298 K.

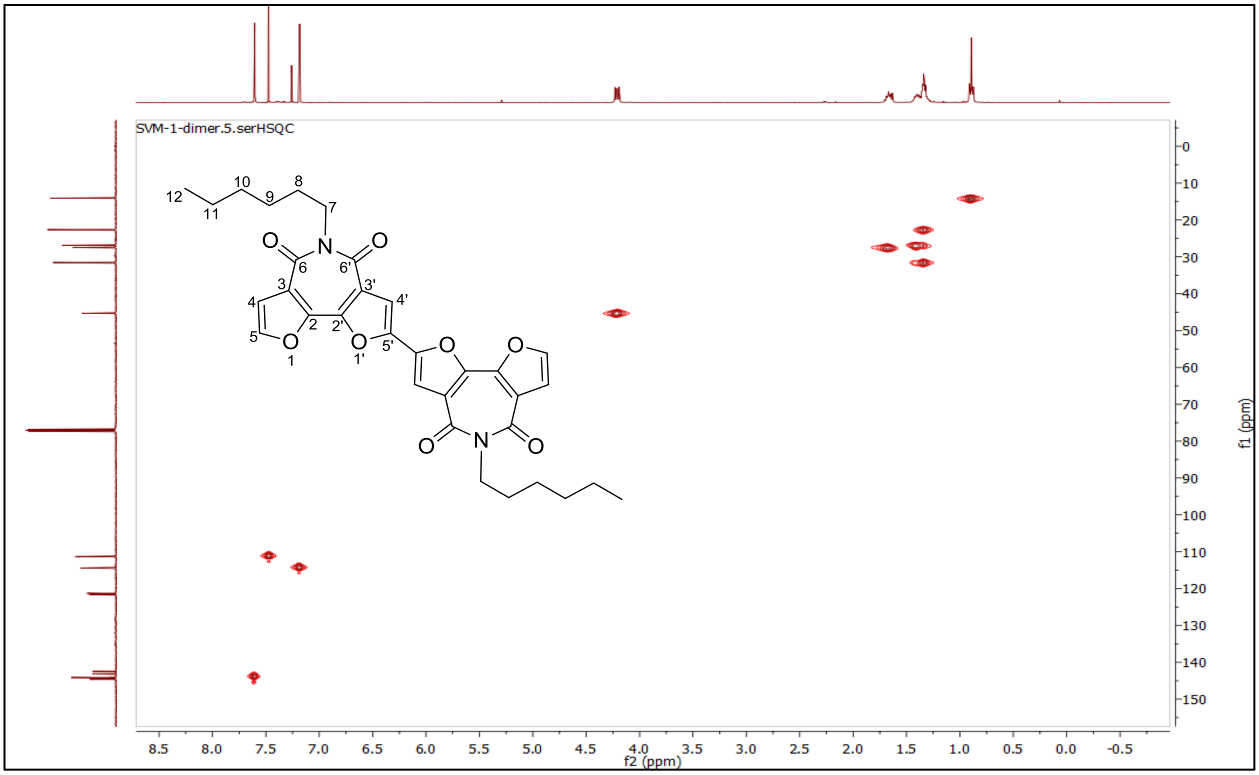

Figure S63. HSQC NMR spectrum of **2BFI-H** in $CDCl_3$, measured at 298 K.

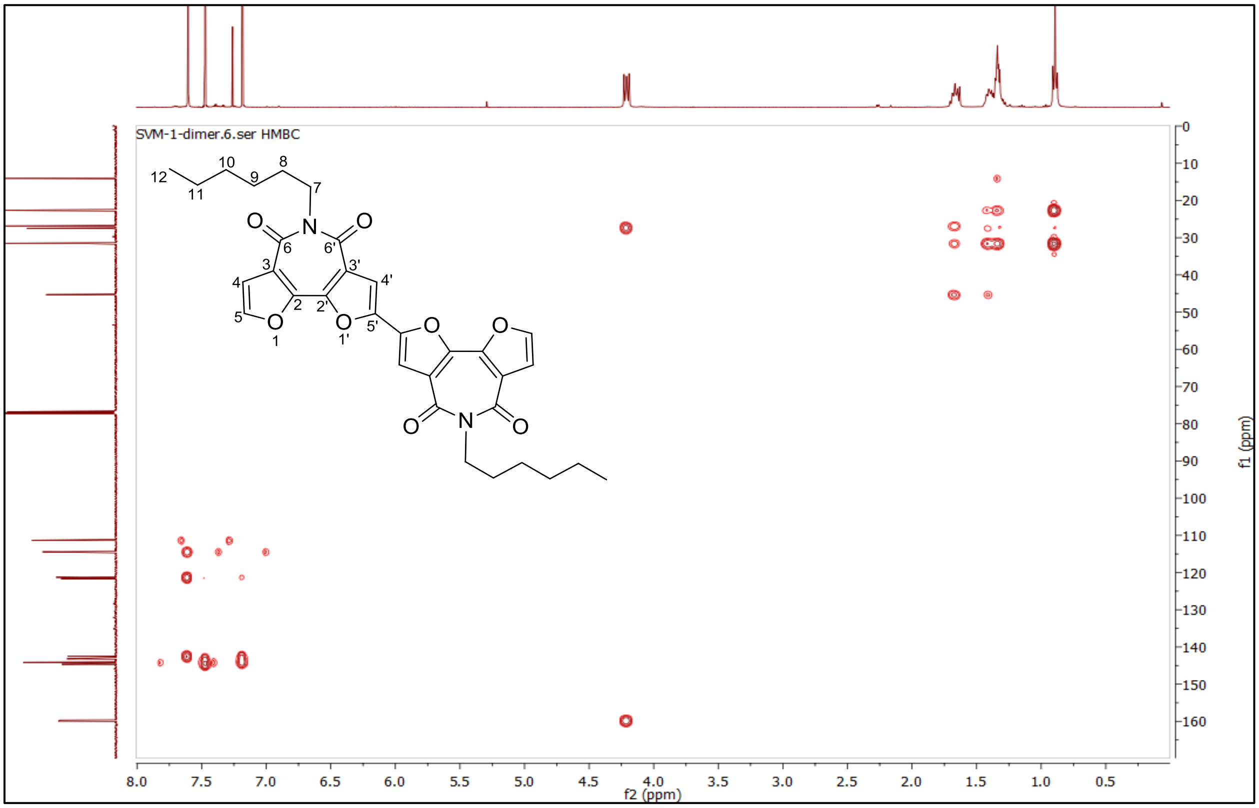

Figure S64. HMBC NMR spectrum of **2BFI-H** in $CDCl_3$, measured at 298 K.

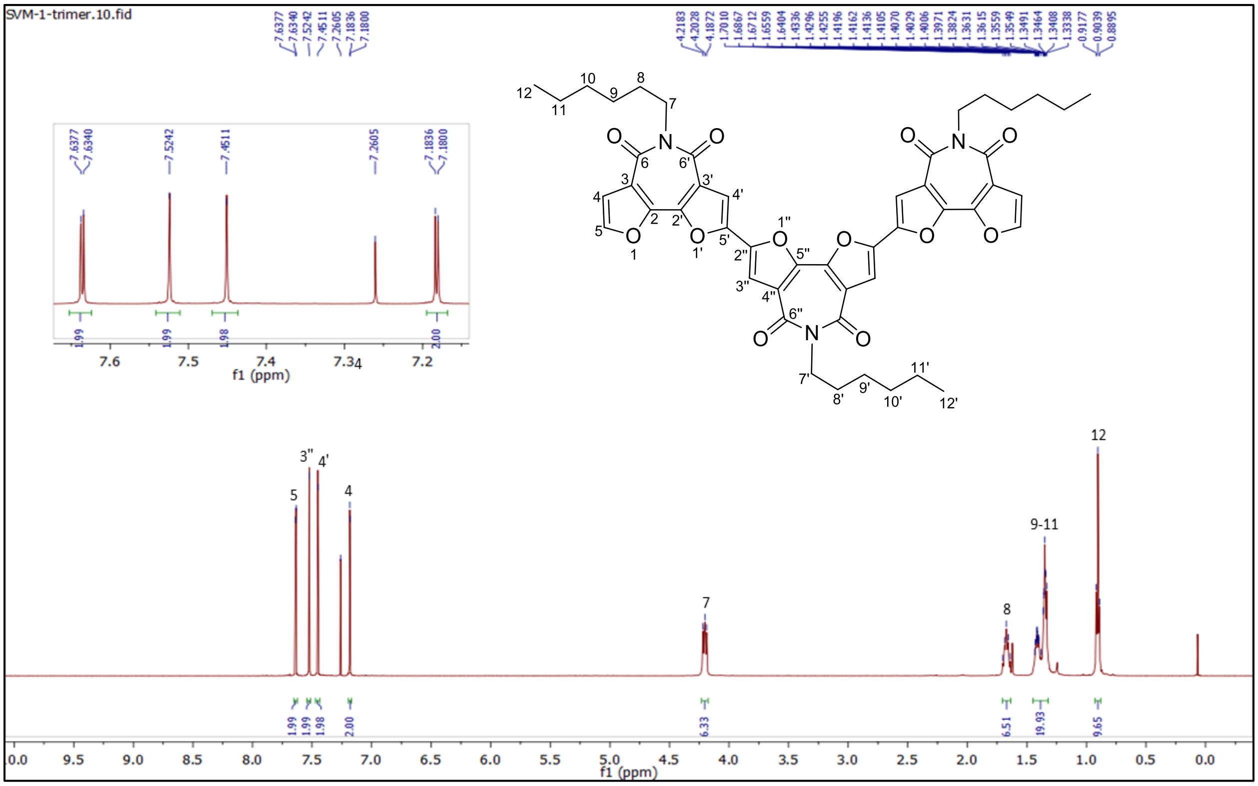

Figure S65. ^{1}H NMR spectrum of **3BFI-H** in CDCl$_3$, measured at 298 K.

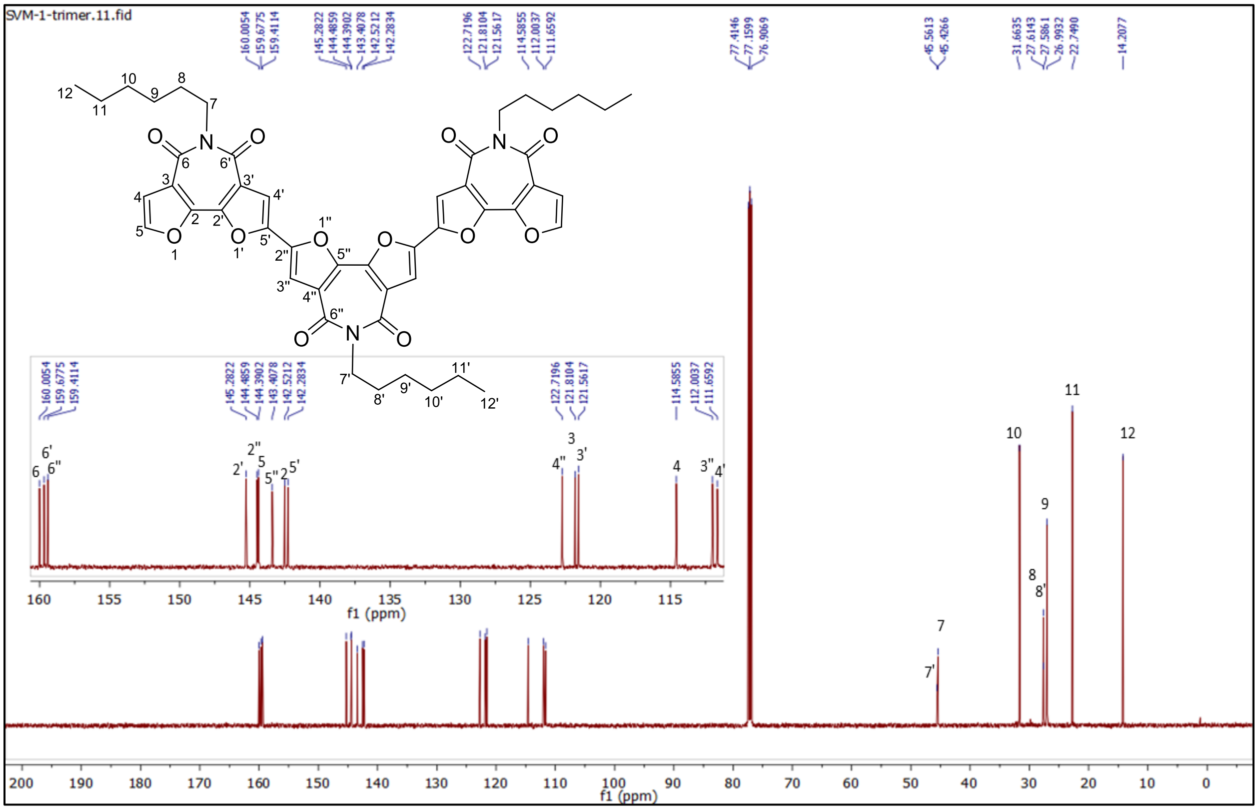

Figure S66. ^{13}C NMR spectrum of **3BFI-H** in CDCl$_3$, measured at 298 K.

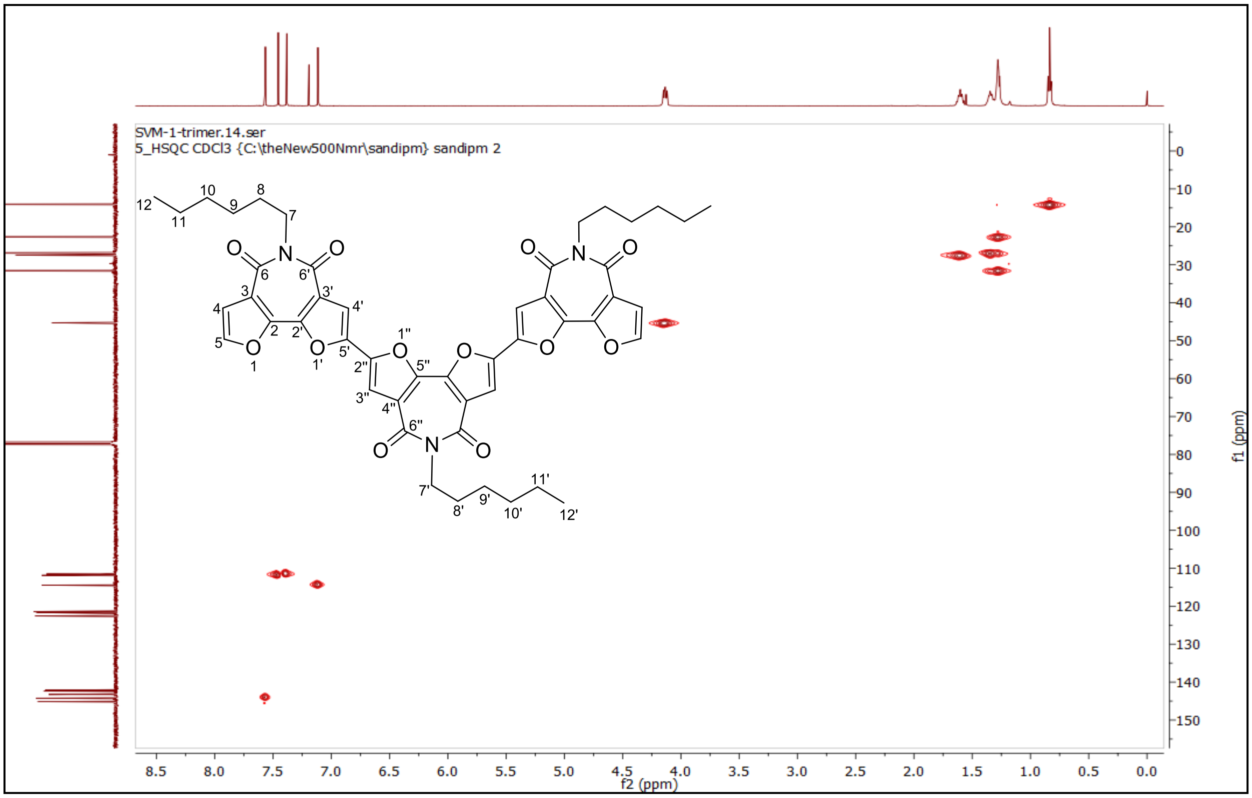

Figure S67. HSQC NMR spectrum of **3BFI-H** in $CDCl_3$, measured at 298 K.

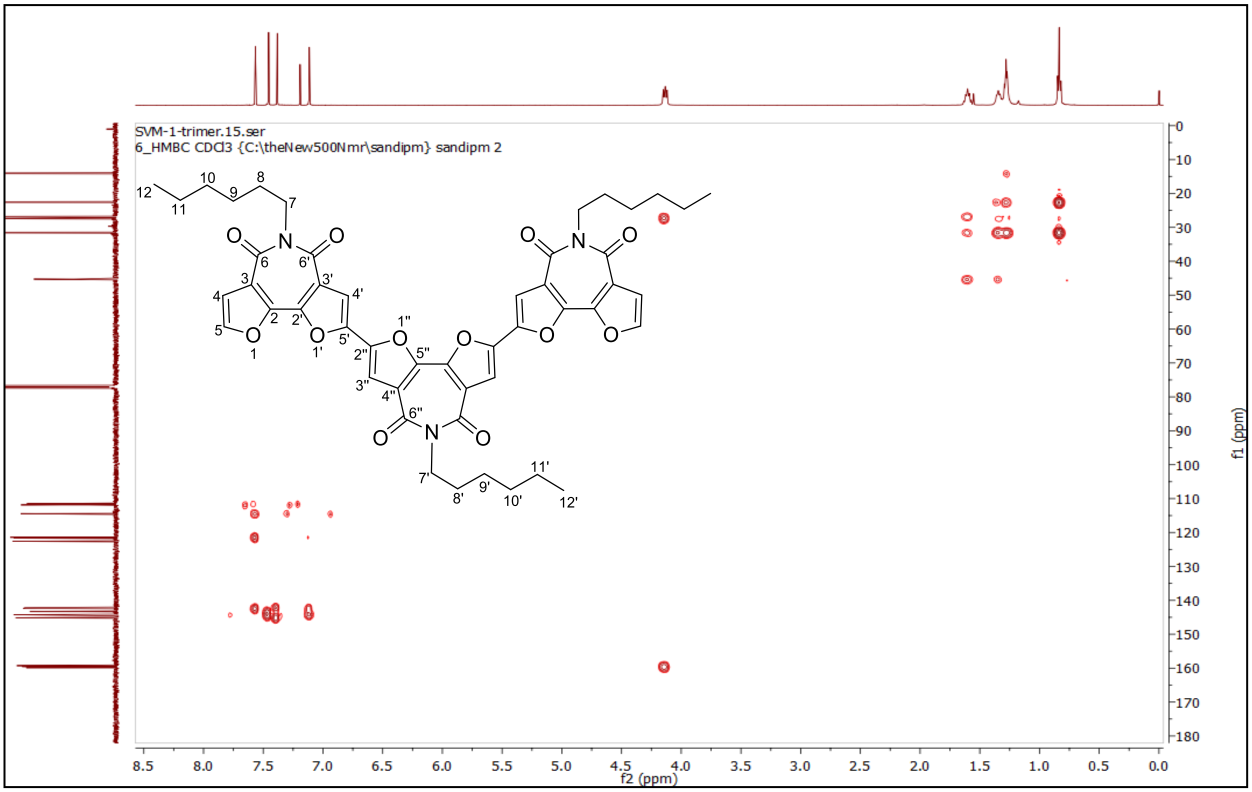

Figure S68. HMBC NMR spectrum of **3BFI-H** in $CDCl_3$, measured at 298 K.

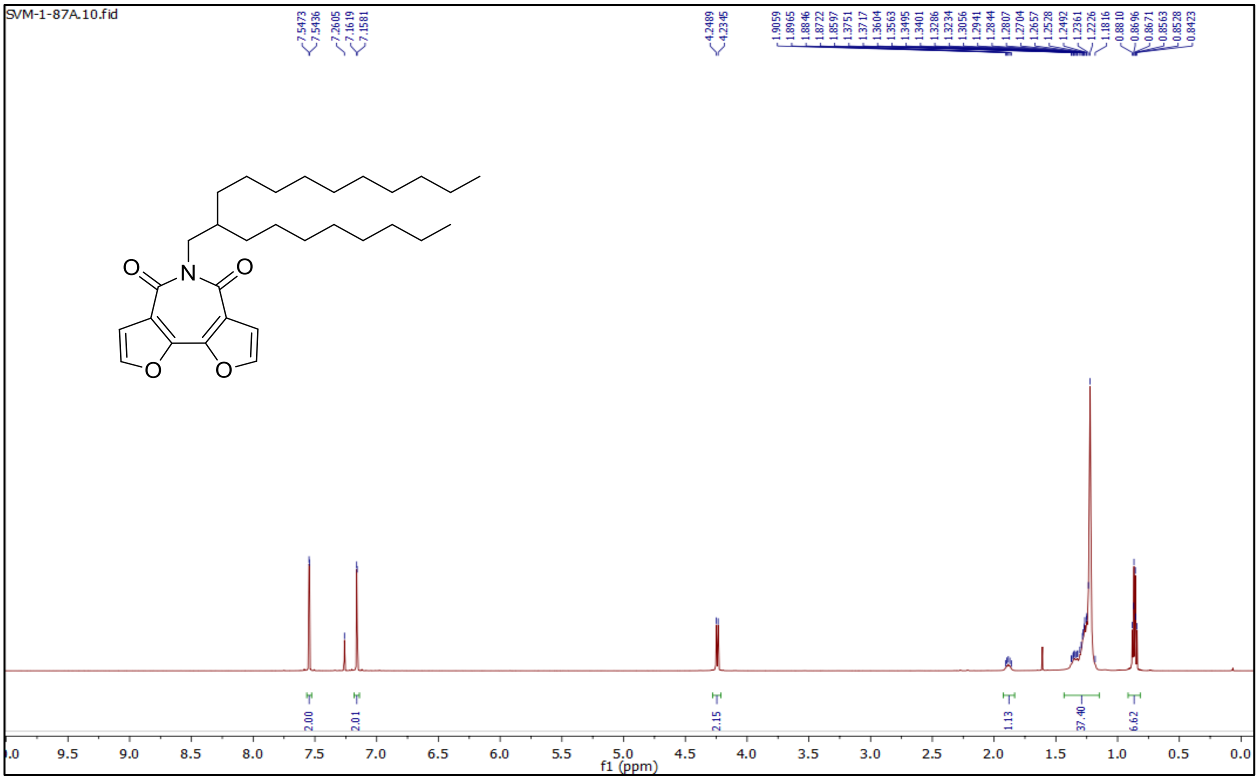

Figure S69. ^{1}H NMR spectrum of **BFI-OD** in $CDCl_3$, measured at 298 K.

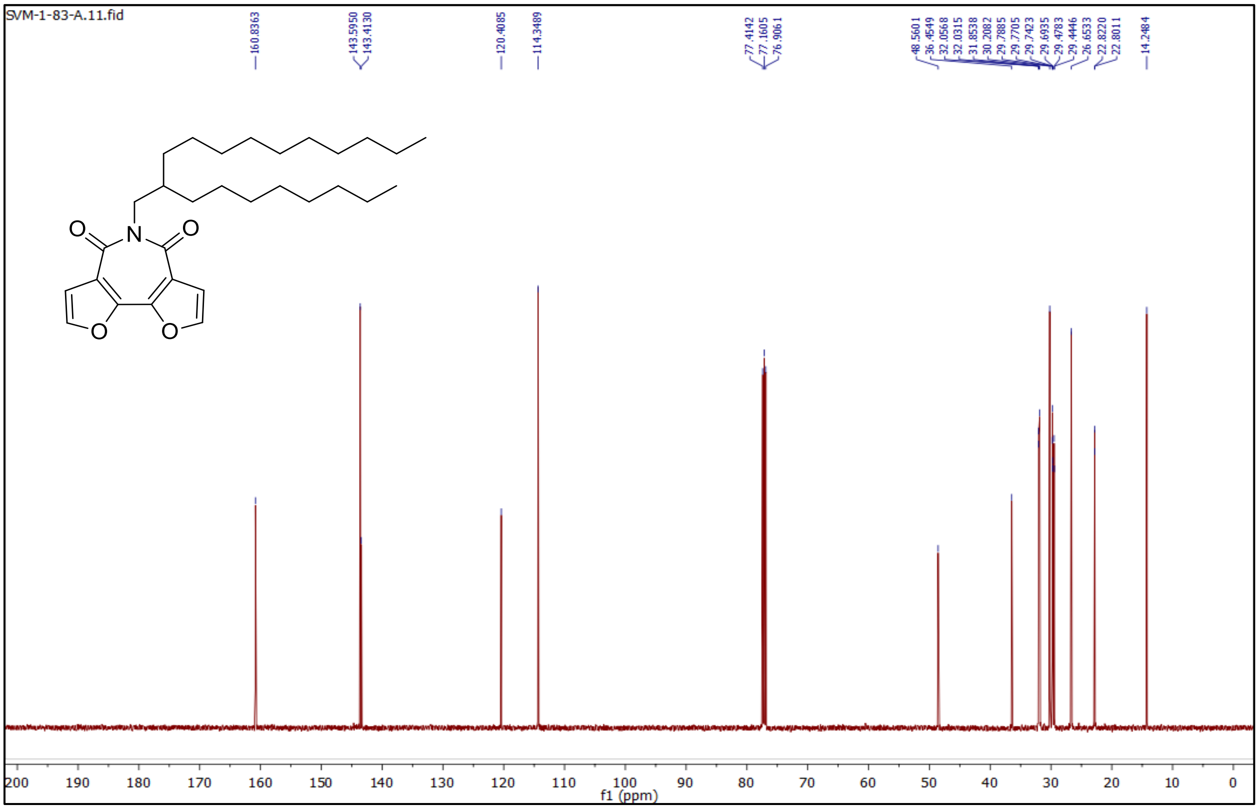

Figure S70. ^{13}C NMR spectrum of **BFI-OD** in $CDCl_3$, measured at 298 K.

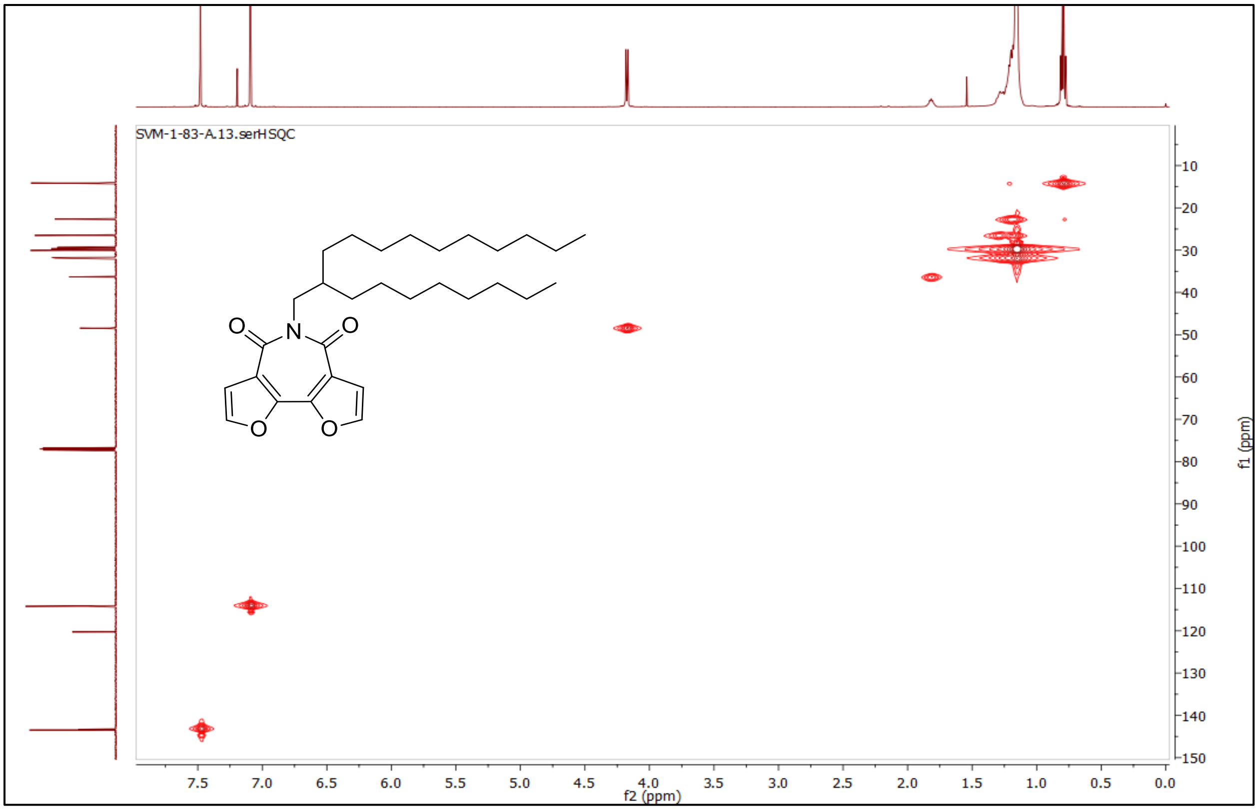

Figure S71. HSQC NMR spectrum of **BFI-OD** in $CDCl_3$, measured at 298 K.

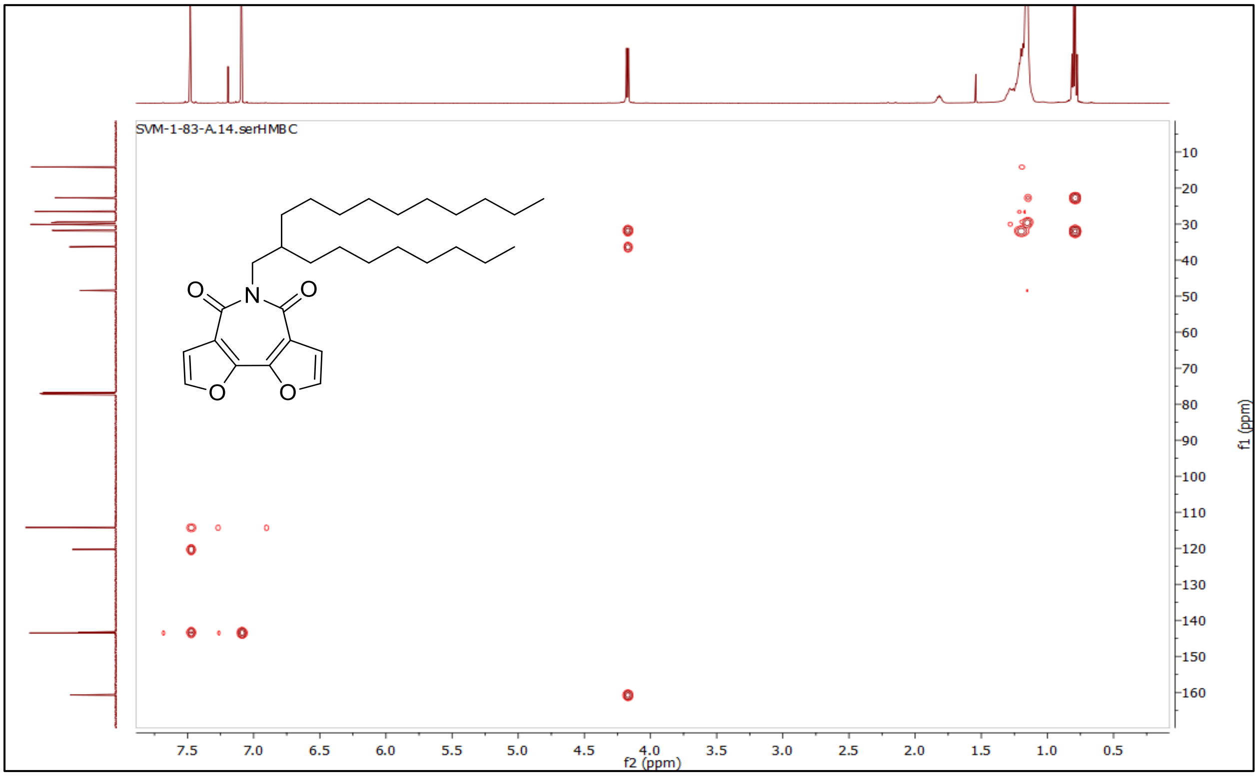

Figure S72. HMBC NMR spectrum of **BFI-OD** in $CDCl_3$, measured at 298 K.

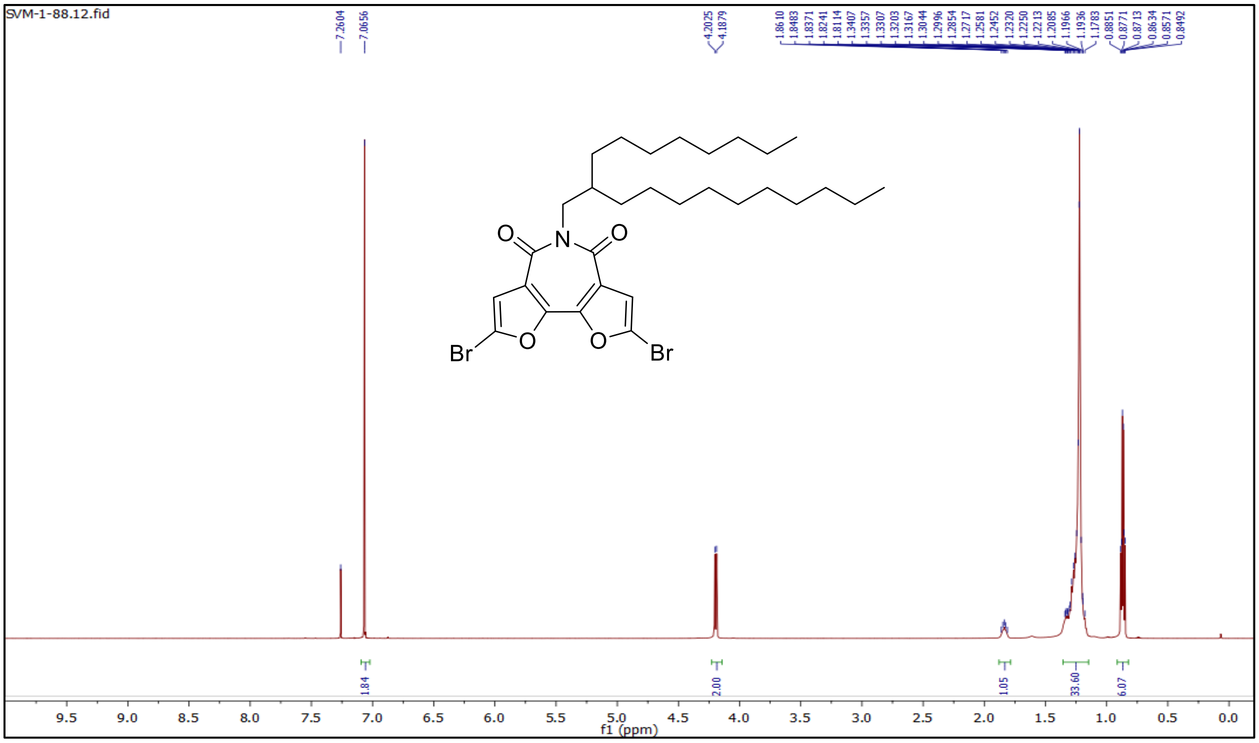

Figure S73. ^{1}H NMR spectrum of **4c** in $CDCl_3$, measured at 298 K.

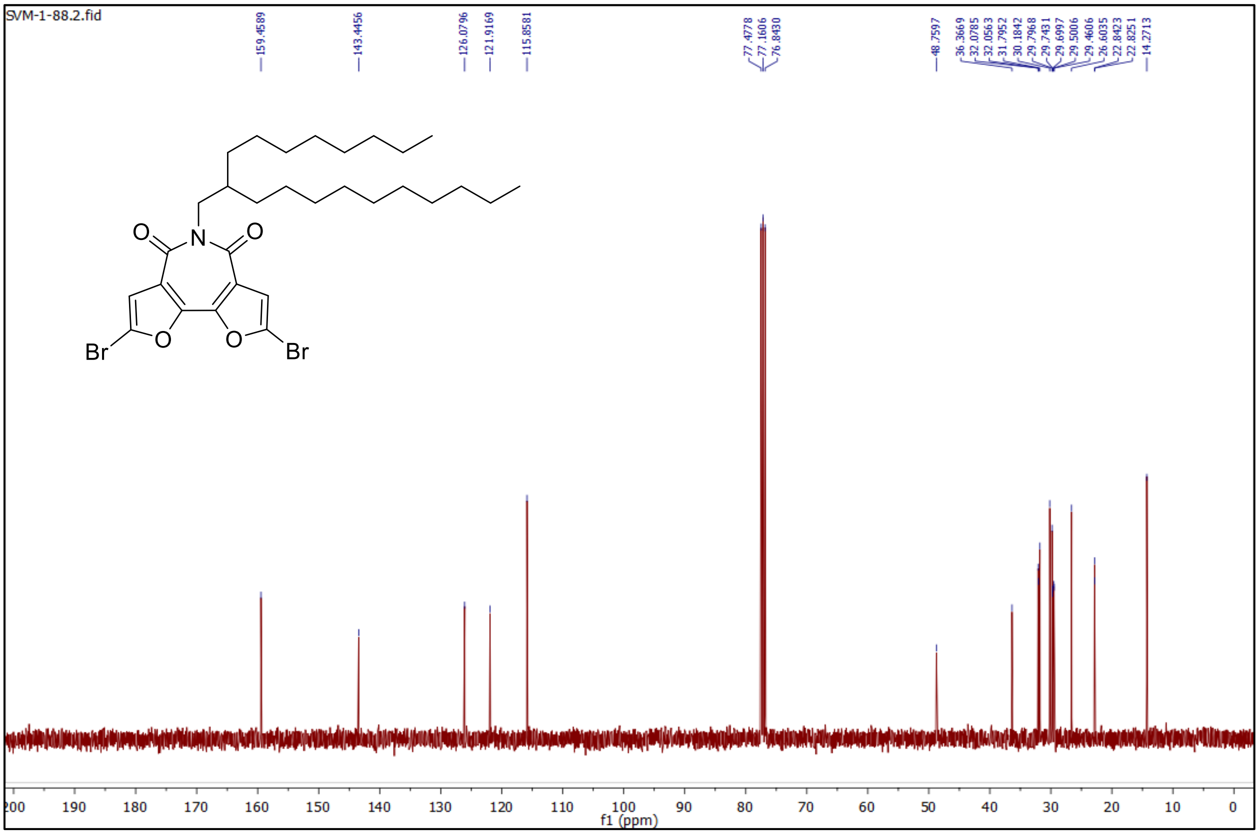

Figure S74. ^{13}C NMR spectrum of **4c** in $CDCl_3$, measured at 298 K.

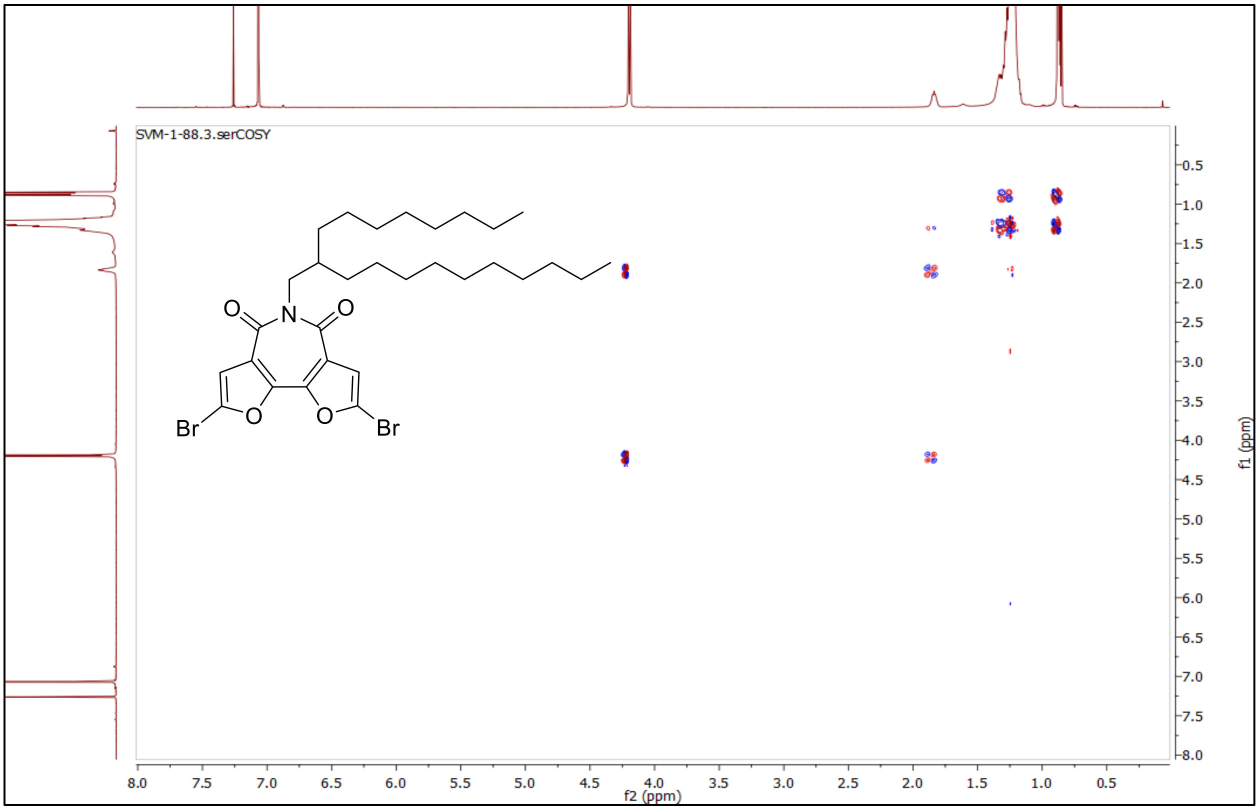

Figure S75. COSY spectrum of **4c** in $CDCl_3$, measured at 298 K.

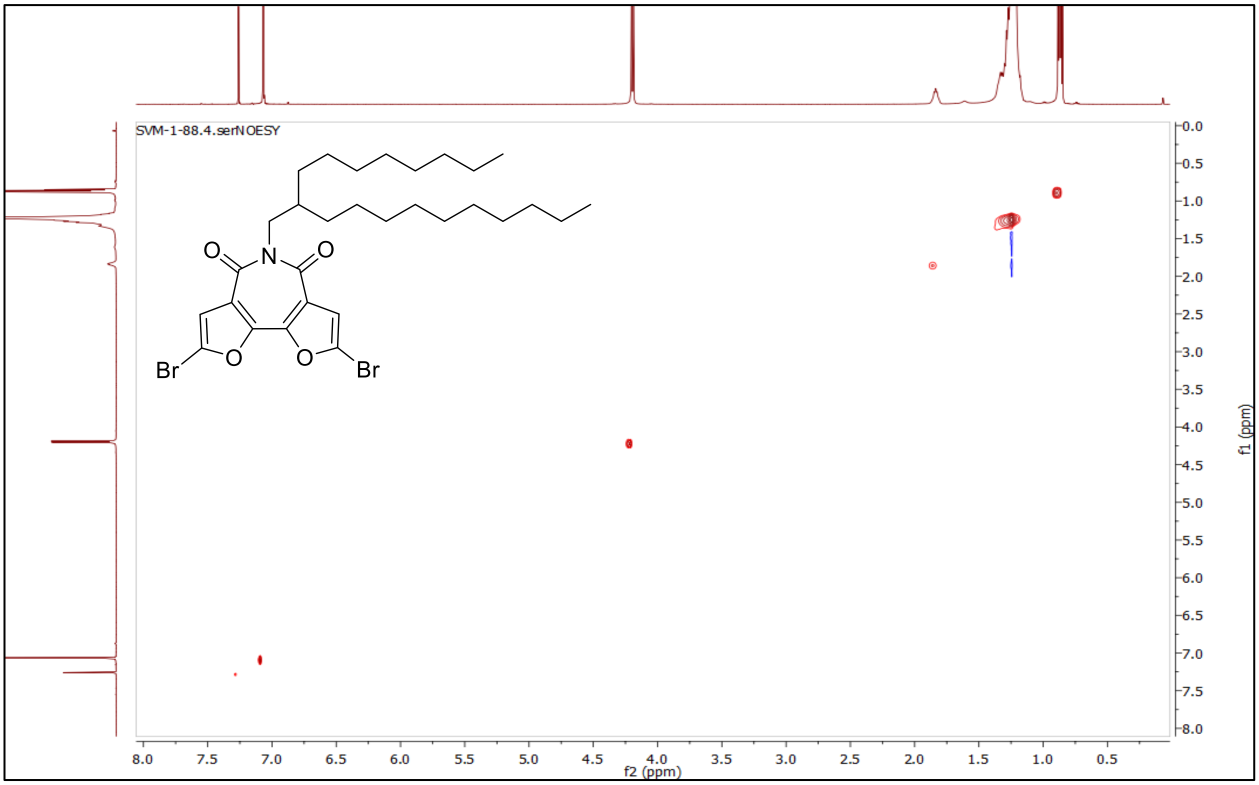

Figure S76. NOESY spectrum of **4c** in $CDCl_3$, measured at 298 K.

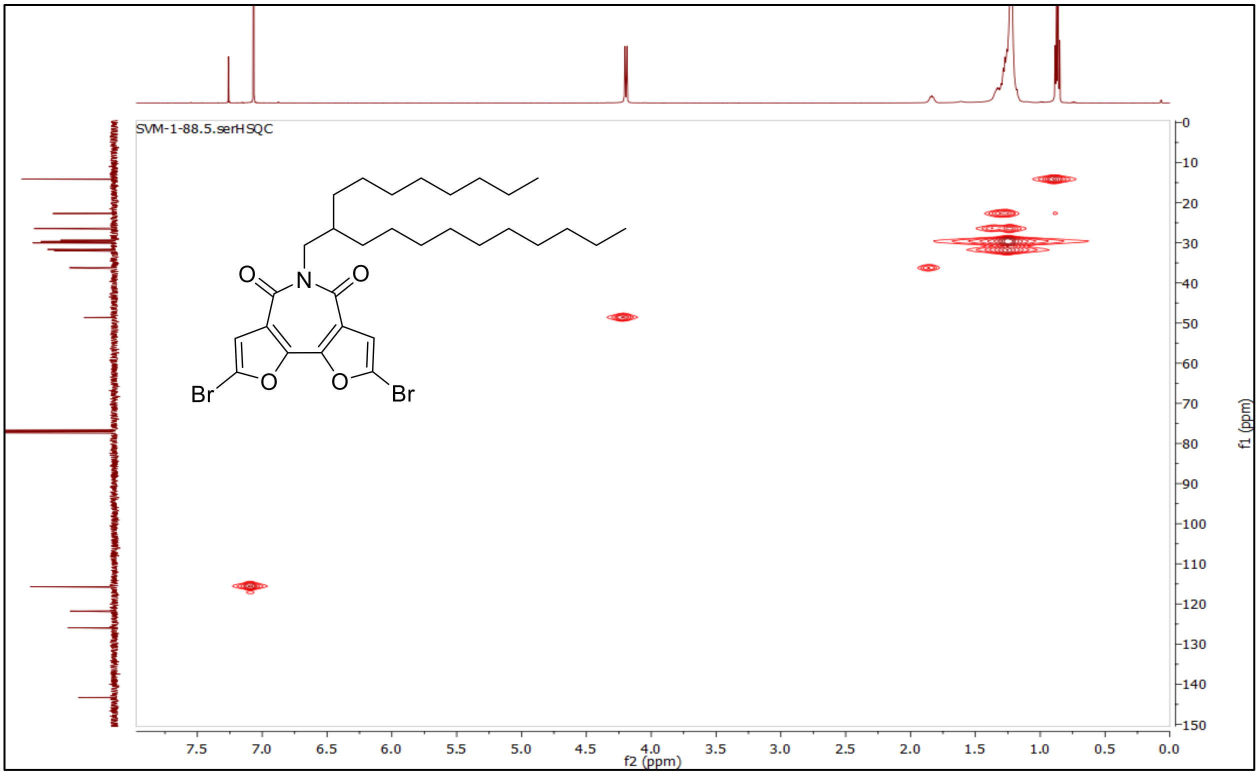

Figure S77. HSQC NMR spectrum of **4c** in $CDCl_3$, measured at 298 K.

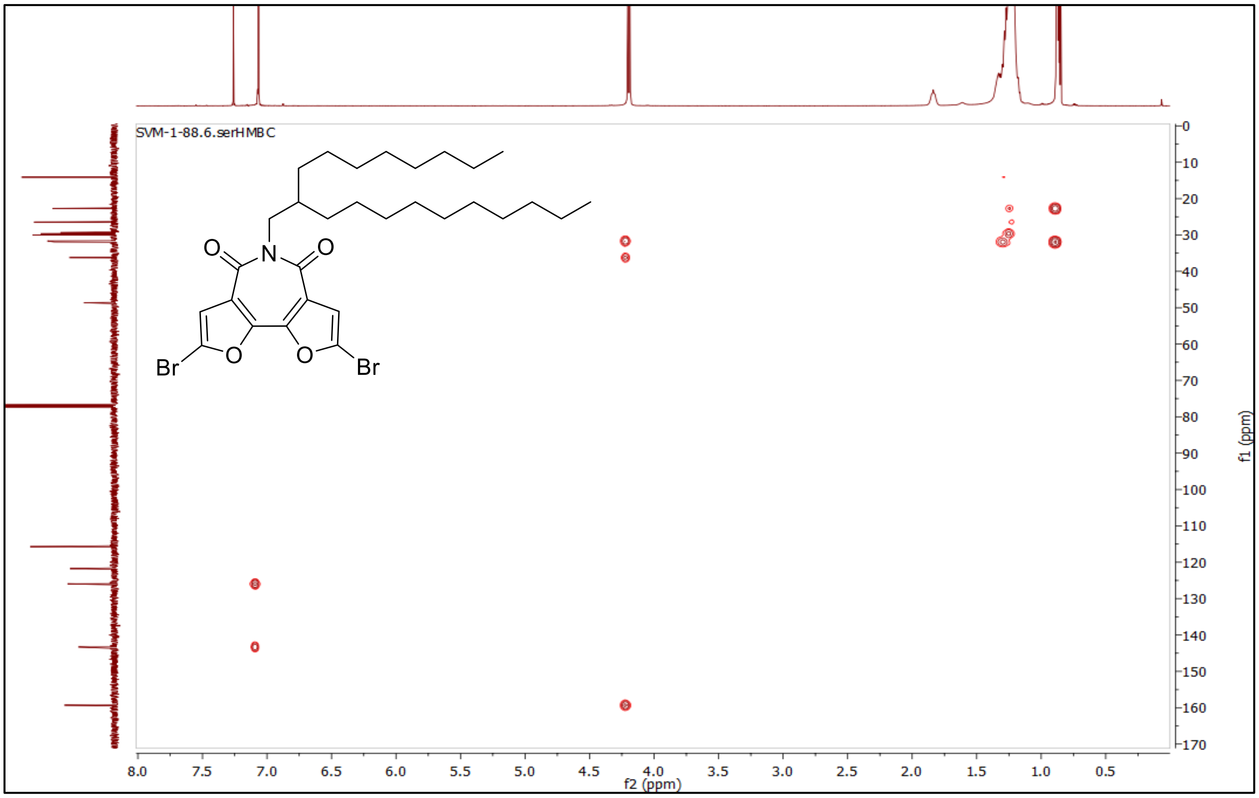

Figure S78. HMBC NMR spectrum of **4c** in $CDCl_3$, measured at 298 K.

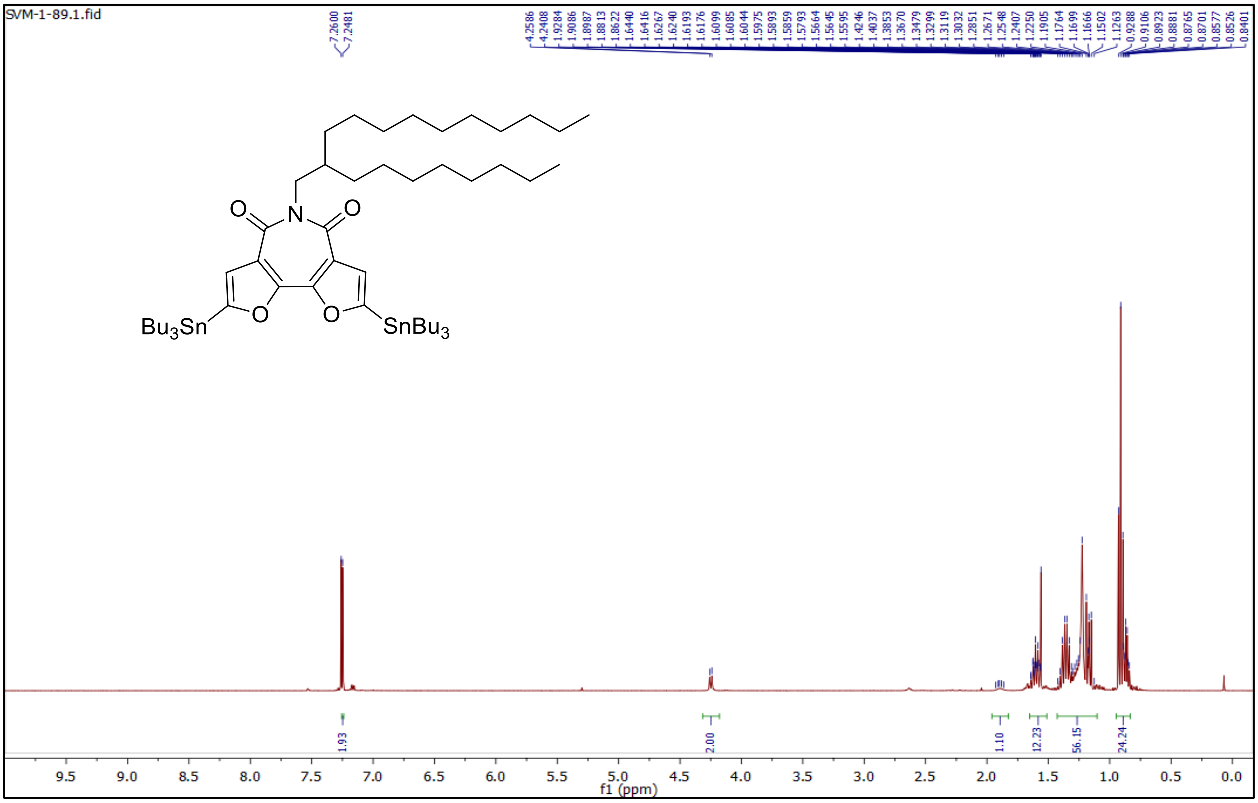

Figure S79. ^{1}H NMR spectrum of **6** in $CDCl_3$, measured at 298 K.

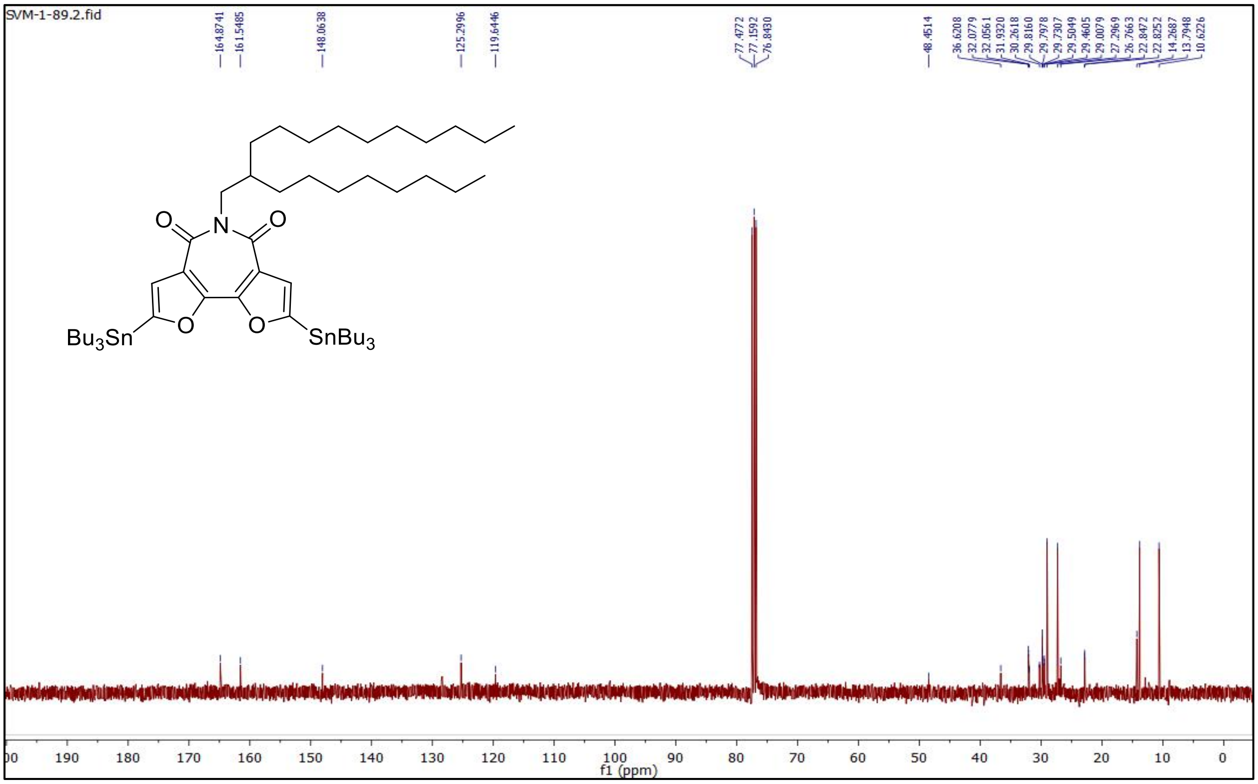

Figure S80. ^{13}C NMR spectrum of **6** in $CDCl_3$, measured at 298 K.

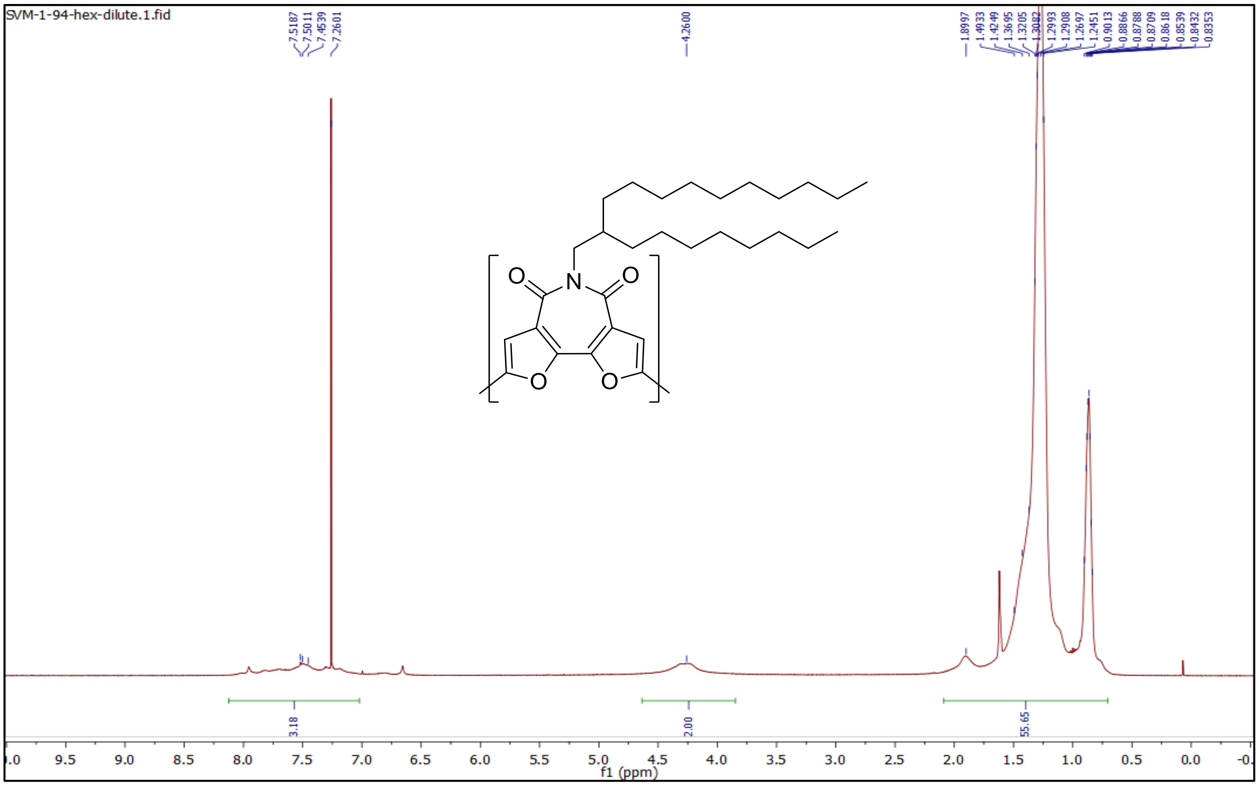

Figure S81. ^{1}H NMR spectrum of **poly(BFI-OD)** in $CDCl_3$, measured at 298 K.

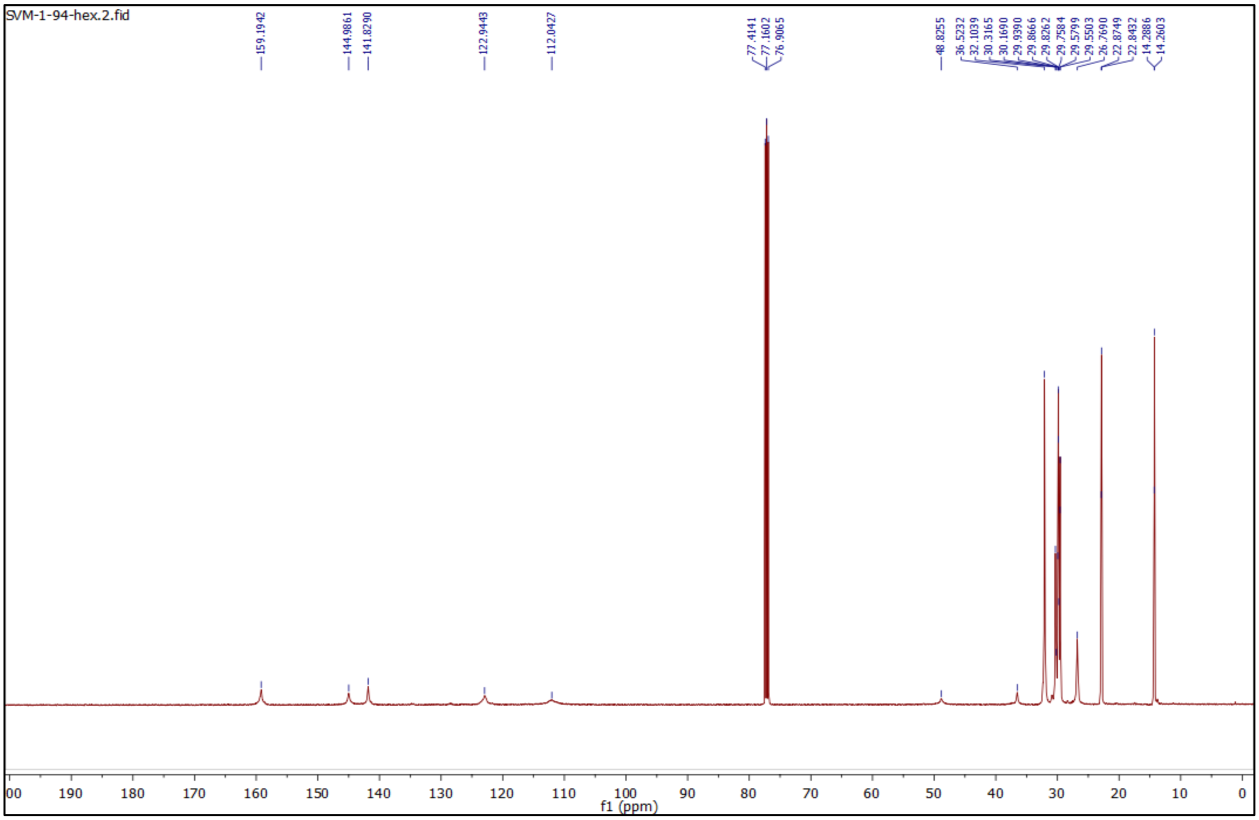

Figure S82. ^{13}C NMR spectrum of **poly(BFI-OD)** in $CDCl_3$, measured at 298 K.

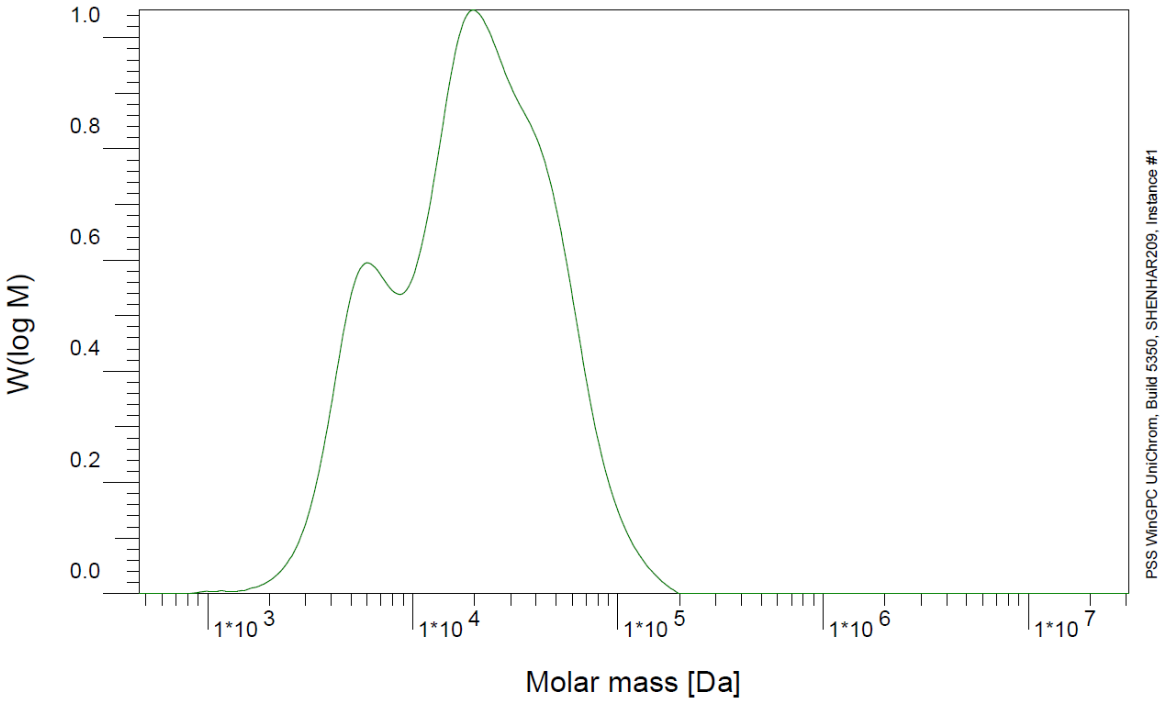

```
Sample :           SVM-01-94 hexane
Integration from:  Tuesday     03/20/18   17:15:08                          5.031 ml
Integration to  :  Tuesday     03/20/18   17:22:12                         12.091 ml
Calibration File : Raju sandip calibration chcl3 21 03 2018.CAL  Eluent :             CHCl3
MHK - A (Cal.):     0.000E+0                                     MHK - K (Cal.):       1.000E+0 ml/g
Int.stand.-cal.:    13.220 ml                                    Int.stand.-sam.:     ------- ml
Pump :             PSS SECcurity                                 Flowrate :             1.000 ml/min
Concentration :      2.531 g/l                                   Inject volume :      100.000 ul
Column 1 :         PSS SDV 5µm                                   Temperature :         35.000 °C
Detector 1 :       PSS SECcurity UV                              Delay volume :         0.000 ml
Detector 2 :       PSS SECcurity RI                              Delay volume :         0.100 ml
Operator :         gpc admin                                     Acquisition interval 1.000 sec
```

```
            PSS SECcurity RI

Mn :       1.2529e4           g/mol
Mw :       2.6622e4           g/mol
Mz :       4.7258e4           g/mol
Mv :       0.000000           g/mol
D  :       2.1249e0
[n]:       0.000000           ml/g
Vp :       9.6333e0           ml
Mp :       1.9726e4           g/mol
A  :       6.446e-2           ml*V
< 460          0.00
w% :         100.00
> 30763500   0.00
```

Figure S83. GPC graph of **poly(BFI-OD)** measured in $CHCl_3$ at room temperature.

S5 X-Ray Data Collection and Structure Refinement

A single crystal of **2**, **3**, **4a**, **4b**, **BFI-H** and **2BFI-H** was attached to a 400/50 MicroMeshes™ with NVH Oil,[3] and transferred to a Bruker SMART APEX CCD X-ray diffractometer equipped with a graphite-monochromator. Maintaining the crystals **3** at -150°C , **BFI-H** at -100°C and **2BFI-H** at -130°C was done with a Bruker KRYOFLEX nitrogen cryostat. The system was controlled by a PC running the SMART software package.[4] Data were collected at room temperature using MoKα radiation (λ=0.71073 Å). Immediately after collection, the raw data frames were transferred to a second PC computer for integration and reduction by the SAINT program package.[5] The structure was solved and refined by the SHELXTL software package.[6] The structures have been deposited with the Cambridge Crystallographic Data Centre (CCDC).

Compounds	**2**	**3**	**BFI-H**
CCDC No.	1839512	1839513	1839516
Formula	$C_{10}H_6O_6$	$C_{10}H_4O_5$	$C_{16}H_{17}NO_4$
Formula Weight	222.15	204.13	287.31
Crystal system	Monoclinic	Monoclinic	Triclinic
Space group	C2/c	$P2_1/c$	$P\bar{1}$-
Crystal size	0.46 x 0.33 x 0.15	0.40 x 0.12 x 0.10	0.48 x 0.30 x 0.30
Temperature (K)	296(1)	123 (1)	173(1)
Wavelength (Å)	0.71073	0.71073	0.71073
a, (Å)	13.226(4)	9.814(2)	12.422(2)
b, (Å)	6.747(2)	18.944(4)	12.868(2)
c, (Å)	10.358(3)	8.825(2)	13.229(2)
α, (°)	90	90	91.138(2)
β, (°)	94.474(4)	92.819(4)	92.183(2)
γ, (°)	90	90	94.864(2)
Volume ($Å^3$)	921.5(4)	1638.7(7)	2104.7(5)
Z	4	8	6
ρ_{calcd},(g cm^{-1})	1.601	1.655	1.360
μ, mm^{-1}	0.136	0.137	0.098
No. of reflection(unique)	4546 (986)	14786 (2878)	19501 (7278)
R_{int}	0.0233	0.0399	0.0236
Completeness to θ (%)	97.5	99.4	98.2
data / restraints / parameters	986/0/86	2878/0/ 271	7278/0/572
goodness-of-fit on F^2	1.181	1.306	1.067
Final R_1 and wR_2 indices [$I > 2\sigma(I)$]	0.0493, 0.1216	0.0758, 0.1485	0.0536, 0.1403
R_1 and wR_2 indices (all data)	0.0510, 0.1230	0.0795, 0.1504	0.0616, 0.1526

Compounds	**4a**	**4b**	**2BFI-H**
CCDC No.	1839515	1839514	1839517
Formula	$C_{16}H_{16}BrNO_4$	$C_{16}H_{15}Br_2NO_4$	$C_{32}H_{32}N_2O_8$ + (1/2 CH_2Cl_2)
Formula Weight	366.21	445.11	615.06
Crystal system **Space group**	Orthorhombic Pbca	Monoclinic $P2_1/c$	Monoclinic $P2_1/c$
Crystal size	0.33 x 0.30 x 0.13	0.52 x 0.21 x 0.12	0.63 x 0.13 x 0.12
Temperature (K)	292(1)	292(1)	143(1)
Wavelength (Å)	0.71073	0.71073	0.71073
a, (Å)	19.822(3)	8.962(1)	16.043(5)
b, (Å)	7.252(1)	22.105(4)	9.527(3)
c, (Å)	21.178(3)	8.691(1)	39.12(1)
α, (°)	90	90	90
β, (°)	90	104.837(3)	95.887
γ, (°)	90	90	90
Volume ($Å^3$)	3044.3(7)	1664.3(5)	5947(3)
Z	8	4	8
ρ_{calcd},(g cm^{-1})	1.598	1.776	1.374
μ, mm^{-1}	2.718	4.889	0.184
No. of reflection(unique)	32361 (3642)	17960 (3630)	53871(10463)
R_{int}	0.0423	0.0376	0.1179
Completeness to θ (%)	98.6	99.6	99.9
data / restraints / parameters	3642/0/200	3630/0/244	10463/0/788
goodness-of-fit on F^2	1.012	1.030	1.134
Final R_1 and wR_2 indices [$I > 2\sigma(I)$]	0.0350, 0.0900	0.0334, 0.0802	0.0949, 0.1940
R_1 and wR_2 indices (all data)	0.0561, 0.1010	0.0494, 0.0849	0.1380, 0.2145

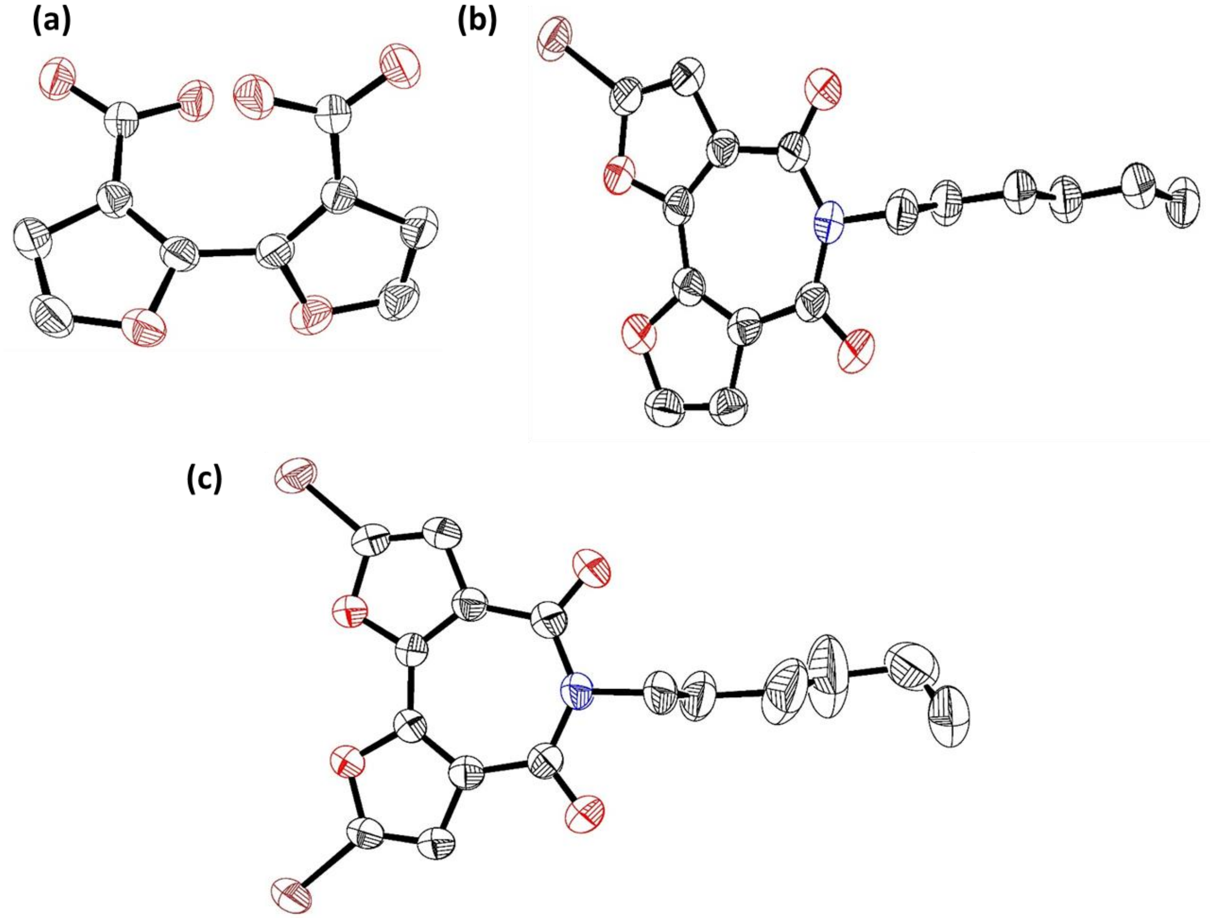

Figure S84. ORTEP representation of (a) 2,2'-bifuran-3,3'-dicarboxylic acid (**2**), (b) *N*-hexyl-5-bromo-2,2'-bifuran-3,3'-dicarboximide (**4a**), and (c) *N*-hexyl-5,5'-dibromo-2,2'-bifuran-3,3'-dicarboximide (**4b**).

S6 Computational Details

All calculations were carried out with the Gaussian 09 series of programs using density function theory (DFT).[7] Becke's three-parameter exchange functional combined with the Lee–Yang–Parr correlation functional (B3LYP) and with the 6-31G(d) basis set was used for all calculations.[8] The optimal geometries for all structures were confirmed as minima by frequency calculations. No negative frequencies were found for any structure presented in this work. For all calculated structures, methyl was used instead of hexyl to reduced computation time.

Compound name	Energy (Hartrees)
1BFI	-779.01236330
2BFI	-1556.84327214
3BFI	-2334.67383742
Poly(2BFI)	-1555.66102250

S7 References

1. Jin, X-H.; Sheberla, D.; Shimon, L. J. W.; Bendikov, M. J. Am. Chem. Soc. 2015, 136, 2592-2601.
2. Letizia, J. A.; Salata, M. R.; Tribout, C. M.; Facchetti, A.; Ratner, M. A.; Marks, T. J. J. Am. Chem. Soc. 2008, 130, 9679-9694.
3. MiTeGen, LLC P.O. Box 3867 Ithaca, NY 14852.
4. SMART-NT V5.6, BRUKER AXS GMBH, D-76181 Karlsruhe, Germany, **2002**.
5. SAINT-NT V5.0, BRUKER AXS GMBH, D-76181 Karlsruhe, Germany, **2002**.
6. SHELXTL-NT V6.1, BRUKER AXS GMBH, D-76181 Karlsruhe, Germany, **2002**.
7. Gaussian 09, Revision D.01: Frisch, M. J.; Trucks, G. W.; Schlegel, H. B.; Scuseria, G. E.; Robb, M. A.; Cheeseman, J. R.; Scalmani, G.; Barone, V.; Petersson, G. A.; Nakatsuji, H.; Li, X.; Caricato, M.; Marenich, A.; Bloino, J.; Janesko, B. G.; Gomperts, R.; Mennucci, B.; Hratchian, H. P.; Ortiz, J. V.; Izmaylov, A. F.; Sonnenberg, J. L.; Williams-Young, D.; Ding, F.; Lipparini, F.; Egidi, F.; Goings, J.; Peng, B.; Petrone, A.; Henderson, T.; Ranasinghe, D.; Zakrzewski, V. G.; Gao, J.; Rega, N.; Zheng, G.; Liang, W.; Hada, M.; Ehara, M.; Toyota, K.; Fukuda, R.; Hasegawa, J.; Ishida, M.; Nakajima, T.; Honda, Y.; Kitao, O.; Nakai, H.; Vreven, T.; Throssell, K.; Montgomery, J. A., Jr.; Peralta, J. E.; Ogliaro, F.; Bearpark, M.; Heyd, J. J.; Brothers, E.; Kudin, K. N.; Staroverov, V. N.; Keith, T.; Kobayashi, R.; Normand, J.; Raghavachari, K.; Rendell, A.; Burant, J. C.; Iyengar, S. S.; Tomasi, J.; Cossi, M.; Millam, J. M.; Klene, M.; Adamo, C.; Cammi, R.; Ochterski, J. W.; Martin, R. L.; Morokuma, K.; Farkas, O.; Foresman, J. B.; Fox, D. J. Gaussian, Inc., Wallingford CT, 2016.
8. (a) Parr, R. G.; Weitao, Y. *Density-Functional Theory of Atoms and Molecules*; Oxford University Press, **1989**; (b) Lee, C.; Yang, W.; Parr, R. G. *Phys. Rev. B: Condens. Matter Mater. Phys.* **1988**, *37*, 785– 789; (c) Becke, A. D. *J. Chem. Phys.* **1993**, *98*, 5648– 5652.